University of Alberta

THE HUMAN NEURAMINIDASE ENZYME, NEU3, REGULATES INTEGRIN-MEDIATED CELL MIGRATION VIA CHANGES IN GLYCOLIPID COMPOSITION

by

Feng Jia

A thesis submitted to the Faculty of Graduate Studies and Research
in partial fulfillment of the requirements for the degree of

Master of Science

Department of Chemistry

Fall 2013
Edmonton, Alberta

DEDICATION

To my parents, family members and friends.

ABSTRACT

The human neuraminidase enzyme, NEU3, is known to cleave sialic acid from ganglioside substrates. However, the biological effects of this cleavage are not clearly understood. This thesis describes our studies of the regulation of β1-integrins by neuraminidase enzymes, and the role of gangliosides in this process. In cell migration assays, NEU3 treatment of cells increased the rate of migration in HeLa. In contrast, NEU4 increased the rate of cell migration. Using a cell line that over-expressed a fluorescent fusion protein of NEU3, we were able to observe that the enzyme colocalized with β1-integrin in cells. These results strengthen the biochemical link between NEU3 and integrin receptors, and suggest that glycolipids may play a more direct role in the regulation of cellular migration.

ACKNOWLEDGEMENTS

I would like to thank all those who assisted me in my studies. First and foremost, I would like to thank my supervisor Dr. Christopher Cairo for his support in my Masters studies. His professional and academic guidance were helpful in my research and in preparing me for my future scientific career. I also want to thank Dr. Simonetta Sipione for her support in my research for cell studies. I would like to thank all the Cairo group members, especially Dr. Carson Li, Cecilia Zou, Blake Zheng and Amgad Albohy for teaching me most of the techniques used in my research and their help when I had difficulties in my studies.

Finally I want to thank my parents, my granduncle Dr. Fu Shiang Chia and my friends, for their enormous support.

TABLE OF CONTENTS

LIST OF TABLES

LIST OF FIGURES

LIST OF ABBREVIATIONS

4MU-NANA	2'-(4-methylumbelliferyl)-alpha-D-N-acetylneuraminic acid
CTB	Cholera toxin B
Cy5	Cyanine 5
Cyto D	Cytochalasin D
DANA	2-deoxy-2,3-didehydro-N-acetylneuraminic acid
DIC	Differential interference contrast
$\mathbf{D_{Macro}}$	Dynamic Macro
DMEM	Dulbecco's Modified Eagle Medium
$\mathbf{D_{micro}}$	Dynamic micro
FITC	Fluorescein isothiocyanate
FN	Fibronectin
G148	Geneticin
GFP	Green fluorescent protein
hNEU	human Neuraminidase
HPTLC	High performance thin layer chromatography
$\mathbf{IC_{50}}$	Half maximal inhibitory concentration
LacCer	Lactosylcerimide
MMP-9	Matrix metallopeptidase 9

MSD	Meso scale discovery
PBS	Phosphate buffered saline
PFA	Paraformaldehyde
pfNEU	Clostridium perfringens neuraminidase
PMA	Phorbol 12-myrisate 13-acetate
R_f	Retardation factor
SDT	Single dye tracking
ST6Gal-1	β-galactosamide-α-2-6-sialytransferase-1
TIRF	Total internal reflection fluorescence microscope
TLC	Thin layer chromatography
TQ	Thymoquinone
TRITC	Tetramethyl Rhodamine isothiocyanate

Chapter 1: The Role of Plasma membrane gangliosides in cell migration

1.1 The plasma membrane of mammalian cells

The plasma membrane is a dynamic structure that acts as a structural barrier between cellular contents and the extracellular environment (*1-4*). The membrane also allows selective passage of specific molecules, allowing it to act as a selectively permeable film. Another important function of the membrane is signal transduction, which is the transfer of information between the extracellular environment and the intracellular compartment. These mechanisms allow the membrane to play crucial roles in many cellular functions including immune response, recognition, protection, and signal transduction.

As the outer surface of the cell, the membrane interacts with components of the extracellular matrix (ECM). The ECM is a milieu of biomolecules, including proteins and glycoproteins, which can be tissue specific. Interactions between the ECM and membrane receptors regulate behavior of cells in differentiation, migration and proliferation. Adherent cells are often anchored through ECM-receptor interactions (*5, 6*). Increasing stiffness of the ECM is known to up-regulate cancer cell proliferation, and the control of proliferation from attachment occurs in cell detachment, cell cleavage, and the cell cycle (e.g. G1-phase) (*7, 8*). Interaction between the cell and the ECM is crucial for cell invasion and migration, and evidence shows that varying the membrane-ECM

interactions can change the type of cell migration, for example, from a mesenchymal to amoebic model (*6*).

The cell membrane can regulate the passage of certain molecules using different mechanisms. Examples include transmembrane protein channels, passive osmosis, and endo- or exocytosis. Recent studies have shown that cancer cells take up more iron than normal cells leading to an upregulation of cell growth (*9, 10*). Another important element is potassium, which can be transported by transmembrane potassium channels. These channels are an important therapeutic target for diseases such as diabetes, migraines, and hypertension. Other evidence shows that G protein-coupled inwardly rectifying K^+ channels (GIRKs) play an important role in lung cancer proliferation (*11*). Larger molecules are transported by endo- and exocytosis through the formation of vesicles, a process important in many cell-cell interactions (*12*). Studies have suggested that tumor cells may transfer DNA or RNA to other cells which may elicit an immune response (*13, 14*).

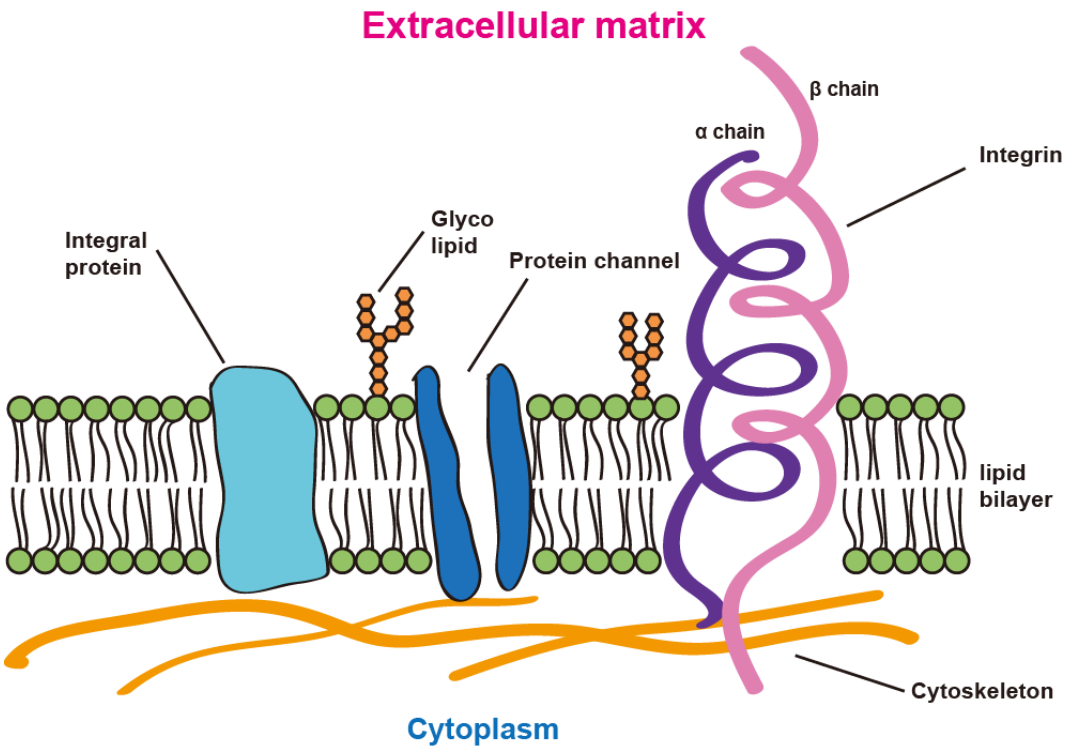

Figure 1.1 Structure of mammalian plasma membrane.

1.1.1 Structure of the cell membrane

The major structural components of the plasma membrane are phospholipids and glycolipids. Individual lipids assemble through non-covalent interactions into a bilayer structure consisting of two leaflets (an outer and inner leaflet) with the hydrophobic tails of the lipids oriented toward each other. Embedded within the membrane are transmembrane proteins which may have structural or functional roles (**Figure 1.1**) (*15*). Many different lipids are found in the plasma membrane, more than 1000 different lipids have been identified in the plasma membrane of mammalian cells (*16*). These structures are usually organized into three main categories: cholesterol, glycerol lipids and ceramide

sphingolipids. The specific lipid composition may vary in different cell lines. The membrane has been equated to a 'lipid sea,' with lipids and proteins flowing in membrane, as proposed in the fluid mosaic model.(*17*) Detailed studies of the diffusion of membrane lipids have found that lipids and components of the membrane do not diffuse freely in the membrane, instead they are often found to follow anomalous diffusion (*18*). This model of diffusion is a result of cytoskeletal contact with the membrane components which restricts the movement of lipids and receptors (*19*). This model better explains movent of membrane proteins and lipids than the mosaic model (*20*).

Cells can control the specific composition of lipids and their subcellular location (*21*). Proteins are often an important constituent of the membrane. Membrane proteins are classified by their interaction with the membrane, and can include membrane-associated proteins or transmembrane proteins. the subject of this thesis will be the interaction of membrane glycolipids with integrins. Integrins are transmembrane proteins which mediate cellular adhesion (*22*).

1.2 Membrane gangliosides and their function

Membrane gangliosides and glycolipids compose a small portion of the lipid bilayer (c.a. <10%) (*23*). Glycolipids are lipids which contain a glycan or oligosaccaride chain. Gangliosides are glycolipids which contain at least one

sialic acid residue (*24*). In mammalian cells, glycolipids are primarily composed of sphingolipids. Gangliosides derive their name from their discovery in bovine brain tissue (*25*). Currently, more than 180 gangliosides have been found in vertebrate cells (*26*). Common structures include GM1, GM3, GD1a and GT1b (*26*, *27*) (**Figure 1.2**). The ganglioside composition of tissues may vary, for example brain tissue often contains glycolipids, such as GD3 and GM3 early in development, while more complex gangliosides (e.g. GT1b and GM1) increase at later times (*28*). This observation suggests that biosynthetic pathways of gangliosides are tightly regulated in the cell. Most gangliosides are derived from LacCer (lactosylceramide), with some exceptions, such as GM4 (derived from GalCer) (*26*).

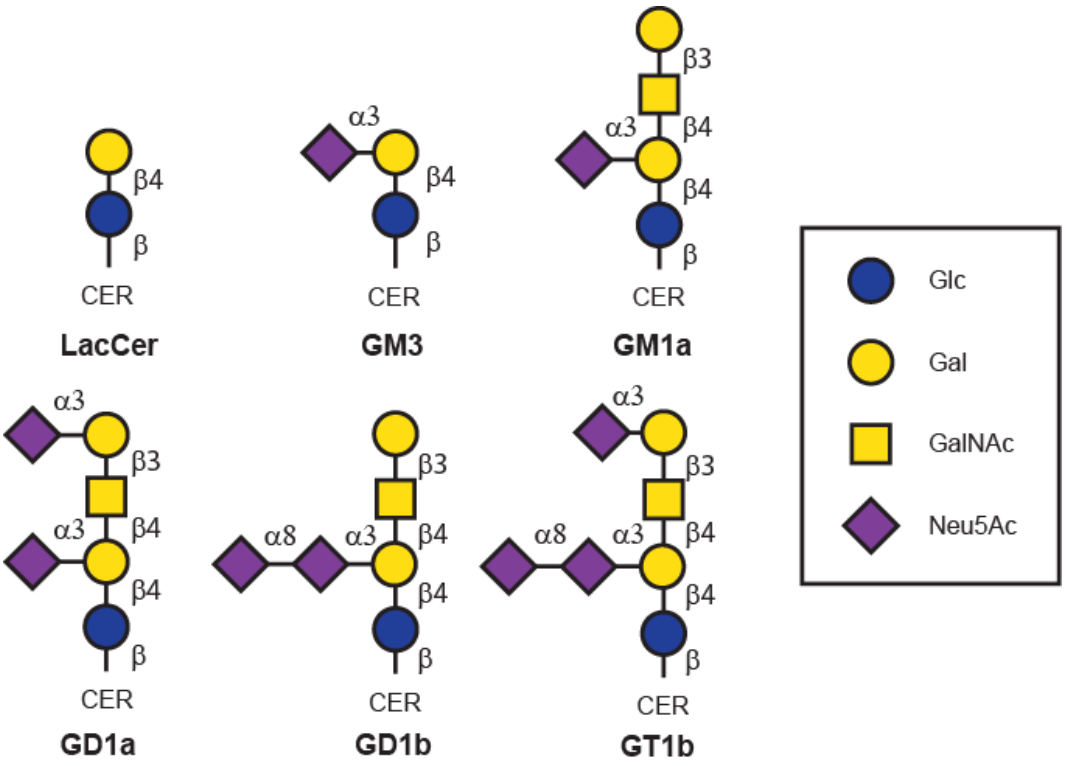

Figure 1.2 Structure of gangliosides LacCer, GM1a, GM3, GD1a, GD1b and GT1b. Glycan structures are represented using the symbolic nomenclature recommended by the CFG (*29*).

Previous studies have suggested that components of the membrane can associate, resulting in the formation of microdomains (*30*). These membrane microdomains have been found to be enriched in gangliosides, and are proposed to play roles in the regulation of cell adhesion, signal transduction and cell-cell recognition (*31*). Membrane microdomains have been defined by their stability in specific detergents (detergent-resistant microdomains, DRM) (*32*). Lack or excess of specific gangliosides can result in disease, especially in neural

systems which have an abundance of gangliosides. The lacking of GM3 will lead to deafness in mice, and recent studies suggested that a concentration change of gangliosides was found in Alzheimer's patients (*33, 34*). Furthermore, alteration of gangliosides occurs not only in the neurons system, but also in other diseases, such as type 2 diabetes where it is known that GM3 content changes in cells(*35*).

Ganglioside GM3 is the simplest ganglioside found in cell membranes, and it is a precursor of other complex gangliosides. GM3 is known to be involved in cell migration, proliferation, adhesion and other cell functions (*36-38*). Research has found that GM3 has an influence on many membrane receptors. GM3 has a proposed effect on the epidermal growth factor receptor (EGFR), which may involve a physical interaction between EGFR and the β1 integrin. GM3 concentration in the cell membrane appears to inhibit tyrosine phosphorylation on EGFR (*39*). Furthermore, GM3 blocks EGFR phosphorylation at the Tyr-1173 residue leading to an inhibition of PI3K/Akt pathways and a down-regulation of cell motility (*40*).

The ganglioside, GM1, is known to regulate cell functions. Examples include modulation of galectin-1 activity due to GM1 expression, which leads to inhibition of cell growth. GM1 is known to be colocalized with galectin-1 on cell membranes (*41, 42*). Other observations show that GM1 can affect T cells by altering galectin-1 secretion in regulatory T cells (*43, 44*). GM1 can also regulate

cells through direct binding to fibroblast growth factor 2 (FGF2) in the presence of heparin sulfate proteoglycans, leading to inhibition of its function, and suppression of angiogenesis (*45*).

In the membrane, it is likely that the presence of several gangliosides result in more complex interactions with membrane receptors. GM2 can inhibit cell motility through suppression of the hepatocyte growth factor (HGF), and its inhibition can be enhanced by addition of nanomolar quantities of GM3. These observations were suggested to indicate the formation of a complex with GM2, GM3 and CD82 in HCV29 cells (*38, 46*). GD1a, a ganglioside found on many tumor cell membranes, is shed from vascular cells, inducing angiogenesis. Recent work has reported that GM3 can inhibit angiogenesis, thus opposing the effect of GD1a (*47*).

1.2.1 The lipid raft hypothesis

The glycosphingolipids of the cell membrane are known to form complexes with certain membrane proteins which are resistant to membrane extraction by detergents. These detergent-resistant microdomains (DRM) have been proposed to exist within the plasma membrane, and have also been termed "lipid rafts" (*48*). These microdomains are proposed to participate in many regulatory pathways in cells (*49-51*). Previous publications have suggested that lipid rafts influence the clustering of G-proteins and other lipid domains (*52*).

Several models of lipid raft structure have been proposed, they are generally thought to include sphingolipids and cholesterol-based lipids. Lipid rafts can be defined by their stability in the presence of specific surfactants which disrupt other lipids of the bilayer. For example, Triton X-100 has been used in study of the model in lipid mixtures (*48*). Recently, a more complex and detailed model was put forward which includes protein-protein as well as protein-lipid interactions. These interactions generate a large platform in the cell membrane, which is suggested to dynamically regulate interaction between membrane proteins and the cytoskeleton (*53*).

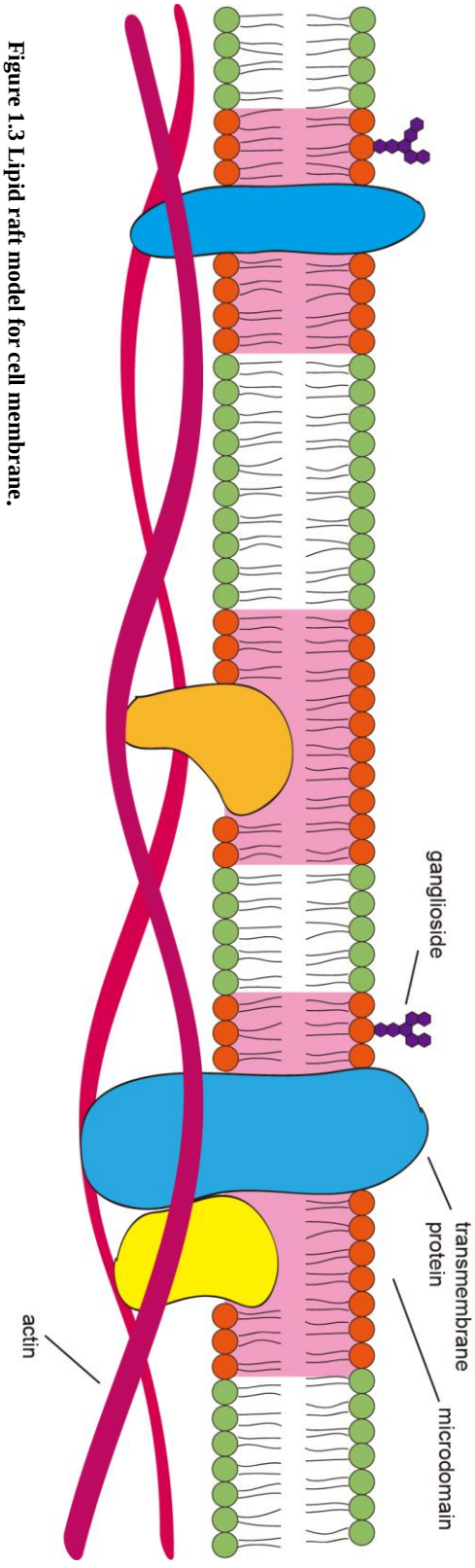

Figure 1.3 Lipid raft model for cell membrane.

1.2.2 Human neuraminidase enzymes regulate cell function.

As discussed above, many glycolipids and glycoproteins contain sialic acid residues, and sialylation is altered in disease states, including cancer (*54*). Previous studies have confirmed that tumor cells treated with bacterial sialidase have reduced cell growth and adhesion, yet the mechanisms of these effects are currently unclear (*55*). Four isoenzymes of human sialidases are known: NEU1, NEU2, NEU3 and NEU4. Evidence suggests that these enzymes may have crucial roles in cell biology. The subcellular localization of the enzymes varies within the cell, and the enzyme substrates include both glycolipids and glycoproteins (**Table 1.1**) (*56, 57*). The NEU enzymes found on the plasma membrane include NEU1, NEU3, and NEU4; thus these isoenzymes are more likely to be involved in regulation of membrane glycolipids (*58, 59*).

NEU3 is a membrane-associated neuraminidase, and is the only isoenzyme known to cleave gangliosides specifically (*58*). Evidence has suggested that NEU3 cleaves gangliosides, such as GD1a, at cell-cell contacts; thus, the enzyme may regulate gangliosides on neighboring cells (*60*). Kakugawa *et al.* tested NEU3 expression in human colon cancer cells by competitive reverse transcription–PCR (RT-PCR) and found an increase of sialidase activity compared with normal tissue. The enzyme was also found to decrease cancer cell

apoptosis. Cell death could be suppressed by an increase of NEU3 expression (*61*).

Enzyme	Location	Representative Substrates	Optimal pH
NEU1	Lysosome, Membrane	Oligosaccharides 4MU-Neu5Ac	4.4-4.6
NEU2	Cytosol	Glycolipid Ganglioside Oligosaccharide 4MU-Neu5Ac	5.0-6.0
NEU3	Lysosome, Membrane	Ganglioside	4.6-4.8
NEU4	Lysosome, Membrane, Mitochondria	Glycolipid Ganglioside Oligosaccharide 4MU-Neu5Ac	4.4-4.5

Table 1.1 Human sialidases and their location, substrates and optimal pH (*62*).

Other observations in transfected cells have suggested that NEU3 regulates cell adhesion. Compared with control cells, cells which overexpressed NEU3 showed increased adhesion to laminins, and decreased adhesion to other ECM components such as fibronectin and collagen. These findings suggested that NEU3 activates adhesion receptors for laminins via desialylation of glycolipids (*63*).

NEU4 has broader substrate specificity than NEU3, and is known to modify glycoprotein, oligosaccharide and glycolipid targets (*59*). Down-regulation of NEU4 by siRNA in cancer cells resulted in an increase of NEU3 expression, which suggested interaction between these two enzymes in cells (*61*). NEU4 induces mucosal cell apoptosis and inhibits cell invasion and migration. This difference in function may be related to the differences in enzyme substrate specificity between NEU3 and NEU4. NEU4 is known to modify glycoproteins, similar to NEU1 (*64*). To date, no glycoprotein substrates have been reported for NEU3.

1.3 Integrins

Integrins are a large family of transmembrane proteins that play important roles in cell adhesion and signal transduction (*65, 66*). In total, there are 24 different integrins found in humans. Integrin receptors are noncovalent

heterodimers, composed of an α- and β-subunit. There are 18 α and 8 β subunits known, individual subunits can have more than one combination (*67*). Previous work has found that knocking out certain integrin subunits in mice will cause distinct phenotypes. In 2002, Hynes and coworkers (*68*) published an integrin review and summarized all phenotypes known from integrin knock outs. For example, silencing the β6 integrin can cause inflammation, while knockout of the αL subunit results in leukocyte functional defections (*68*). Even though a cell may have various integrins on the membrane, they may not all be active at a given time. A good example is αIIbβ3, which is abundant on the surface of platelets, but it is inactive in most circumstances (*69*). The activation of αIIbβ3 can make platelets bind to ECM and fibrinogen in plasma, preventing blood loss from wounds. Improper activation of the same integrin will cause platelet aggregation in blood vessels leading to thrombosis (*70*).

Integrins can transmit signals in two directions through the plasma membrane — usually termed as "inside-out" and "outside-in" processes (*71*). Integrin signaling is known to regulate functions including cell migration, proliferation, angiogenesis, and apoptosis (*72-75*). Intracellular signals can cause actin polymerization, driving the cytoskeleton in the direction of cell migration. Integrin signaling can alter the binding affinity between integrin and ECM (*76*). Meanwhile, the binding between an integrin and the ECM can act as a feedback

signal to actin, resulting in cytoskeletal changes (*77*).

In the plasma membrane, integrins may interact with other receptors. One example is the matrix metalloproteases (MMPs). MMPs can form a complex with the αMβ2 integrin. This interaction is through the β2 subunit, and can be broken or inhibited by peptides (*78*). Integrins are also known to bind with gangliosides. Recent studies have suggested that GT1b regulates the α5β1 integrin, decreasing cell adhesion and migration (*79*).

1.3.1 The α4 and α5 integrins

The α4 and α5 integrin chains both associate with the β1 subunit. The resulting complexes (α4β1 and α5β1) are involved in cell adhesion in a number of cell types, and bind to fibronectin (FN) in the ECM. The α5β1 integrin was the first integrin to be isolated, and is considered the prototypical integrin receptor for FN (*80, 81*). Recent studies have suggested that the α4 integrin can decrease cell migration through inhibition of the α5 and αV integrins. Stimulation of the α4 integrin up-regulates α5 and αV, leading to a net increase of cell migration. Furthermore, blocking any one of the α4, α5 or αV integrins can increase expression of the other two (*82*). Many cancer cells have low expression of α4β1 on the cell surface due to the increased expression of an oncogene (*83*). This suggests that the loss of the α4β1 integrin could be an important phenomenon in cancer cell development and invasion(*84*). Recent studies have shown that

integrin α5β1 levels are regulated by syntaxin 6, which can cause angiogenesis. Inhibition of syntaxin 6 will decrease integrin α5β1 expression (*85*).

1.4 Hypothesis and project objectives

As discussed above, neuraminidase enzymes may play important roles in regulation of membrane composition. In turn, adhesion receptors are regulated by a variety of signals, including the presence of specific glycolipids. The precise mechanisms that relate membrane composition to receptor function are currently unclear.

Recent studies have linked sialylation at the cell membrane to tumor formation (*86*). As an example, ST6Gal-I, a glycosyltransferase, can add sialic acid to glycoproteins with an α2-6 linkage. Bellis *et al*. reported that increased expression of ST6Gal-I up-regulated α2-6 sialylation of the β1 integrin (*87, 88*). The suppression of ST6Gal-I by shRNA decreased cell migration and adhesion through the β1-integrin ligand, collagen I (*89*). Human neuraminidases have an opposing biochemical role to sialyltransferases. It can hydrolyze and cleave sialic acid from glycoproteins and glycolipids. Miyagi *et al.* suggested that NEU3 activation could enhance Rac-1 signaling and increase cell migration in human tumor cells (*61, 89*) . However, another human neuraminidase, NEU4, has been shown to inhibit cell invasion and migration. NEU4 is known to modify

glycoproteins as well as glycolipids (*64*). Together, these observations suggest that sialylation is important to the function of integrins, and that pathways which alter glycosylation may be critical to regulation of cell adhesion.

We hypothesized that human neuraminidase enzymes which could alter glycolipid composition of the membrane, NEU3 and NEU4, could act as regulators of cell migration. To test this hypothesis, we developed an assay to quantitate changes in cell migration through β1-integrin–fibronectin mediated adhesion. Using this assay, we tested the effect of exogenously added NEU3 and NEU4 on the rate of cell migration. Additionally, we tested inhibitors of the enzymes and found that both the enzymes and non-specific inhibitors have large effects on cell migration. To explore the mechanism of this effect, we also characterized the subcellular localization of gangliosides, integrin, and the enzyme NEU3 in human epithelial cells. These studies reveal an important role for the human neuraminidase enzymes in regulating integrin function.

1.5 References

1. Cossetti, C., Smith, J. A., Iraci, N., Leonardi, T., Alfaro-Cervello, C., and Pluchino, S. (2012) Extracellular membrane vesicles and immune regulation in the brain, *Frontiers in physiology 3*, 117.

2. Vorup-Jensen, T. (2012) On the roles of polyvalent binding in immune recognition: perspectives in the nanoscience of immunology and the immune response to nanomedicines, *Advanced drug delivery reviews 64*, 1759-1781.

3. Guagliardo, N. A., Yao, J., Hu, C., and Barrett, P. Q. (2012) Minireview: aldosterone biosynthesis: electrically gated for our protection, *Endocrinology 153*, 3579-3586.

4. Kuroki, K., Furukawa, A., and Maenaka, K. (2012) Molecular recognition of paired receptors in the immune system, *Frontiers in microbiology 3*, 429.

5. van Dijk, M., Goransson, S. A., and Stromblad, S. (2013) Cell to extracellular matrix interactions and their reciprocal nature in cancer, *Experimental cell research*.

6. Friedl, P., and Wolf, K. (2010) Plasticity of cell migration: a

multiscale tuning model, *The Journal of cell biology 188*, 11-19.

7. Lu, P., Weaver, V. M., and Werb, Z. (2012) The extracellular matrix: a dynamic niche in cancer progression, *The Journal of cell biology 196*, 395-406.

8. Assoian, R. K., and Klein, E. A. (2008) Growth control by intracellular tension and extracellular stiffness, *Trends in cell biology 18*, 347-352.

9. Kwok, J. C., and Richardson, D. R. (2002) The iron metabolism of neoplastic cells: alterations that facilitate proliferation?, *Critical reviews in oncology/hematology 42*, 65-78.

10. Pahl, P. M., and Horwitz, L. D. (2005) Cell permeable iron chelators as potential cancer chemotherapeutic agents, *Cancer investigation 23*, 683-691.

11. Wischmeyer, E., Lentes, K. U., and Karschin, A. (1995) Physiological and molecular characterization of an IRK-type inward rectifier K+ channel in a tumour mast cell line, *Pflugers Archiv : European journal of physiology 429*, 809-819.

12. Gutierrez-Vazquez, C., Villarroya-Beltri, C., Mittelbrunn, M., and Sanchez-Madrid, F. (2013) Transfer of extracellular vesicles during immune cell-cell interactions, *Immunological reviews 251*, 125-142.

13. Belting, M., and Wittrup, A. (2008) Nanotubes, exosomes, and nucleic acid-binding peptides provide novel mechanisms of intercellular

communication in eukaryotic cells: implications in health and disease, *The Journal of cell biology 183*, 1187-1191.

14. Balaj, L., Lessard, R., Dai, L., Cho, Y. J., Pomeroy, S. L., Breakefield, X. O., and Skog, J. (2011) Tumour microvesicles contain retrotransposon elements and amplified oncogene sequences, *Nature communications 2*, 180.

15. Escriba, P. V., Ozaita, A., Ribas, C., Miralles, A., Fodor, E., Farkas, T., and Garcia-Sevilla, J. A. (1997) Role of lipid polymorphism in G protein-membrane interactions: nonlamellar-prone phospholipids and peripheral protein binding to membranes, *Proceedings of the National Academy of Sciences of the United States of America 94*, 11375-11380.

16. van Meer, G., Voelker, D. R., and Feigenson, G. W. (2008) Membrane lipids: where they are and how they behave, *Nature reviews. Molecular cell biology 9*, 112-124.

17. Singer, S. J., and Nicolson, G. L. (1972) The fluid mosaic model of the structure of cell membranes, *Science 175*, 720-731.

18. Regner, B. M., Vucinic, D., Domnisoru, C., Bartol, T. M., Hetzer, M. W., Tartakovsky, D. M., and Sejnowski, T. J. (2013) Anomalous diffusion of single particles in cytoplasm, *Biophysical journal 104*, 1652-1660.

19. Saxton, M. J. (1994) Anomalous diffusion due to obstacles: a Monte

Carlo study, *Biophysical journal 66*, 394-401.

20. Burrage, K., Hancock, J., Leier, A., and Nicolau, D. V., Jr. (2007) Modelling and simulation techniques for membrane biology, *Briefings in bioinformatics 8*, 234-244.

21. Daleke, D. L. (2003) Regulation of transbilayer plasma membrane phospholipid asymmetry, *Journal of lipid research 44*, 233-242.

22. Goni, F. M. (2002) Non-permanent proteins in membranes: when proteins come as visitors (Review), *Molecular membrane biology 19*, 237-245.

23. Cantu, L., Del Favero, E., Sonnino, S., and Prinetti, A. (2011) Gangliosides and the multiscale modulation of membrane structure, *Chemistry and physics of lipids 164*, 796-810.

24. Feizi, T. (1985) Demonstration by monoclonal antibodies that carbohydrate structures of glycoproteins and glycolipids are onco-developmental antigens, *Nature 314*, 53-57.

25. Zeller, C. B., and Marchase, R. B. (1992) Gangliosides as modulators of cell function, *The American journal of physiology 262*, C1341-1355.

26. Yu, R. K., Tsai, Y. T., Ariga, T., and Yanagisawa, M. (2011) Structures, biosynthesis, and functions of gangliosides--an overview, *Journal of oleo science 60*, 537-544.

27. Sonnino, S., Mauri, L., Chigorno, V., and Prinetti, A. (2007) Gangliosides as components of lipid membrane domains, *Glycobiology 17*, 1R-13R.

28. Ishii, A., Ikeda, T., Hitoshi, S., Fujimoto, I., Torii, T., Sakuma, K., Nakakita, S., Hase, S., and Ikenaka, K. (2007) Developmental changes in the expression of glycogenes and the content of N-glycans in the mouse cerebral cortex, *Glycobiology 17*, 261-276.

29. http://www.functionalglycomics.org/static/consortium/Nomenclature.shtml.

30. Tsukahara, S., Kamiya, Y., and Fujiwara, T. (2009) In situ measurements of emission transition dipole moment of individual ordered microdomain of diprotonated tetraphenylporphine aggregate formed at dodecane/aqueous H2SO4 interface, *Analytical and bioanalytical chemistry 395*, 1047-1053.

31. Hakomori, S., Handa, K., Iwabuchi, K., Yamamura, S., and Prinetti, A. (1998) New insights in glycosphingolipid function: "glycosignaling domain," a cell surface assembly of glycosphingolipids with signal transducer molecules,involved in cell adhesion coupled with signaling, *Glycobiology 8*, xi-xix.

32. Nishiyama, A., Isobe, H., Iwao, Y., Takano, T., Hung, W. C., Taneike, I., Nakagawa, S., Dohmae, S., Iwakura, N., and Yamamoto, T. (2012)

Accumulation of staphylococcal Panton-Valentine leukocidin in the detergent-resistant membrane microdomains on the target cells is essential for its cytotoxicity, *FEMS immunology and medical microbiology 66*, 343-352.

33. van Echten-Deckert, G., and Walter, J. (2012) Sphingolipids: critical players in Alzheimer's disease, *Progress in lipid research 51*, 378-393.

34. Yoshikawa, M., Go, S., Takasaki, K., Kakazu, Y., Ohashi, M., Nagafuku, M., Kabayama, K., Sekimoto, J., Suzuki, S., Takaiwa, K., Kimitsuki, T., Matsumoto, N., Komune, S., Kamei, D., Saito, M., Fujiwara, M., Iwasaki, K., and Inokuchi, J. (2009) Mice lacking ganglioside GM3 synthase exhibit complete hearing loss due to selective degeneration of the organ of Corti, *Proceedings of the National Academy of Sciences of the United States of America 106*, 9483-9488.

35. Inokuchi, J. (2010) Membrane microdomains and insulin resistance, *FEBS letters 584*, 1864-1871.

36. Prokazova, N. V., Samovilova, N. N., Gracheva, E. V., and Golovanova, N. K. (2009) Ganglioside GM3 and its biological functions, *Biochemistry. Biokhimiia 74*, 235-249.

37. Toledo, M. S., Suzuki, E., Handa, K., and Hakomori, S. (2004) Cell growth regulation through GM3-enriched microdomain (glycosynapse) in human lung embryonal fibroblast WI38 and its oncogenic transformant VA13, *The Journal*

of biological chemistry 279, 34655-34664.

38. Todeschini, A. R., Dos Santos, J. N., Handa, K., and Hakomori, S. I. (2008) Ganglioside GM2/GM3 complex affixed on silica nanospheres strongly inhibits cell motility through CD82/cMet-mediated pathway, *Proceedings of the National Academy of Sciences of the United States of America 105*, 1925-1930.

39. Wang, X. Q., Sun, P., and Paller, A. S. (2003) Ganglioside GM3 blocks the activation of epidermal growth factor receptor induced by integrin at specific tyrosine sites, *The Journal of biological chemistry 278*, 48770-48778.

40. Huang, X., Li, Y., Zhang, J., Xu, Y., Tian, Y., and Ma, K. (2013) Ganglioside GM3 inhibits murine ascites hepatoma cell motility and migration in vitro through inhibition of phosphorylation of EGFR at specific tyrosine sites and PI3K/AKT signaling pathway, *Journal of cellular biochemistry*.

41. Kopitz, J., Bergmann, M., and Gabius, H. J. (2010) How adhesion/growth-regulatory galectins-1 and -3 attain cell specificity: case study defining their target on neuroblastoma cells (SK-N-MC) and marked affinity regulation by affecting microdomain organization of the membrane, *IUBMB life 62*, 624-628.

42. Fajka-Boja, R., Blasko, A., Kovacs-Solyom, F., Szebeni, G. J., Toth, G. K., and Monostori, E. (2008) Co-localization of galectin-1 with GM1

ganglioside in the course of its clathrin- and raft-dependent endocytosis, *Cellular and molecular life sciences : CMLS 65*, 2586-2593.

43. Brumeanu, T. D., Preda-Pais, A., Stoica, C., Bona, C., and Casares, S. (2007) Differential partitioning and trafficking of GM gangliosides and cholesterol-rich lipid rafts in thymic and splenic CD4 T cells, *Molecular immunology 44*, 530-540.

44. Wang, P., Zhang, J., Bian, H., Wu, P., Kuvelkar, R., Kung, T. T., Crawley, Y., Egan, R. W., and Billah, M. M. (2004) Induction of lysosomal and plasma membrane-bound sialidases in human T-cells via T-cell receptor, *The Biochemical journal 380*, 425-433.

45. Rusnati, M., Urbinati, C., Tanghetti, E., Dell'Era, P., Lortat-Jacob, H., and Presta, M. (2002) Cell membrane GM1 ganglioside is a functional coreceptor for fibroblast growth factor 2, *Proceedings of the National Academy of Sciences of the United States of America 99*, 4367-4372.

46. Todeschini, A. R., Dos Santos, J. N., Handa, K., and Hakomori, S. I. (2007) Ganglioside GM2-tetraspanin CD82 complex inhibits met and its cross-talk with integrins, providing a basis for control of cell motility through glycosynapse, *The Journal of biological chemistry 282*, 8123-8133.

47. Kanda, T., Yoshino, H., Ariga, T., Yamawaki, M., and Yu, R. K. (1994)

Glycosphingolipid antigens in cultured bovine brain microvascular endothelial cells: sulfoglucuronosyl paragloboside as a target of monoclonal IgM in demyelinative neuropathy [corrected], *The Journal of cell biology 126*, 235-246.

48. Edidin, M. (2003) The state of lipid rafts: from model membranes to cells, *Annual review of biophysics and biomolecular structure 32*, 257-283.

49. Benarroch, E. E. (2007) Lipid rafts, protein scaffolds, and neurologic disease, *Neurology 69*, 1635-1639.

50. Debruin, L. S., and Harauz, G. (2007) White matter rafting--membrane microdomains in myelin, *Neurochemical research 32*, 213-228.

51. Delacour, D., and Jacob, R. (2006) Apical protein transport, *Cellular and molecular life sciences : CMLS 63*, 2491-2505.

52. Funari, S. S., Prades, J., Escriba, P. V., and Barcelo, F. (2005) Farnesol and geranylgeraniol modulate the structural properties of phosphatidylethanolamine model membranes, *Molecular membrane biology 22*, 303-311.

53. Pike, L. J. (2006) Rafts defined: a report on the Keystone Symposium on Lipid Rafts and Cell Function, *Journal of lipid research 47*, 1597-1598.

54. Kim, Y. J., and Varki, A. (1997) Perspectives on the significance of altered glycosylation of glycoproteins in cancer, *Glycoconj J 14*, 569-576.

55. Hakomori, S. (1996) Tumor malignancy defined by aberrant glycosylation and sphingo(glyco)lipid metabolism, *Cancer research 56*, 5309-5318.

56. Miyagi, T., Wada, T., Yamaguchi, K., and Hata, K. (2004) Sialidase and malignancy: a minireview, *Glycoconj J 20*, 189-198.

57. Miyagi, T., Wada, T., Iwamatsu, A., Hata, K., Yoshikawa, Y., Tokuyama, S., and Sawada, M. (1999) Molecular cloning and characterization of a plasma membrane-associated sialidase specific for gangliosides, *The Journal of biological chemistry 274*, 5004-5011.

58. Monti, E., Bassi, M. T., Papini, N., Riboni, M., Manzoni, M., Venerando, B., Croci, G., Preti, A., Ballabio, A., Tettamanti, G., and Borsani, G. (2000) Identification and expression of NEU3, a novel human sialidase associated to the plasma membrane, *The Biochemical journal 349*, 343-351.

59. Monti, E., Bassi, M. T., Bresciani, R., Civini, S., Croci, G. L., Papini, N., Riboni, M., Zanchetti, G., Ballabio, A., Preti, A., Tettamanti, G., Venerando, B., and Borsani, G. (2004) Molecular cloning and characterization of NEU4, the fourth member of the human sialidase gene family, *Genomics 83*, 445-453.

60. Papini, N., Anastasia, L., Tringali, C., Croci, G., Bresciani, R., Yamaguchi, K., Miyagi, T., Preti, A., Prinetti, A., Prioni, S., Sonnino, S., Tettamanti,

G., Venerando, B., and Monti, E. (2004) The plasma membrane-associated sialidase MmNEU3 modifies the ganglioside pattern of adjacent cells supporting its involvement in cell-to-cell interactions, *The Journal of biological chemistry 279*, 16989-16995.

61. Kakugawa, Y., Wada, T., Yamaguchi, K., Yamanami, H., Ouchi, K., Sato, I., and Miyagi, T. (2002) Up-regulation of plasma membrane-associated ganglioside sialidase (Neu3) in human colon cancer and its involvement in apoptosis suppression, *Proceedings of the National Academy of Sciences of the United States of America 99*, 10718-10723.

62. Zhang, Y., Albohy, A., Zou, Y., Smutova, V., Pshezhetsky, A. V., and Cairo, C. W. (2013) Identification of selective inhibitors for human neuraminidase isoenzymes using C4,C7-modified 2-deoxy-2,3-didehydro-N-acetylneuraminic acid (DANA) analogues, *Journal of medicinal chemistry 56*, 2948-2958.

63. Kato, K., Shiga, K., Yamaguchi, K., Hata, K., Kobayashi, T., Miyazaki, K., Saijo, S., and Miyagi, T. (2006) Plasma-membrane-associated sialidase (NEU3) differentially regulates integrin-mediated cell proliferation through laminin- and fibronectin-derived signalling, *The Biochemical journal 394*, 647-656.

64. Yamanami, H., Shiozaki, K., Wada, T., Yamaguchi, K., Uemura, T.,

Kakugawa, Y., Hujiya, T., and Miyagi, T. (2007) Down-regulation of sialidase NEU4 may contribute to invasive properties of human colon cancers, *Cancer science 98*, 299-307.

65. Berrier, A. L., and Yamada, K. M. (2007) Cell-matrix adhesion, *Journal of cellular physiology 213*, 565-573.

66. Giancotti, F. G., and Ruoslahti, E. (1999) Integrin signaling, *Science 285*, 1028-1032.

67. Springer, T. A., and Wang, J. H. (2004) The three-dimensional structure of integrins and their ligands, and conformational regulation of cell adhesion, *Advances in protein chemistry 68*, 29-63.

68. Hynes, R. O. (2002) Integrins: bidirectional, allosteric signaling machines, *Cell 110*, 673-687.

69. Savage, B., Almus-Jacobs, F., and Ruggeri, Z. M. (1998) Specific synergy of multiple substrate-receptor interactions in platelet thrombus formation under flow, *Cell 94*, 657-666.

70. Tao, L., Zhang, Y., Xi, X., and Kieffer, N. (2010) Recent advances in the understanding of the molecular mechanisms regulating platelet integrin alphaIIbbeta3 activation, *Protein & cell 1*, 627-637.

71. Kim, M., Carman, C. V., and Springer, T. A. (2003) Bidirectional

transmembrane signaling by cytoplasmic domain separation in integrins, *Science 301*, 1720-1725.

72. Yamada, K. M. (1997) Integrin signaling, *Matrix biology : journal of the International Society for Matrix Biology 16*, 137-141.

73. Arnaout, M. A., Goodman, S. L., and Xiong, J. P. (2007) Structure and mechanics of integrin-based cell adhesion, *Current opinion in cell biology 19*, 495-507.

74. Mainiero, F., Murgia, C., Wary, K. K., Curatola, A. M., Pepe, A., Blumemberg, M., Westwick, J. K., Der, C. J., and Giancotti, F. G. (1997) The coupling of alpha6beta4 integrin to Ras-MAP kinase pathways mediated by Shc controls keratinocyte proliferation, *The EMBO journal 16*, 2365-2375.

75. Schwartz, M. A., and Ingber, D. E. (1994) Integrating with integrins, *Molecular biology of the cell 5*, 389-393.

76. Goldfinger, L. E., Tzima, E., Stockton, R., Kiosses, W. B., Kinbara, K., Tkachenko, E., Gutierrez, E., Groisman, A., Nguyen, P., Chien, S., and Ginsberg, M. H. (2008) Localized alpha4 integrin phosphorylation directs shear stress-induced endothelial cell alignment, *Circulation research 103*, 177-185.

77. Geiger, B., Bershadsky, A., Pankov, R., and Yamada, K. M. (2001) Transmembrane crosstalk between the extracellular matrix--cytoskeleton crosstalk,

Nature reviews. Molecular cell biology 2, 793-805.

78. Stefanidakis, M., Bjorklund, M., Ihanus, E., Gahmberg, C. G., and Koivunen, E. (2003) Identification of a negatively charged peptide motif within the catalytic domain of progelatinases that mediates binding to leukocyte beta 2 integrins, *The Journal of biological chemistry 278*, 34674-34684.

79. Paller, A. S., Arnsmeier, S. L., Chen, J. D., and Woodley, D. T. (1995) Ganglioside GT1b inhibits keratinocyte adhesion and migration on a fibronectin matrix, *J Invest Dermatol 105*, 237-242.

80. Mould, A. P., and Humphries, M. J. (1991) Identification of a novel recognition sequence for the integrin alpha 4 beta 1 in the COOH-terminal heparin-binding domain of fibronectin, *The EMBO journal 10*, 4089-4095.

81. Ruoslahti, E. (1994) Fibronectin and its alpha 5 beta 1 integrin receptor in malignancy, *Invasion & metastasis 14*, 87-97.

82. Zhang, Y., Lu, H., Dazin, P., and Kapila, Y. (2004) Functional differences between integrin alpha4 and integrins alpha5/alphav in modulating the motility of human oral squamous carcinoma cells in response to the V region and heparin-binding domain of fibronectin, *Experimental cell research 295*, 48-58.

83. Ignatoski, K. M., Maehama, T., Markwart, S. M., Dixon, J. E., Livant, D. L., and Ethier, S. P. (2000) ERBB-2 overexpression confers PI 3'

kinase-dependent invasion capacity on human mammary epithelial cells, *British journal of cancer 82*, 666-674.

84. Jia, Y., Zeng, Z. Z., Markwart, S. M., Rockwood, K. F., Ignatoski, K. M., Ethier, S. P., and Livant, D. L. (2004) Integrin fibronectin receptors in matrix metalloproteinase-1-dependent invasion by breast cancer and mammary epithelial cells, *Cancer research 64*, 8674-8681.

85. Tiwari, A., Jung, J. J., Inamdar, S. M., Brown, C. O., Goel, A., and Choudhury, A. (2011) Endothelial cell migration on fibronectin is regulated by syntaxin 6-mediated alpha5beta1 integrin recycling, *The Journal of biological chemistry 286*, 36749-36761.

86. Sproviero, D., Julien, S., Burford, B., Taylor-Papadimitriou, J., and Burchell, J. M. (2012) Cyclooxygenase-2 enzyme induces the expression of the alpha-2,3-sialyltransferase-3 (ST3Gal-I) in breast cancer, *The Journal of biological chemistry 287*, 44490-44497.

87. Seales, E. C., Jurado, G. A., Brunson, B. A., Wakefield, J. K., Frost, A. R., and Bellis, S. L. (2005) Hypersialylation of beta1 integrins, observed in colon adenocarcinoma, may contribute to cancer progression by up-regulating cell motility, *Cancer research 65*, 4645-4652.

88. Dalziel, M., Dall'Olio, F., Mungul, A., Piller, V., and Piller, F. (2004)

Ras oncogene induces beta-galactoside alpha2,6-sialyltransferase (ST6Gal I) via a RalGEF-mediated signal to its housekeeping promoter, *European journal of biochemistry / FEBS 271*, 3623-3634.

89. Shaikh, F. M., Seales, E. C., Clem, W. C., Hennessy, K. M., Zhuo, Y., and Bellis, S. L. (2008) Tumor cell migration and invasion are regulated by expression of variant integrin glycoforms, *Experimental cell research 314*, 2941-2950.

Chapter 2: The human neuraminidase, NEU3, regulates cell migration through alteration of the plasma membrane glycolipid composition[1, 2]

1. GFP transfected HeLa cells GFP-NEU3/A10 and NEU3-GFP/C2 were provided by L.C. Morales and S. Sipione, University of Alberta.

2. NEU3 and NEU4 were provided by Blake Zheng and Amgad Albohy, University of Alberta.

2.1 Introduction

The extracellular matrix (ECM) surrounds tissues and organs and interacts with epithelial cells. Adhesion receptors on the cell membrane bind with different ECM components, including glycoprotein fibronectin, laminins and collagen. They can stimulate cell migration, differentiate and cause cell metastasis. Cell adhesion by integrin receptors to the ECM, which are trans-membrane proteins, can regulate trans-membrane signals (*1*, *2*). Each integrin has an α chain and β chain and is regulated by trans-membrane signals (*3*). Specific cell types express different integrins; for example, lymphocytes express β2 integrins including the αLβ2, and αMβ2 integrins, while epithelial cells express α4β1 and α5β1 integrins (*4*, *5*).

Integrins are a major class of receptors for ECM on cells, and mechanisms which regulate these interactions are of interest in the design of new therapeutics. Previously, gangliosides (sialic acid-containing glycolipids) have been found to regulate the interaction of integrins with ECM. For example, GT1b is known to significantly reduce cell motility, spreading, and adhesion on FN (*6*, *7*). Some evidence suggests that GT1b binds with the α5 tail of the α5β1 integrin, leading to reduced binding of the integrin with FN (*8*). The ganglioside, GM3, has been found to affect cell migration and invasion by controlling expression of matrix

metalloproteinase-9 (MMP-9), an effect which is not FN-specific. MMP-9 interacts with α5β1 when epithelial cells adhere on fibronectin-surfaces. Increased presence of GM3 at the plasma membrane can reduce MMP-9 expression and activation, leading to inhibition of cell motility (*9*). Thus, the composition of membrane glycolipids may regulate the activity of integrins.

Glycolipid and glycoconjugates at the cell surface may vary in their sialic acid content, which is regulated by sialidase (also called neuraminidase) and sialyltransferase enzymes. Sialyltransferases are a large class of enzymes, most of which are found intracellularly (*10*). However, sialyltransferase activity has been found at the plasma membrane and extracellularly (*11-14*). It has long been known that malignant cells have increased amounts of sialic acid, and these changes have been proposed to alter cell behaviors including cell migration, differentiation and growth (*15*). Four human sialidase enzyme are currently known (*16*), several of which are found at the cell membrane (NEU1, NEU3, NEU4) (*17-19*). The NEU3 isoenzyme is known to be plasma membrane-associated, and specifically hydrolyzes the terminal sialic acid residues of gangliosides (*20*). This activity has been proposed to be important both *in-cis* (on the same membrane) and *in-trans* (on the membrane of an apposing cell) where it may regulate cell-cell interactions (*17*).

Our group has been working to develop specific inhibitors of the human

neuraminidase enzymes in order to investigate their role in cellular adhesion. The general sialidase inhibitor, 2-deoxy-2,3-didehydro-*N*-acetylneuraminic acid (DANA), has activity against both human, bacterial and viral neuraminidase enzymes (*21*). Previous studies have shown that DANA has micromolar IC_{50} against all isoforms of human neuraminidase enzymes (*22*). Magesh *et al.* have identified a NEU1-specific inhibitor with low micromolar activity (*23*). Our group has reported inhibitors with specificity for NEU2, NEU3 (*22*), and NEU4 (*24*) . However, neither DANA nor these newly identified compounds have been used to investigate the role of native sialidase enzymes in the regulation of integrin adhesion.

Cell migration can be observed using a variety of different assays. We consider these as separated into two groups: 2D migration assays and 3D migration assays (*25*). Cell scratch assays, also called wound healing assays, are widely applied in cell migration studies due their simplicity and low cost. The assay consists of a cultured monolayer of cells which is “wounded” by physical manipulation. The scratch results in a region of the monolayer with no cells, and the migration of new cells into the space is observed to quantitate the rate of cell motility. Cell migration can be measured by microscopy with software analysis (*26*). Currently, with the development of 3D optical microscopy technology, 3D cell migration assays are also improved (*27, 28*). 3D migration assays can mimic

the *in vivo* environment better than 2D migration (*25*).

In this chapter, we have investigated the role of human neuraminidase enzymes in the regulation of β2 integrin-regulated cell migration. We implemented a scratch assay to measure changes in the rate of cell migration under various conditions. Additionally, we employed immunofluorescence and single-dye tracking to observe changes in the subcellular location and diffusion of integrin receptors. To gain insight into the role of specific glycolipids in this process, we have used recombinant glycolipid processing enzymes (NEU3), neuraminidase inhibitors (DANA), and gangliosides (LacCer, GM1, GM3, GD1a, GD1b and GT1b).

2.2 Results

2.2.1 Determination of ganglioside composition by HPTLC

We studied the composition of cellular gangliosides using high performance thin layer chromatography (HPTLC). This method can be used to examine glycolipids extracted from cells, or for purified substrates (*29*).

Cellular gangliosides can be analyzed by HPTLC, which is a relatively simple and straightforward assay. In 1978, Susumo Ando *et al*. used HPTLC to determine and analyze gangliosides from brain (*30*). They extracted ganglioside mixtures from different species of brains and then separated them using TLC.

High-performance TLC uses a much thinner layer of silica for better separation than standard TLC; thus, providing an improved method for analysis of complex gangliosides.

2.2.2 Glycolipid composition of cells is altered by NEU3 treatment and inhibition.

In order to investigate the role of human neuraminidase enzymes in the regulation of glycolipid composition, we used an HPTLC assay. Cell extracts were first analyzed to determine the most abundant glycolipids. Each band was measured one time, and then a ratio of the intensity for LacCer was determined by dividing by that of GM3 (LacCer:GM3; asialo:sialo) (**Figure 2.2**). Measurements were performed only once, so no error analysis is shown. In both cell lines (HeLa and A549) examined, we found that the major gangliosides were analogs of LacCer and GM3, which likely vary in their fatty acid compositions (generating broader bands).

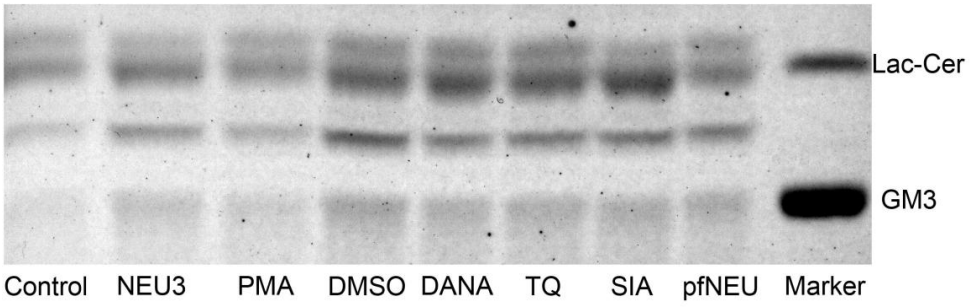

Figure 2.1 Extracted cellular gangliosides from HeLa analyzed by HPTLC. HeLa cells were treated with

same conditions used in the migration assay (see below) for 3 hours at 37 ℃ (5% CO_2), and then harvested. The suspension was washed with PBS twice and centrifuged. Gangliosides were extracted by 1:1 methanol and chloroform for 30 min, followed by centrifugation to remove any precipitates. The solution was dried by N_2 and then dissolved again in a small amount of 1:1 methanol and chloroform. The TLC plate was eluted with 1:2:1 acidic acid, *n*-butanol and 0.5% $CaCl_2$ (aq) and then stained with oricinol sulfuric acid stain. In order to keep the same number of cells in each sample, cells were counted and split into flasks at a concentration of $1x10^6$ cells mL^{-1}.

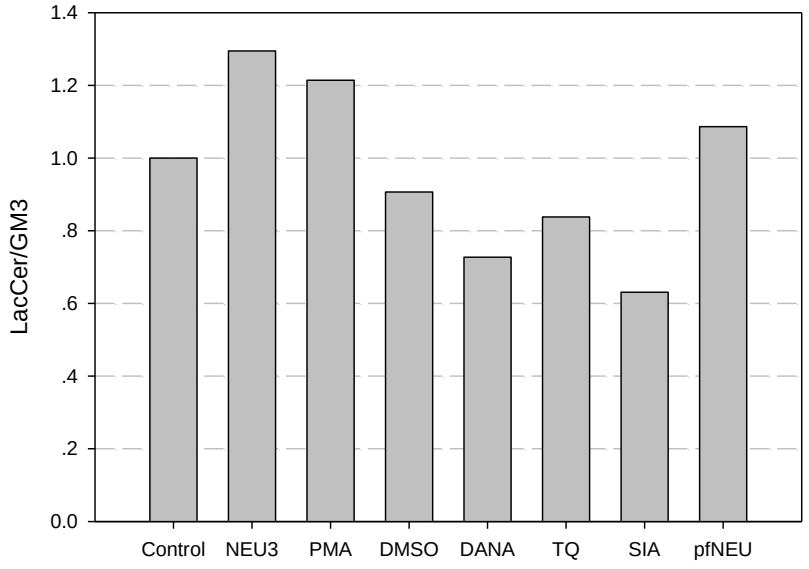

Figure 2.2 TLC analysis of glycolipids from HeLa. TLC plates were scanned and measured with Image J (*31*). Each band was tested once, and the normalized ratio of LacCer to GM3 was determined for each condition.

We then tested changes in glycolipid composition as a result of conditions known to alter integrin-mediated adhesion and migration in epithelial cells.

Activation of the protein kinase C pathway by phorbol esters, such as PMA, is known to increase cell adhesion and migration through the α5β1 integrin (*32*). In HeLa cells, we observed an increase in asialo glycolipids after PMA treatment. We also examined changes induced by treatment of cells with exogenous neuraminidase enzymes. In both cell lines, we observed that recombinant NEU3 and *Clostridium perfringens* NEU (*pf*NEU) increased the content of asialo glycolipids. Treatment of cells with sialic acid (SIA) increased the ratio of sialylated glycolipids. Treatment of cells with DANA, a non-specific inhibitor of human sialidase enzymes, resulted in a decrease in asialo lipids (**Figure 2.2**) (*33*). These results confirm that exogenous sialidase enzymes can alter the membrane glycolipid composition, and that inhibition of native sialidase enzymes has an opposite effect.

Previous reports have suggested that thymoquinone (TQ) can activate the human NEU4 enzyme (*34*), which is known to cleave both glycoproteins and glycolipids (*35*, *36*). We therefore tested whether treatment of cells with TQ would result in a detectable change in glycolipid composition. We found that TQ induced a decrease in the asialo:sialo lipid ratio in HeLa cells, consistent with an activation of the NEU4 enzyme.

We also extracted gangliosides from A549 cells (lung epithelia) under these conditions (see Appendix), which gave similar results.

2.2.3 Human NEU3 and NEU4 are α2,3 and α2,8 sialidases

The human NEU3 and NEU4 enzymes are known to use glycolipids as substrates (*15*). NEU3 is currently thought to target only glycolipids as substrates, while NEU4 cleaves both glycolipids and glycoproteins. NEU3 has been found to have an inherent preference for glycolipid substrates due to a hydrophobic binding pocket (*20*). In 2007, Azuma *et al.* (*37*) showed that NEU3 could change the level of gangliosides in human lymphoma cells (Jurkat), and that NEU3 expression was induced by etoposide. The expression of GM2, GM3 and GD3 increased on these cells, while GM1 and GD1a decreased when treated with etoposide. Previous results have also suggested that NEU3 can cleave α(2,3), α(2,8) (*38*) as well as α(2,6) (*39*) sialic acid linkages in gangliosides. However, these experiments are often conducted with unpurified enzymes. Our group uses purified recombinant enzymes of NEU2, NEU3, and NEU4 (*22*).

We decided to test the substrate specificity of recombinant NEU3 and NEU4 produced in our lab (*22, 40, 41*). Lipid substrates were incubated *in vitro* with the enzyme and the products were detected using an HPTLC assay. As previously discussed, it is difficult to obtain quantitative data from HPTLC; however, we employed the assay here to develop a qualitative understanding of the substrate specificity of these two enzymes. Substrates were used at identical concentrations and were incubated with enzyme samples at the same level of

activity (as calibrated using a 4MU-NANA assay (*41*)).

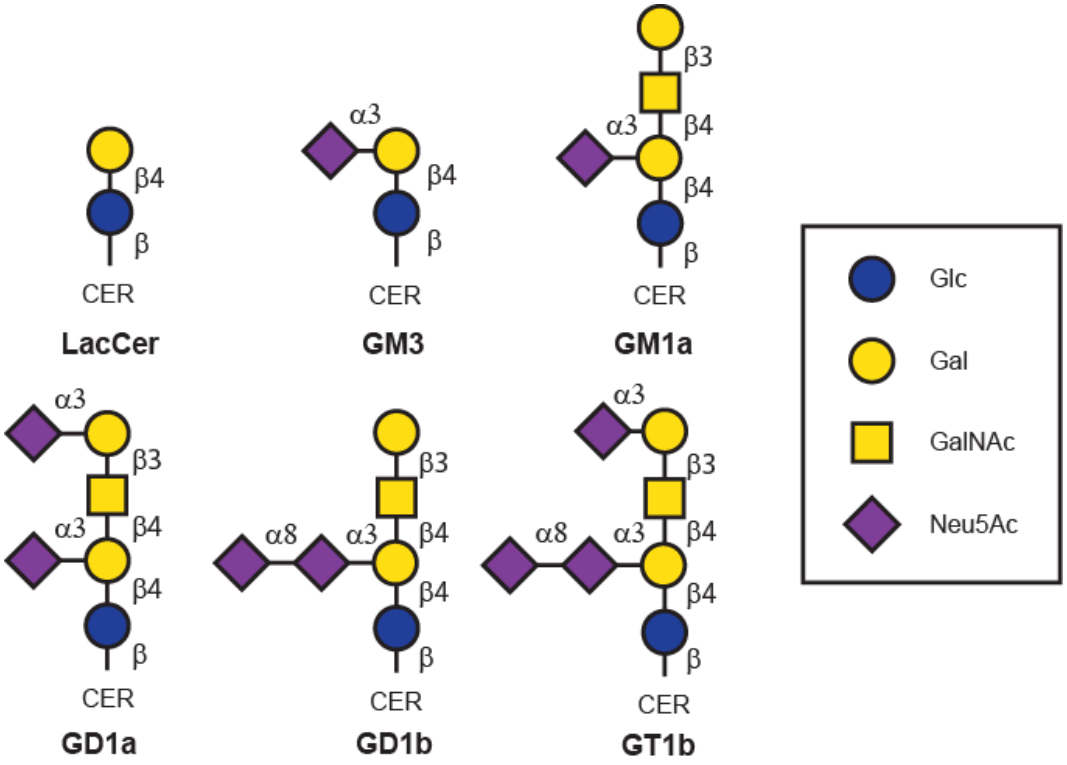

Figure 2.3 Structures of LacCer, GM1a, GM3, GD1a, GD1b and GT1b. Glycosidic linkages are indicated by the anomeric configuration (α or β) and the hydroxyl of the reducing end sugar.

We treated gangliosides GM1, GM3, GD1a, GD1b and GT1b under the same conditions with three neuraminidase enzymes: NEU3, NEU4 and *pf*NEU (*41*). Gangliosides were incubated with enzyme for 1 hour at 37 ℃ and then extracted and analyzed by TLC. An analysis of GM1 and GM3 is shown in **Figure 2.4** (TLC eluent: 1:2:1 acetic acid, *n*-butanol and 0.5% $CaCl_2$) which shows clear resolution between the starting materials and products. Samples required desalting using C18, otherwise bands were often not visible or were too

diffuse to detect (see Appendix). We proceeded to analyze all glycolipid substrates using this method.

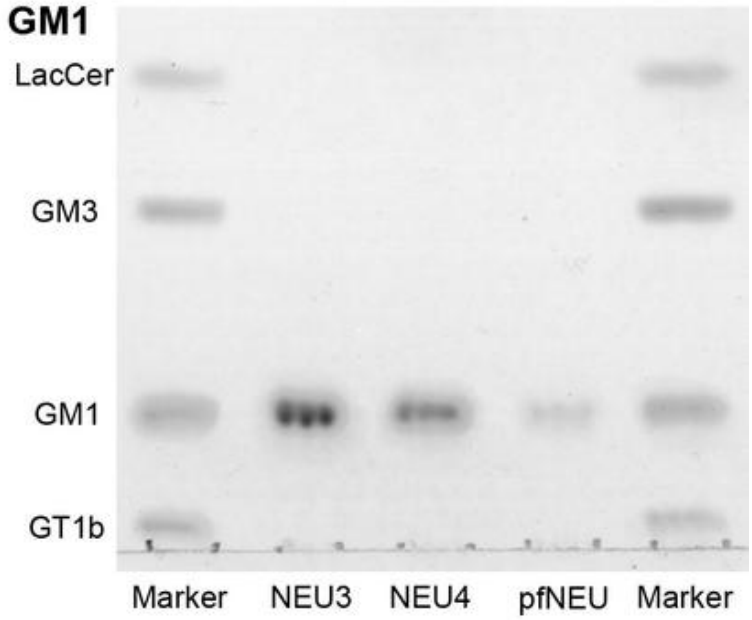

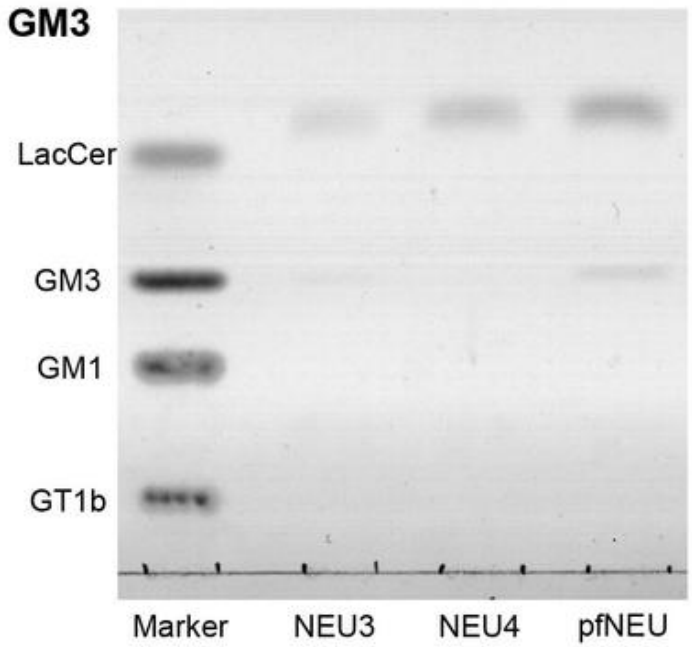

Figure 2.4 TLC analysis of of GM1 and GM3. GM1 or GM3 were treated with sialidase for 1 hour at 37 ℃ and then precipitated by 1:1 methanol and chloroform. The sample was centrifuged and the aqueous layer was removed. After drying, the organic layer was dissolved in 1:1 methanol and chloroform again and then run on TLC by 1:2:1 acetic acid/n-butanol/0.5% $CaCl_2$ (aq.). The plate was stained by orcinol sulfuric acid and heated for 30 min at 80 ℃.

The TLC results (**Figure 2.4**) suggested that NEU3, NEU4, and *pf*NEU are able to cleave the α2-3 linked sialic acid of GM3; however, none of the enzymes were able to cleave the same linkage in GM1 – not even the promiscuous *pf*NEU enzyme (*42*). We observed that GT1b, which contains both α2,3 and α2,8 linkages was a substrate for all three enzymes. A new band was observed for all three enzymes at the R_f of GM1, consistent with cleavage of the α2,8 linkage to form GM1. All three enzymes show a minor band between the R_f of GT1b and GM1, which we hypothesized could be either GD1a or GD1b.

To determine the identity of the band observed between GM1 and GT1b, we tested authentic samples of GD1a and GD1b. These two gangliosides are isomers, and thus have a similar polarity. We identified TLC conditions that could resolve these two components (**Figure 2.5**). We found that all three enzymes could generate GD1b in varying amounts; however, GD1a was not a product of any of the enzymes.

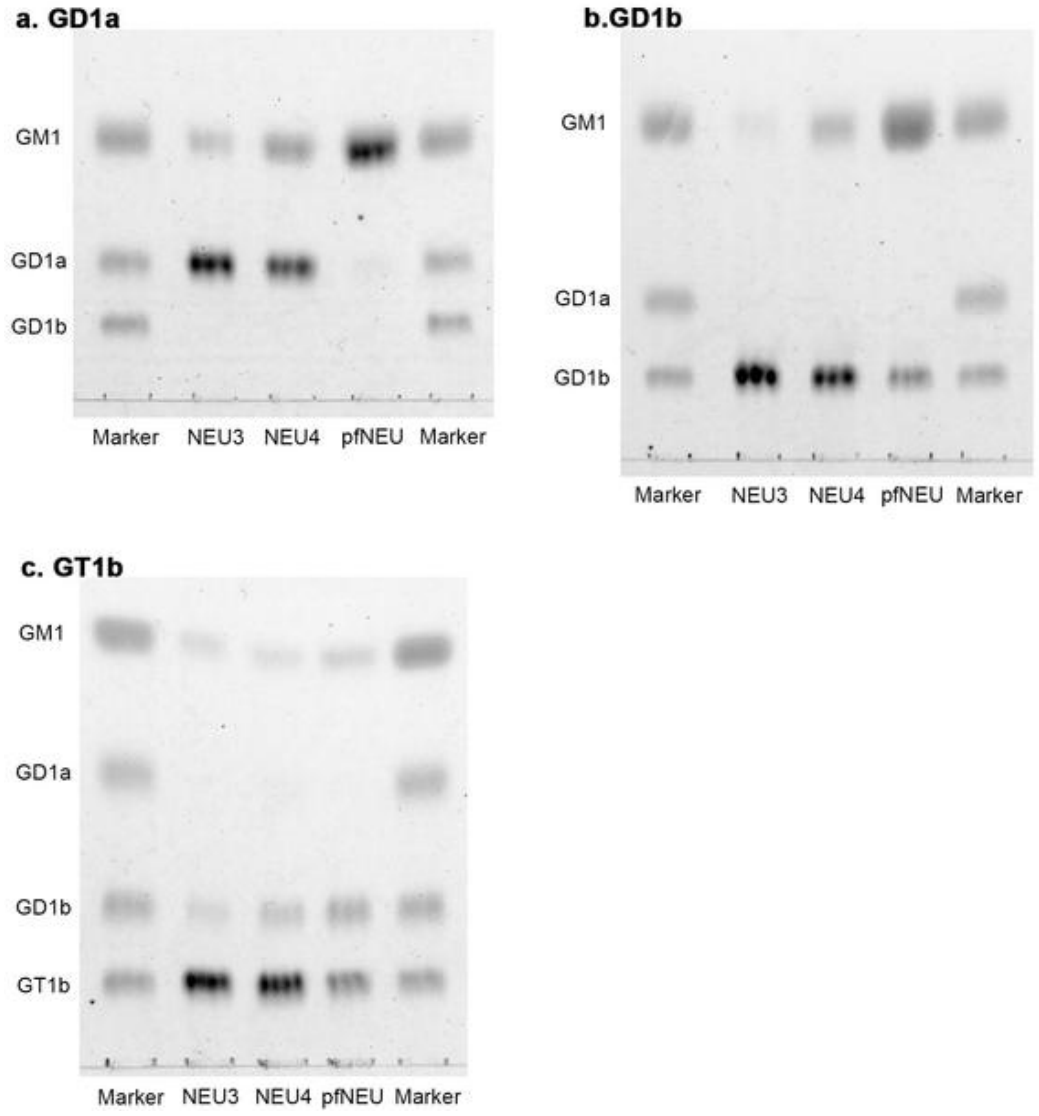

Figure 2.5 TLC analysis of GD1a, GD1b and GT1b cleavage. All sialidase enzymes were exchanged into assay buffer using a 10k spin column to remove glycerol. (a.) GD1a, (b.) GD1b, and (c.) GT1b samples were treated with sialidases for 1 hour at 37 ℃. Protein was precipitated with 1:1 methanol and chloroform and then separated by centrifugation to remove proteins. After drying, the residue was desalted by a C18 tip and dried by N_2. The solid was dissolved in 1:1 methanol and chloroform, and then run on TLC with 60:40:8

chloroform, methanol and 0.25% KCl (aq.) as eluent. The plate was stained by orcinol sulfuric acid and heated for 30 min at 80 ℃.

GM3

	LacCer	**GM3**
NEU3	73%	27%
NEU4	98%	2%
pfNEU	75%	25%

GD1a

	GM1	**GD1a**
NEU3	19%	80.8%
NEU4	35%	65%
pfNEU	98%	2%

GD1b

	GM1	GD1b
NEU3	6%	94%
NEU4	25%	75%
pfNEU	63%	37%

GT1b

	GM1	GD1a	GD1b	GT1b
NEU3	11%	2%	10%	77%
NEU4	9%	2%	17%	73%
pfNEU	18%	<1%	32%	50%

Table 2.1 Quantitation of enzyme cleavage of GM3, GD1a, GD1b, and GT1b by neuraminidase enzymes as followed by TLC. Each ganglioside (GM3, GD1a, GD1b, and GT1b) was run on a separate TLC plate (one image for each). Bands representing the substrate were measured by densitometry relative to any observed product bands in Image J, each band is calculated as a percentage of total staining per lane. Data represent a single image.

	Substrate for			Product	Linkage
	NEU3	**NEU4**	**pfNEU**		
GM1	-	-	-	GA1	α2,3(internal)
GM3	++	+++	++	Lac-Cer	α2,3
GD1a	+	++	+++	GM1a	α2,3
GD1b	-	+	++	GM1a	α2,8
GT1b	+	+	++	GD1b,GM1a	α2,3

Table 2.2 Substrate selectivity of NEU3 and NEU4. This table summarizes the data from Table 2.3.

-, Product observed <10%; +, Product observed 10~30%; ++, Product observed 30~90%; +++, Starting material left <10%.

Table 2.1 and **2.2** summarize the analysis of data in **Figure 2.4** and **2.5** by densitometry. We found that α2,3 linkages at a non-branching Gal residue appear to be the preferred target of NEU3, NEU4 and *pf*NEU. NEU3 and NEU4 completely hydrolyzed GM3 (with ~25% remaining), while the same linkage found in GT1b was only partially cleaved (70% remaining). The α2,8 linkage of ganglioside GD1b was not a good substrate for NEU3 and NEU4, and only a quarter of the substrate was hydrolyzed by NEU4, and even less (6%) with NEU3. The internal α2,3 linkage of GM1 was not cleaved by NEU3, NEU4 or *pf*NEU, and may indicate that the recognition of the substrate requires a free C4-hydroxyl

of the internal galactose residue (*41*). The bacterial *pf*NEU is the least selective of these enzymes, and cleaved the largest amount of α2,3 and α2,8 substrates (~40% GD1b.)

A summary of the substrate activities determined from our TLC results is provided in **Figure 2.6**. Having established the substrate specificity of two hNEU, we next turned our attention to the functional role of these enzymes and their interaction with cell adhesion pathways.

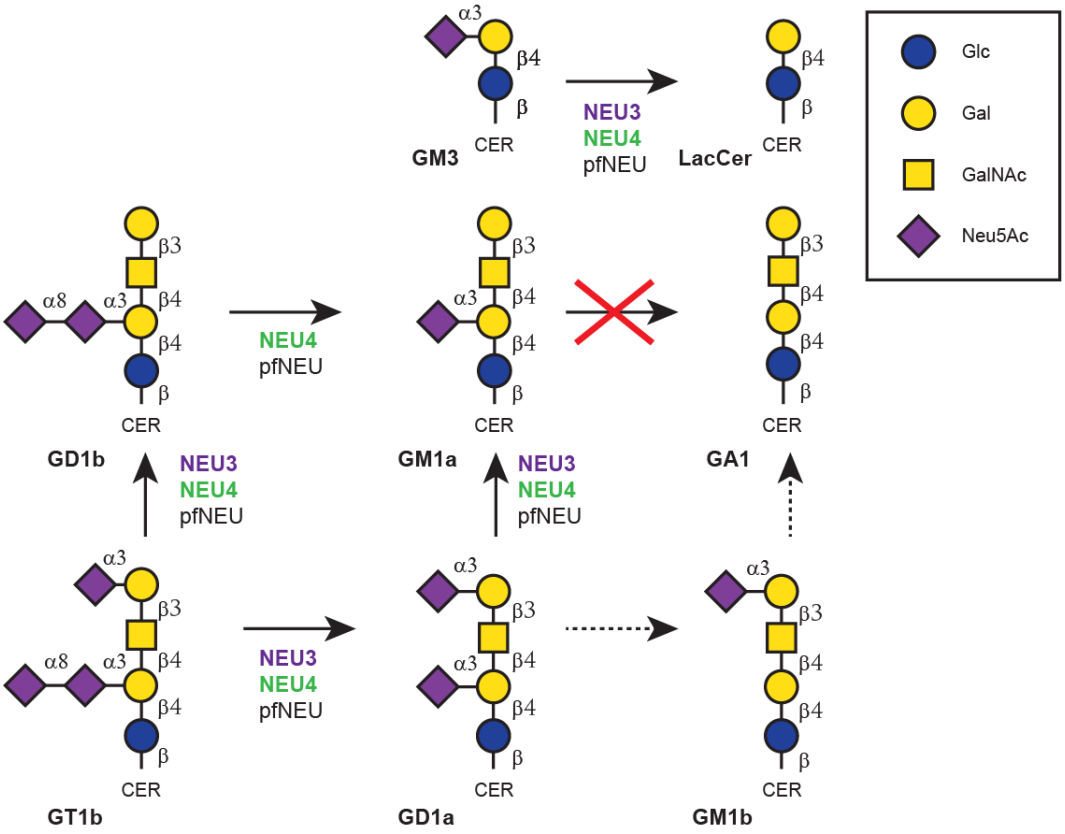

Figure 2.6 Substrate activity of gangliosides for NEU3, NEU4 and pfNEU.

2.3 Cell migration on fibronectin is regulated by NEU3 and NEU4

We proceeded to test the role of hNEU in cellular adhesion using a cell migration assay. A variety of assays can be used to evaluate changes in cell adhesion and migration (*43*). We selected a scratch assay as it is easy to implement, and could be used to measure small changes in cell migration rates by microscopy. We selected two human cell lines: HeLa and A549 cells. HeLa cells are derived from human cervical adenocarcinoma cells, an epithelial cell line.

A549 cells are derived from human lung carcinoma cells (**Figure 2.7**).

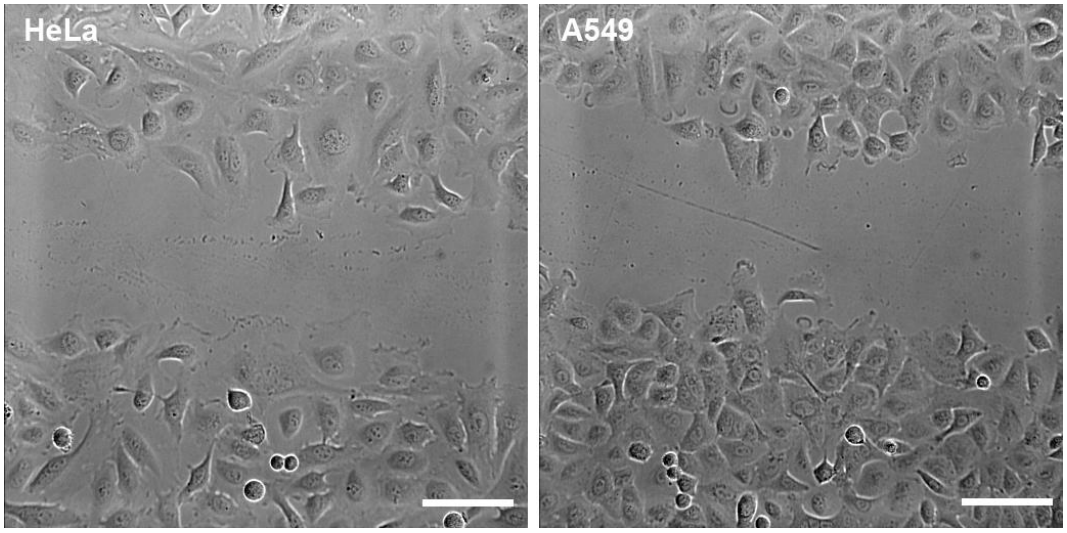

Figure 2.7 Imaging of HeLa and A549 cells in a scratch assay. A fibronectin (FN) treated plate was seeded with HeLa or A549 cells in growth medium. The plate was incubated at 37 ℃, 5% CO_2 overnight. The cell monolayer was wounded using a gel-loading pipette, and the media was changed to the indicated conditions. Images were acquired with a 20x objective 3h after the scratch. Scale bar = 100μm.

In order to provide a controlled surface, and to allow cells to firmly adhere to the substrate, surfaces were coated with fibronectin (FN). Fibronectin is a component of the extracellular matrix, which plays important roles in cell migration and adhesion. It can bind with integrins, for example, α4β1 and α5β1 integrins are known ligands (*44*).

HeLa cells were grown to a monolayer on FN-coated plates, and a wound was generated using a pipette (*26*). We found a 200 μL gel-loading pipette tip was

sharp enough to give a gap of the appropriate size, but did not damage the polystyrene surface. Monolayers were observed over an 8 hour time period, with measurements taken at 1.5 hour intervals. To measure the migration of cells, images of 6 fields along the scratch were acquired at each time point. Image analysis software (NIS-Elements v3.5, Nikon USA) was used to measure the distance between the cell front at each side of the scratch. We initially tested conditions including cells treated with buffer (control), recombinant NEU3 enzyme, and the general sialidase inhibitor, DANA. The raw data for all three conditions is shown in **Figure 2.8**. We found that the data were well fit to a linear curve (r^2 values 0.92-0.99). Although more complex equations also fit the data (such as an exponential, $y=ae^{bx}$), we selected the linear form as it has the fewest variables and provided a reasonable fit (**Table 2.3**). These preliminary data suggested that DANA could inhibit cell migration. Thus, we proceeded to use the assay to probe a variety of conditions in both cell lines.

Condition	N	Migration rate [μm h^{-1}]	St Dev
Control	6	0.091	0.009
DANA	4	0.068	0.008
NEU3	4	0.101	0.005

Table 2.3 Cell migration data for HeLa 7.5h. All 3 conditions were tested with an N >= 4, and data were fit to the equation ($y=ae^{bx}$) and used b as migration rate.

Based on previous studies, we expected that NEU3 would activate cell migration (*45*); however, our results only showed a small increase in migration.

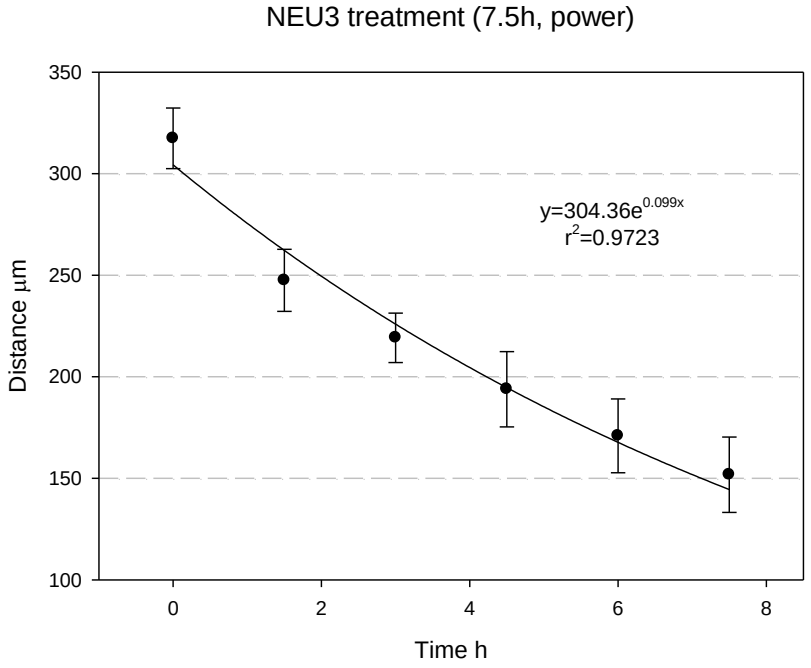

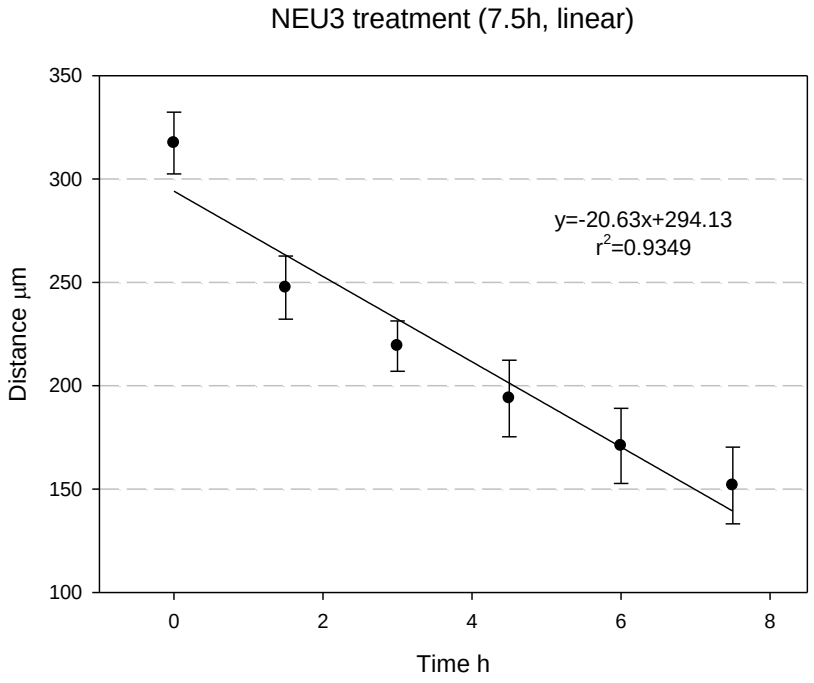

Figure 2.8 NEU3 migration data fit by power and linear equations. NEU3 treated cells were analyzed in the cell migration assay. Data were fit to a power equation ($y=ae^{bx}$) or a linear equation ($y=-ax+b$) in SigmaPlot.

Closer examination of the data suggested that larger differences could be observed in the early parts of the curve. (**Table 2.4, Figure 2.9**). This suggested the assay would be more sensitive if we observed the initial 3 hr period of cell migration. This finding may indicate that the enzyme, NEU3, has a short-acting effect on cells. Previous work has found that the recombinant enzyme degrades after 3 hrs at 37 ℃ (Albohy and Cairo, unpublished), and this is the most likely explanation for our results. We therefore proceeded to test the effect of hNEU over this timeframe using the cell migration assay. All assays with NEU3 were

conducted over a 3 hr period, with four timepoints (including t = 0). Previous testing of NEU4 had indicated that it was stable for a shorter window than NEU3; therefore, NEU4 experiments were conducted over 1 hr, with four time points (including t = 0) (**Figure 2.10**). Due to this difference, additional controls were included for comparison with NEU4 over this shorter duration. Then the final optimized migration assay and data analysis were showed in **Figure 2.11** and **Figure 2.12**.

Time [h]	Mean Distance [µm]	Δd [µm]
0	317.4	0
1.5	247.47	69.93
3	219.18	28.29
4.5	193.86	25.32
6	170.91	22.95
7.5	151.76	19.15

Table 2.4 Fit results for NEU3 treated cells in migration assay. The distance between the two cell fronts from 10 images were averaged for each time point. Δd is the difference between subsequent points, and suggests that longer time points show smaller changes in migration rates.

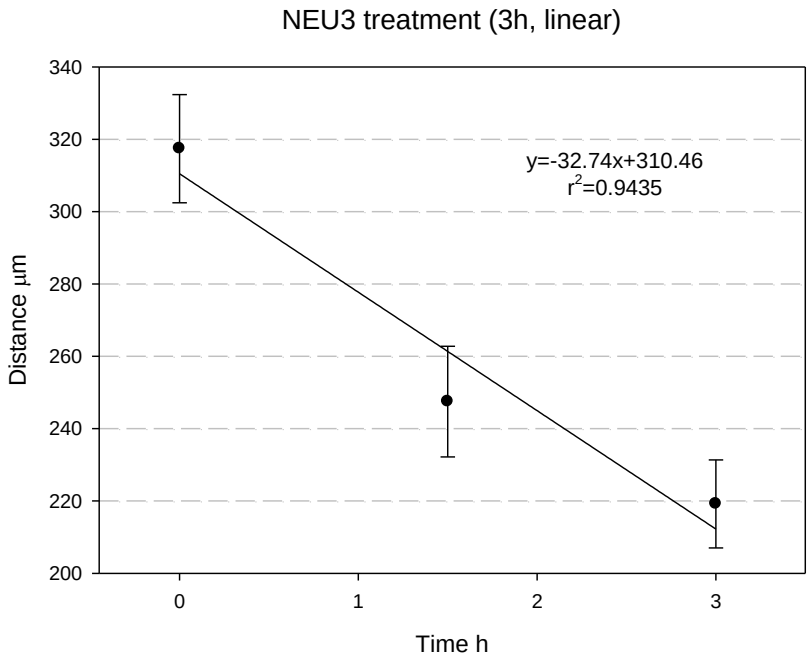

Figure 2.9 Linear fit of migration data for NEU3 treated cells (3 hrs). NEU3 data was fit by linear regression (y=-ax+b) in SigmaPlot.

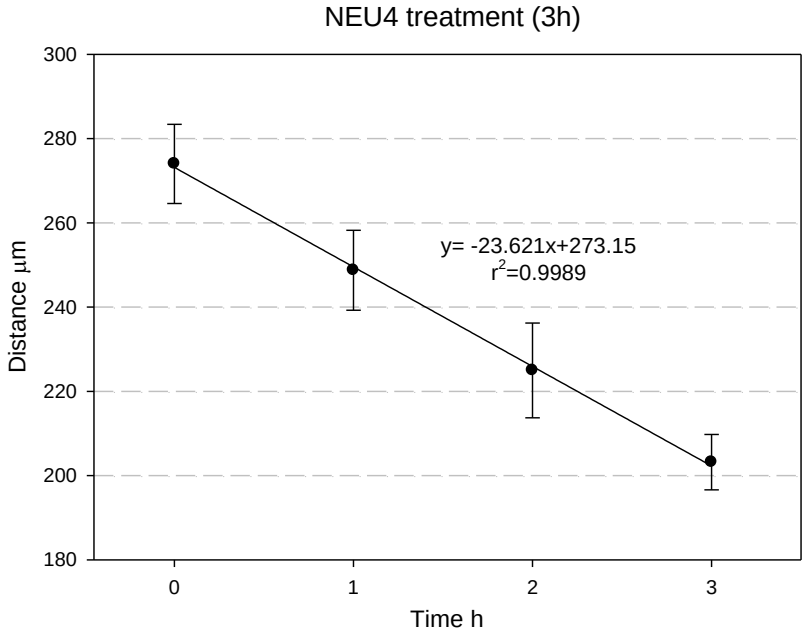

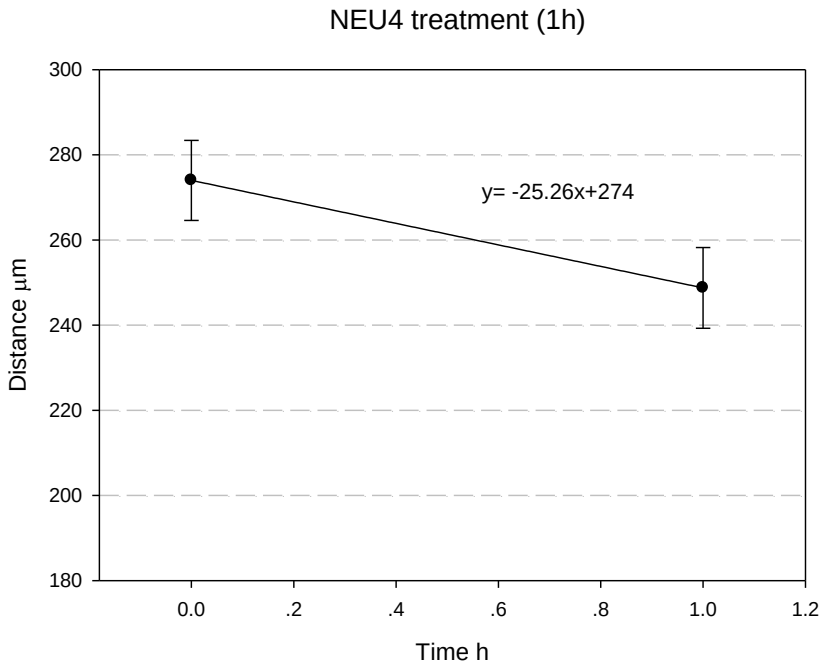

Figure 2.10 Linear fit of migration data for NEU4 treated cells over 3 hrs and 1 hr. NEU4 data was fit by linear regression (y=-ax+b) in SigmaPlot.

Another source of variability in the assay is the concentration and variable activity of the enzyme samples. To assure that all enzyme samples used were of the same activity, we calibrated the activity of individual samples using a fluorogenic assay based on the 4MU-NANA substrate (*41*). The K_m of this substrate has been reported for NEU3 and NEU4 (*40*). Since our experiments were to be conducted in cell culture at physiological pH, we conducted the assay at pH 7. All NEU samples were used at an activity of 600 mU per sample at pH = 7.

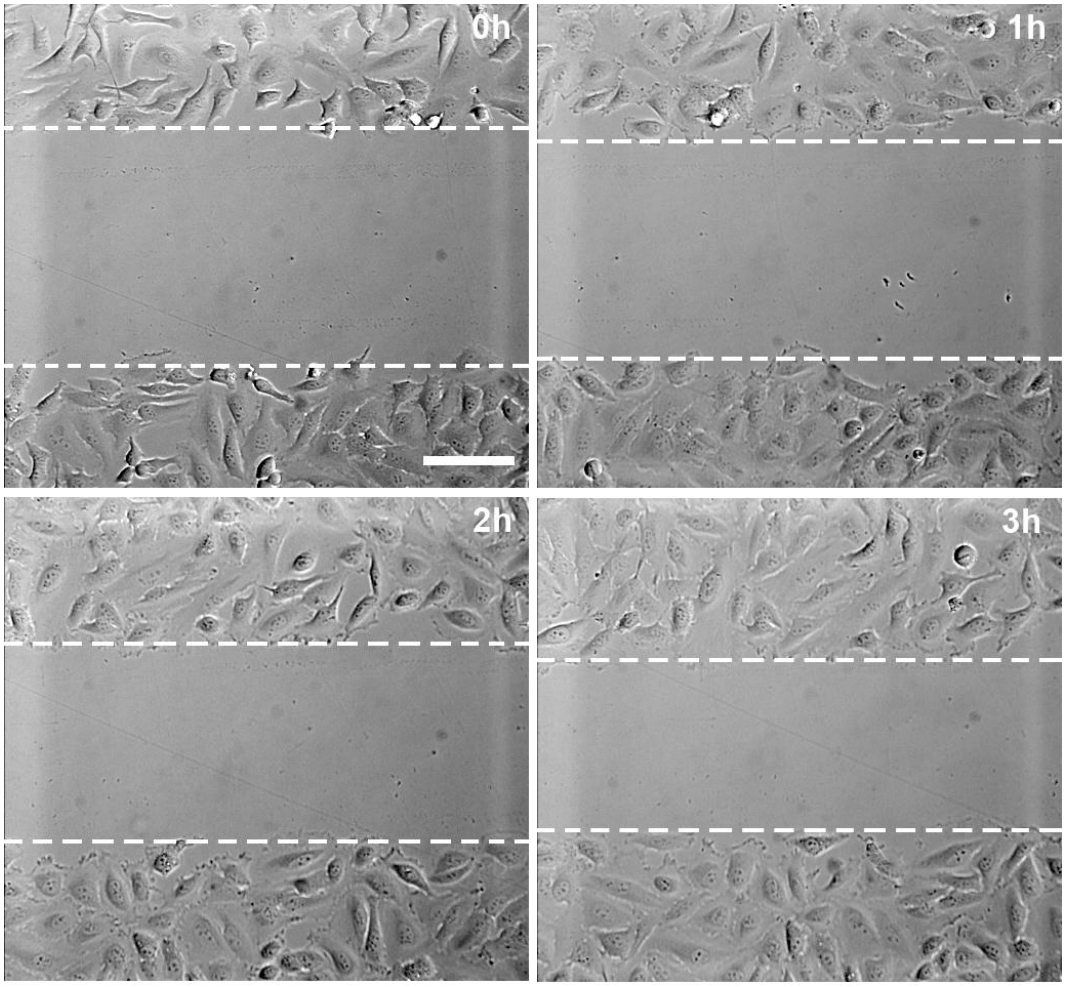

Figure 2.11 Cell migration over 3 hours (HeLa cells control condition). A fibronectin (FN) treated plate was seeded (HeLa: 1 mL, 4 x 10^5 cells mL^{-1}; A549: 1 mL, 5x10^5 cells mL^{-1}) and growth medium (1 mL). The plate was incubated at 37 ℃, 5% CO_2 overnight. The monolayer was scratched with a gel-loading pipette, and fresh medium was added with the indicated conditions. Images were acquired every hour for 3h (20x objective).

Time [hr]	Distance [µm]	St dev.
0	377.77	14.32
1	352.36	14.35
2	332.46	15.79
3	311.17	12.97

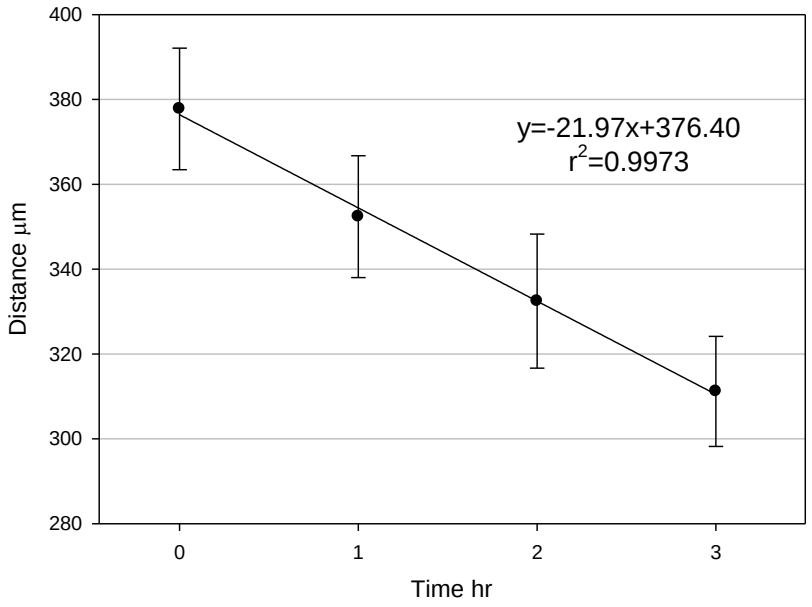

Figure 2.12 Data analysis for HeLa cells control condition. HeLa cell migration data were analyzed in NIS-Elements software (Nikon, USA) and fit data by linear regression (y=-ax+b).

With a cell migration assay established, we then proceeded to test the effects of conditions which might alter cell adhesion to FN. We chose to examine

three groups of conditions: (1) neuraminidase enzymes, (2) chemical inhibitors, and (3) glycolipids. We examined three different neuraminidase enzymes including the human neuraminidase isoenzymes NEU3 and NEU4, and the *Clostridium perfringens* neuraminidase (*pf*NEU). To provide a negative control, we also examined an inactive enzyme mutant, NEU3-Y370F (*41*). Glycolipids were selected based on our substrate studies (*vide supra*) to include possible native products (LacCer, GM1, GD1a) and substrates (GM3, GD1a, GD1b, GT1b) of NEU3. Chemical inhibitors that might disrupt NEU3 (DANA), activate NEU4 (TQ) (*46*), or disrupt integrin adhesion (cytoD)(*47*) were also included.

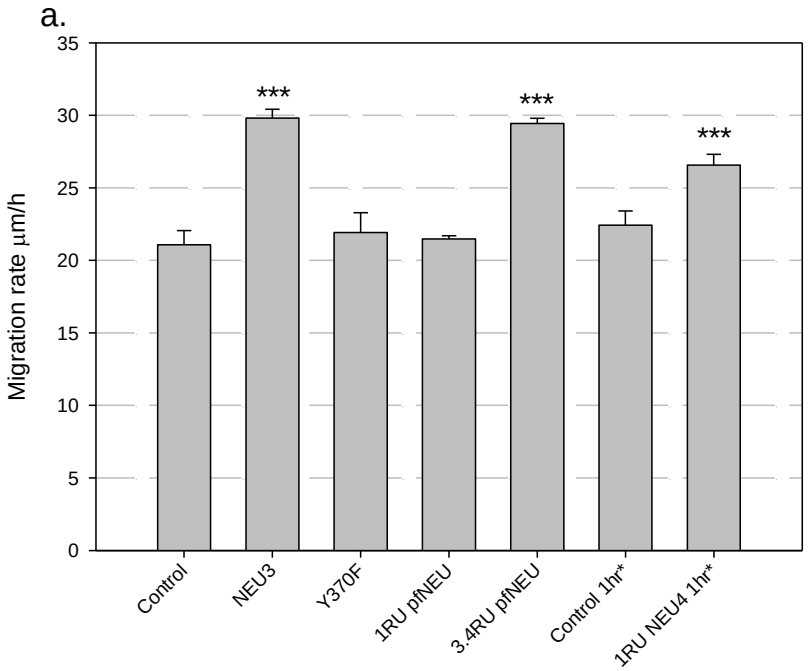

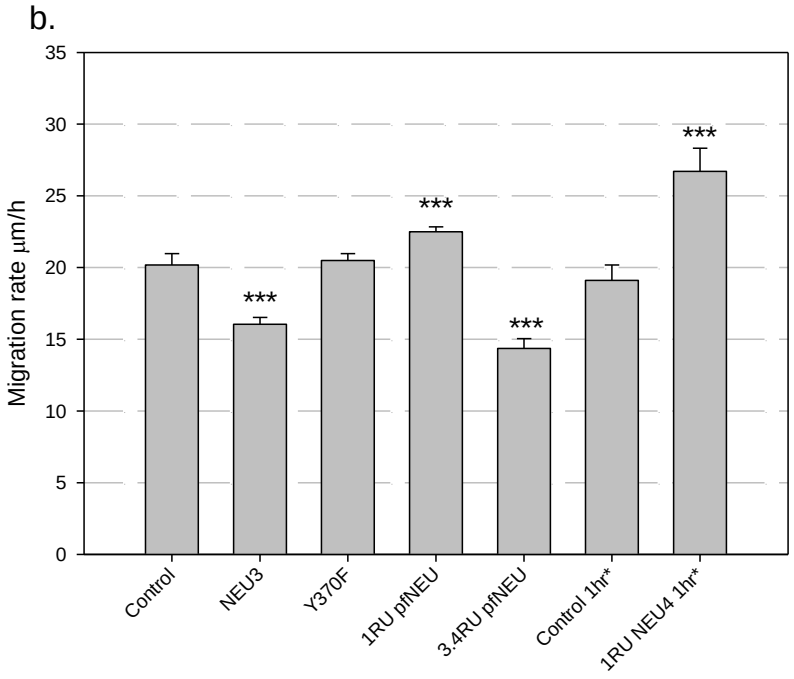

Figure 2.13 Cell migration of HeLa and A549 treated with sialidases. a. HeLa b. A549 cell. Cells were pre-treated as described in **Figure2.11**, and then washed with PBS and the medium was changed to the indicated conditions. Images were acquired every hour for 3 hours, and analyzed. Each condition was repeated 3 times. The NEU3 activity was used as the standard for other sialidases, and 1 relative unit (RU) was set equal to the activity used in this test. * Cells were treated with NEU4 for 1 hr, due to enzyme instability. These data are compared to a 1 hr control for statistical analysis. *** $p<0.001$.

Among the neuraminidase enzymes tested with HeLa cells (**Figure 2.13a**), NEU3, NEU4, and *pf*NEU were all found to increase the rate of cell migrations. The effect of NEU3 was confirmed to be a result of the enzyme activity, as an inactive NEU3-Y370F mutant showed no effect on migration rates. Importantly, more calibrated units of *pf*NEU enzyme activity were required to generate the

same effect as that of NEU3 on the cells. This result is consistent with NEU3 having greater specificity for the target substrate(s) which lead to altered migration.

Corresponding experiments in A549 cells (**Figure 2.13b**) found that NEU3 and *pf*NEU could reduce the rate of cell migration, in contrast to our results in HeLa. The effect of NEU3 was again dependent upon enzyme activity, as the Y370F-NEU3 protein did not alter the rate of migration from control. However, NEU4 resulted in a similar increase in cell migration, similar to our observations in HeLa.

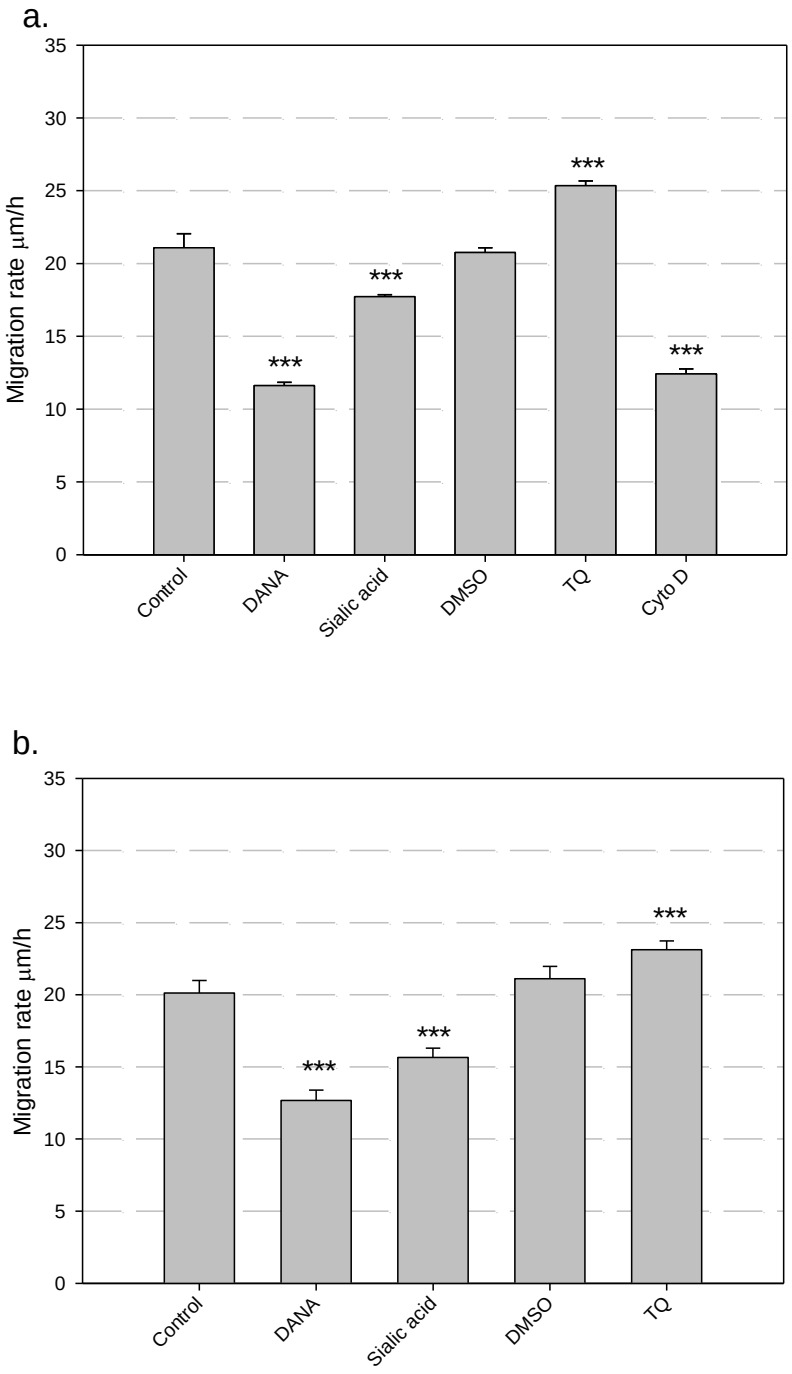

Figure 2.14 Cell migration of HeLa and A549 treated with drugs. a. HeLa b. A549 cell. Cells were

pre-treated as described in **Figure 2.11**, and then washed with PBS and the medium was changed to the indicated conditions. Images were acquired every hour for 3 hours, and analyzed. Each condition was repeated 3 times. *** $p<0.001$.

We also examined changes in cell migration when cells were treated with a non-selective inhibitor of sialidases, DANA (**Figure 2.14**). In both cell lines, we observed that DANA (100 μM) resulted in suppression of cell migration to almost half of the rate of control. We also tested the effect of sialic acid, and found that it also suppressed cell migration, though not as dramatically as DANA. Low concentrations of DMSO had no measurable effect on cell migration, this is an important control as we use DMSO as a vehicle for delivery of other compounds. We also tested the effect of thymoquinone (TQ) a compound proposed to increase the activity of NEU4 in cells (*46*). In our experiments, TQ induced a small increase in the rate of cell migration. Although this may be the result of NEU4 activation, further experiments will be required to confirm the mechanism. Experiments with low concentrations of cytochalasin D (cytoD), a cytoskeletal disrupting agent, resulted in unstable monolayers of cells which were much more sensitive to damage when scratched at the start of the assay. We were able to measure the effect of CytoD on the rate of cell migration in HeLa, which was similar to the effect of DANA. This finding highlights the remarkable potency of DANA as an anti-adhesive, and likely indicates a central role for human

neuraminidase enzymes in integrin adhesion.

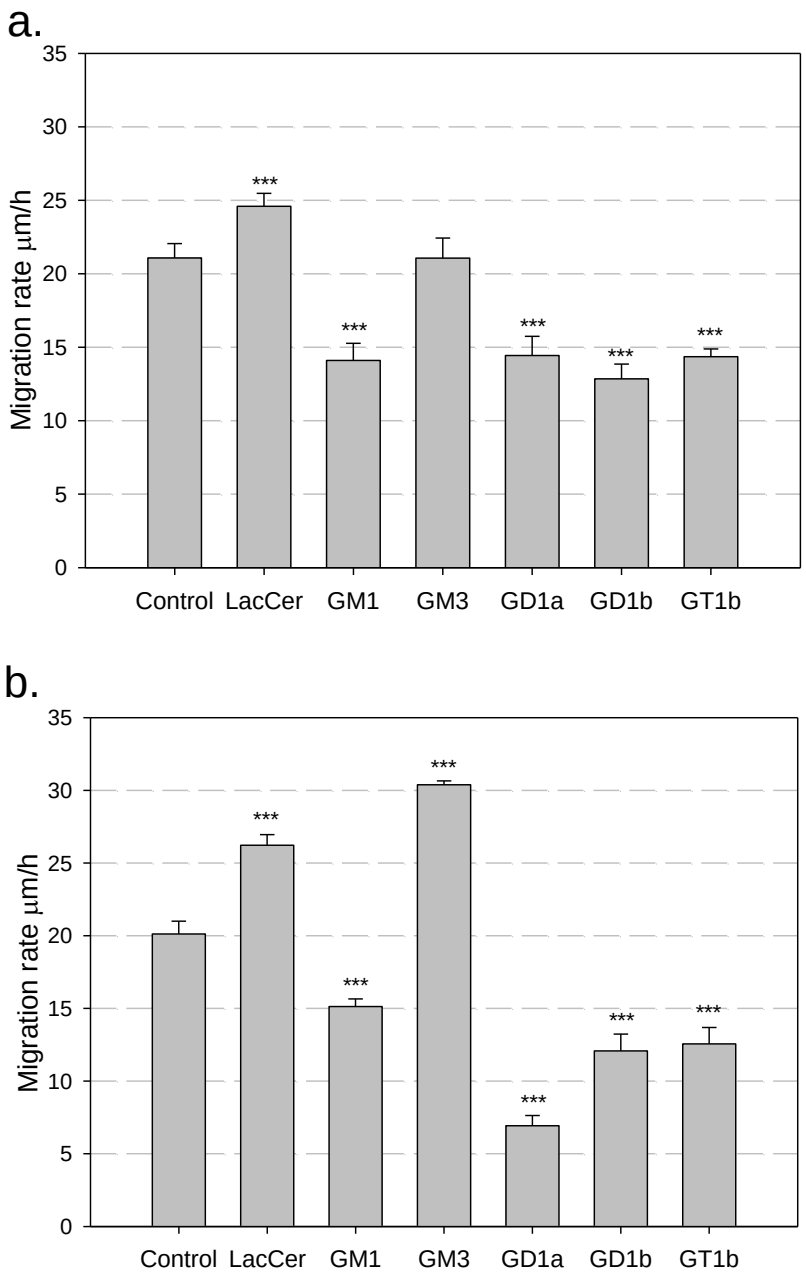

Figure 2.15 Cell migration of HeLa and A549 treated with glycolipids. a. HeLa b. A549 cell. Cells were pre-treated as described in **Figure 2.11**, and then washed with PBS and the medium was changed to the indicated conditions. Images were acquired every hour for 3 hours, and analyzed. Each condition was

repeated 3 times. *** p<0.001.

We next examined the effect of specific glycolipids on cell adhesion when added exogenously to cells (**Figure 2.15**). Glycolipids are known to insert into the plasma membrane when added exogenously to cells (*48*). Therefore, these experiments allow us to explore the specific effect of enriching the membrane in a particular glycolipid. We again found similar results between both cell types. The LacCer glycolipid resulted in enhanced cell migration in both cell types. However, GM3 resulted in enhanced migration for HeLa cells, but not for A549 cells. In contrast, all other complex gangliosides tested (GM1, GD1a, GD1b, GT1b) resulted in suppression of cell migration.

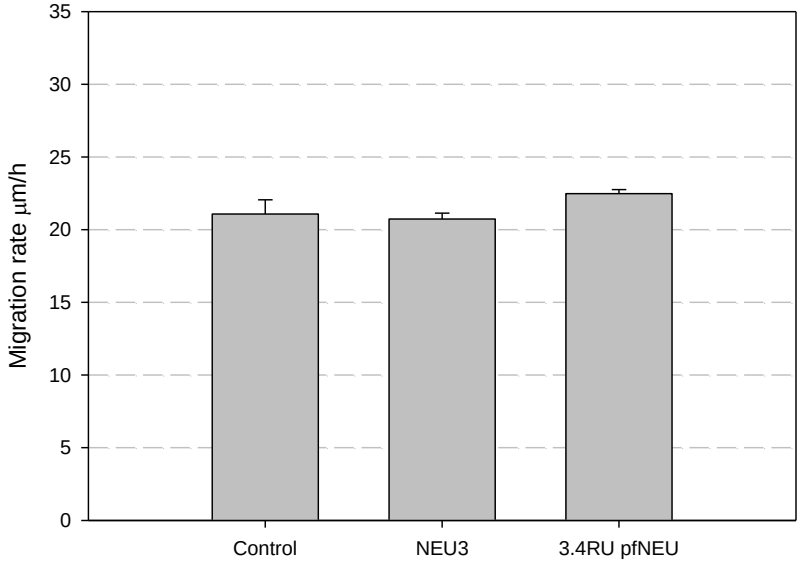

Figure 2.16 Pre-treatment of fibronectin with sialidases does not affect cell migration. Fibronectin was

pre-coated on the culture dish surface, and then exposed to sialidase enzyme. The sample was incubated for 3 hrs at 37℃, 5% CO_2. The surface was washed to remove the enzyme, and then the plate was seeded with HeLa cells. A subsequent migration assay was conducted as above.

So far, we have interpreted the effect of exogenous neuraminidase enzymes as modifying the glycan structures of the cell membrane. However, it is possible that the enzyme is instead altering the sialic acid content of the FN substrate. To test this possibility, we pre-treated the FN matrix with two of the neuraminidase enzymes that gave increased cell migration: NEU3 and *pf*NEU, and examined the rates of migration for cells adherent to this matrix (**Figure 2.16**). We found no significant differences between these conditions, allowing us to conclude that the target of the enzyme is not the FN matrix, but is a component of the cells.

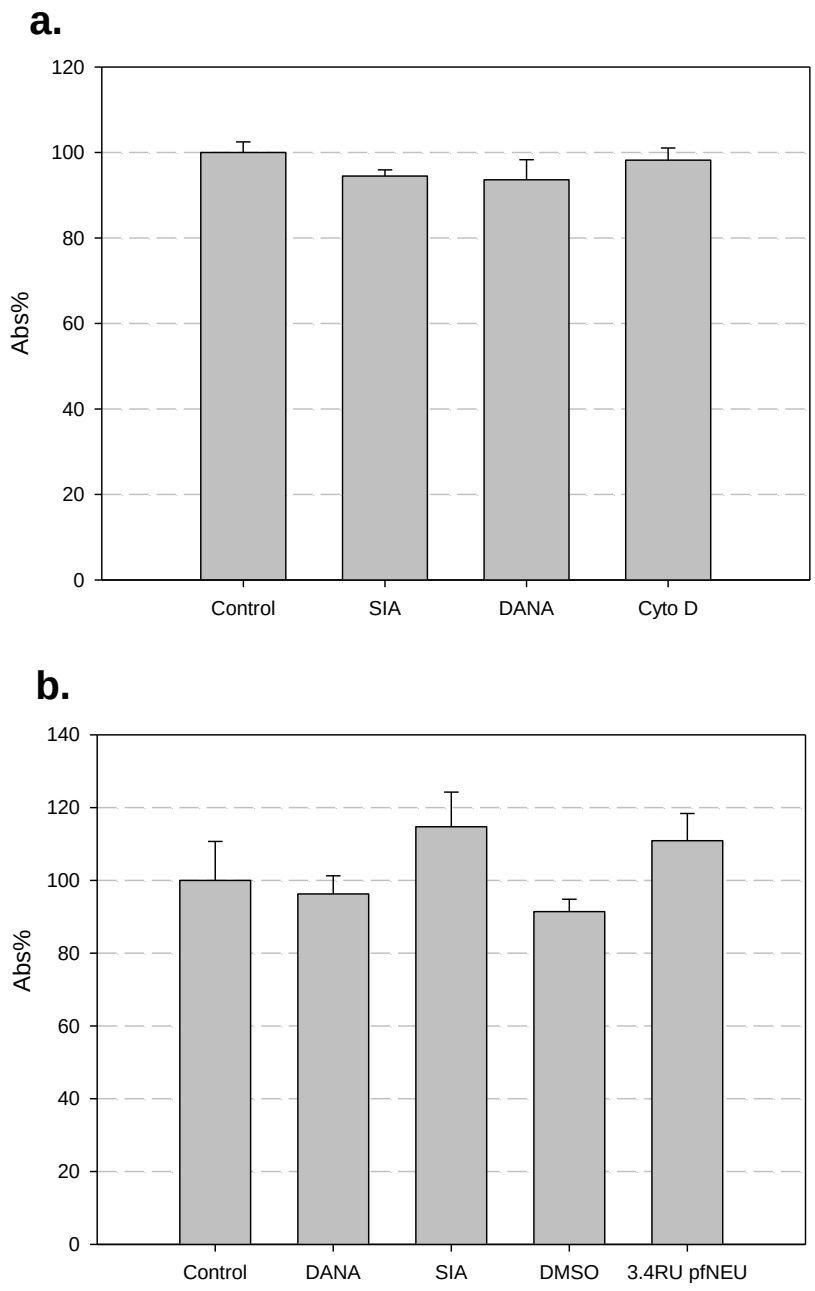

Figure 2.17. Toxicity assays for migration conditions in HeLa and A549 cells. Cells were seeded into a 96-well plate (50μL/well, $1x10^5$ cell/mL). Media containing the indicated condition was added to each well, and the plate was incubated for 48 hrs at 37 ℃, 5% CO_2, followed by addition of 20μL MTS solution per well. After 2 hr incubation, the absorbance was read at 490 nm using a plate reader. (a.) HeLa and (b.) A549 cells

were tested separately.

It is possible that the reduced migration of cells treated with DANA or sialic acid could be the result of toxic effects of these reagents on cells. To test this hypothesis, we treated cells under the same conditions and measured their viability using an MTS assay (*49*) (**Figure 2.17**). We observed little or no effect of any of the conditions tested on cell viability. Therefore, we conclude that the effects on cell migration are a result of specific biochemical effects on the integrin-FN interaction, not a result of cell toxicity.

The migration data from HeLa and A549 cells strongly support the hypothesis that native sialidase activity regulates integrin-mediated adhesion in these cells. NEU3 had a dramatic positive effect on adhesion in HeLa cells, but appeared to have a slightly negative effect in A549 cells. However, experiments with *pf*NEU confirmed that non-specific neuraminidase activity resulted in increased cell migration. In agreement with this finding, the general sialidase inhibitor, DANA, resulted in a dramatic decrease in cell migration. Together, these results are consistent with more than one sialidase enzyme in cells, and likely different substrate targets of these enzymes playing a role in regulating cell adhesion. Our experiments with specific glycolipids suggest that most complex gangliosides are negative regulators of integrin-mediated adhesion (GM1, GD1a, GD1b, GT1b), while LacCer appears to be a positive regulator. We propose a

model which incorporates these results at the end of the chapter.

2.4 Immuno-fluorescence labeling

In order to understand the interaction between gangliosides and integrin receptors on the cell membrane, we employed immuno-fluorescence labeling techniques. Fluorescent dyes can be used to label antibodies or other proteins, which specifically label biomolecules. The localization of these labels can then be used to detect changes in subcellular localization and co-localization. Previous reports have shown that GT1b can inactivate the α5β1 integrin and cause changes in the cell membrane (*8*). Our studies on GT1b (Sec 2.3) found that increased amounts of this glycolipid in the membrane result in decreased cell migration. Other reports have suggested that GM3 can bind with α5β1, resulting in up-regulation of cell adhesion in rat cells (*50*).

2.4.1 Localization of integrins by immuno-fluorescent labeling

In human epithelial cell adhesion, the primary integrins that bind with ECM are the α5β1 and α4β1 integrins (*51*). We employed an anti-α4 antibody with HeLa cells (clone BU49). The antibody was conjugated with a Cy5 NHS ester to allow for observation by fluorescence (**Figure 2.18**).

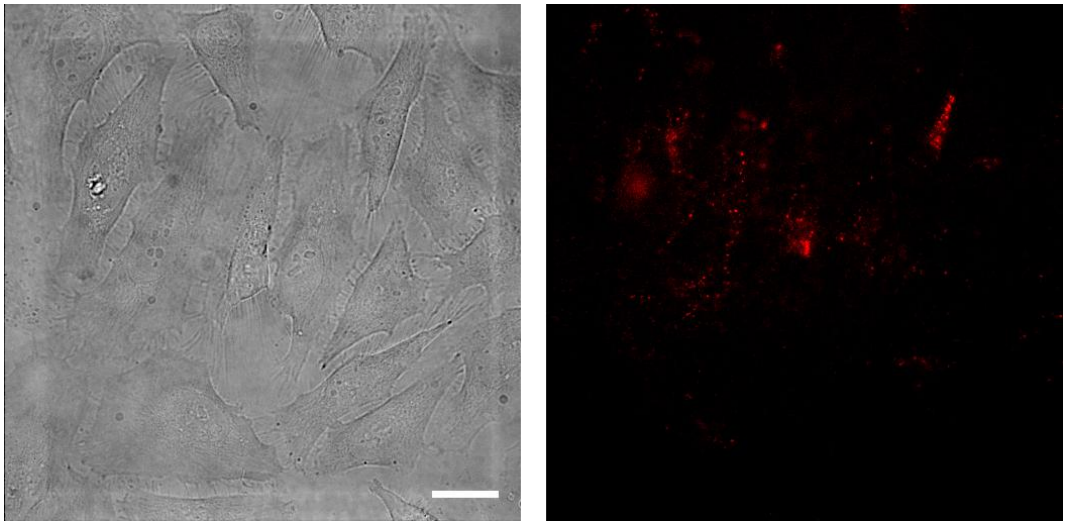

Figure 2.18 HeLa cells labeled with anti-α4 antibody conjugated with Cy5 NHS ester. HeLa cells were cultured in a confocal dish overnight at 37 ℃, with 5% CO_2, and then washed with PBS twice. Cells were immuno-labeled with 50 ng Cy5-anti-α4 antibody conjugate for 10 min at room temperature and then washed with PBS. Images were taken by DIC (left) and TIRF (right) with 633 nm laser excitation. Scale bar = 25 μm.

Labeling of cells with the Cy5-anti-α4 antibody did not show strong labeling on HeLa cells. Increasing the amount of antibody used from 10 ng to 50 ng did not show significant improvement. Previous studies have suggested that adherent cells do not express large amounts of α4β1 integrin (*52*), and this likely explains the low labeling observed in our experiment.

To address this issue, we labeled cells with a Cy5-anti-α5 antibody. The antibody (clone SAM-1) was conjugated with a Cy5-NHS ester as before, and then applied to cells (**Figure 2.19**). Labeling with the anti-α5 antibody resulted in much more intense staining of cells, and revealed a large number of small puncta

on the cell membrane. These puncta are likely microclusters of receptors, and appear to be relatively diffuse on the cell surface.

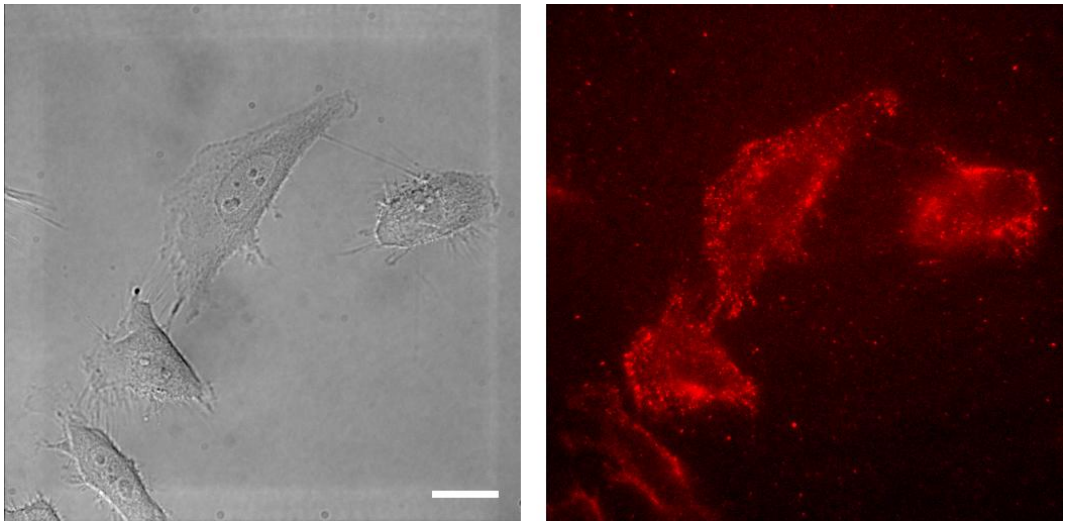

Figure 2.19 HeLa cells labeled with anti-α5 antibody conjugated with Cy5 NHS ester. HeLa cells were cultured in a confocal dish overnight at 37 ℃, with 5% CO_2, and then washed with PBS twice. Cells were immuno-labeled with 50 ng Cy5-anti-α5 antibody conjugate for 10 min at room temperature and then washed with PBS. Images were taken by DIC (left) and TIRF (right) with excitation by a 633 nm laser. Scale bar = 25 μm.

In order to detect membrane ganglioside localization on cells, the GM1-binding protein, cholera toxin B (CTB), is often employed (*53*). We used CTB conjugated with a fluorescent dye (FITC). We first examined the binding of CTB in fixed HeLa cells. There are several ways to fix live cells, such as methanol, acetone and paraformaldehyde treatment (*54*). Fixing HeLa with

methanol (50% and then 100% methanol), followed by labeling with CTB-FITC showed significant staining of intracellular structures. A bright nucleus and weak staining of the membrane was observed for all cells (**Figure 2.20**). We concluded that cell fixation resulted in too much membrane permeabilization, and would not allow visualization of membrane staining.

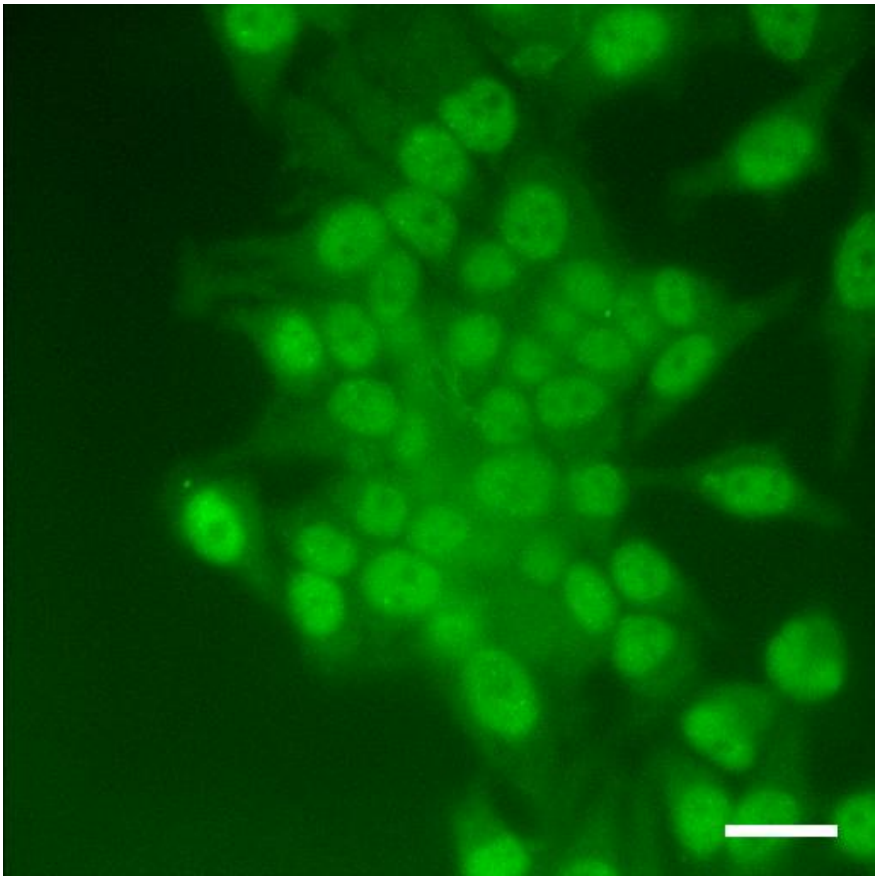

Figure 2.20 HeLa cells fixed by methanol 1 hr and labeled by CTB-FITC. HeLa cells were cultured in a confocal dish overnight at 37 ℃, with 5% CO_2, and then washed with PBS twice. A fixative solution was added to the culture (50% methanol/PBS) and treated for 30 min, and then changed to 100% methanol for another 30 min. Cells were washed with PBS twice and 2 μg CTB-FITC was added for 10 min. Images were

taken by TIRF with excitation by a 488 nm laser. Scale bar = 25 μm.

In order to reduce damage to the cell membrane by methanol, we reduced treatment time from 1 hr to 30 min, but this change had no major effect (**Figure 2.21**).

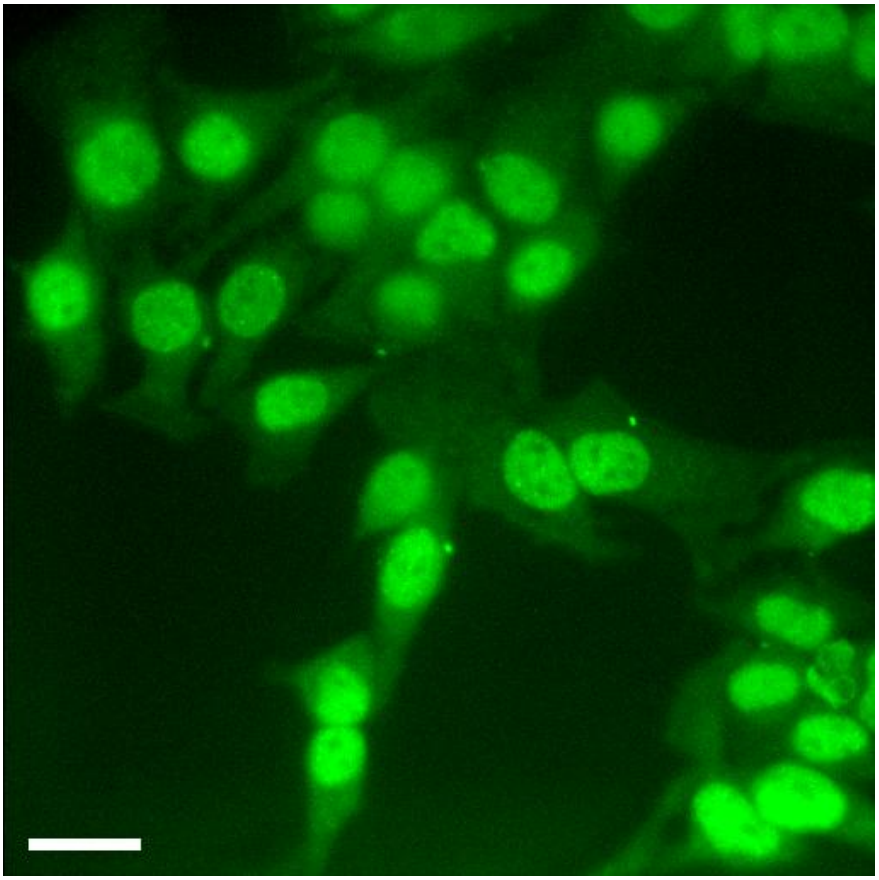

Figure 2.21 HeLa cells fixed by methanol 30 min and labeled by CTB-FITC. HeLa cells were cultured in a confocal dish overnight at 37 ℃, with 5% CO_2, and then washed with PBS twice. A fixative solution was added to the culture (50% methanol/PBS) and treated for 15 min, and then changed to 100% methanol for another 15 min at 4 ℃. Cells were washed with PBS twice and 2 μg CTB-FITC was added for 10 min.

Images were taken by TIRF with excitation by a laser at 488 nm. Scale bar = 25 μm.

Next we tried paraformaldehyde (PFA) as a fixative. Cells were treated with 4% PFA at 4 ℃ for 10 min (**Figure 2.22**).

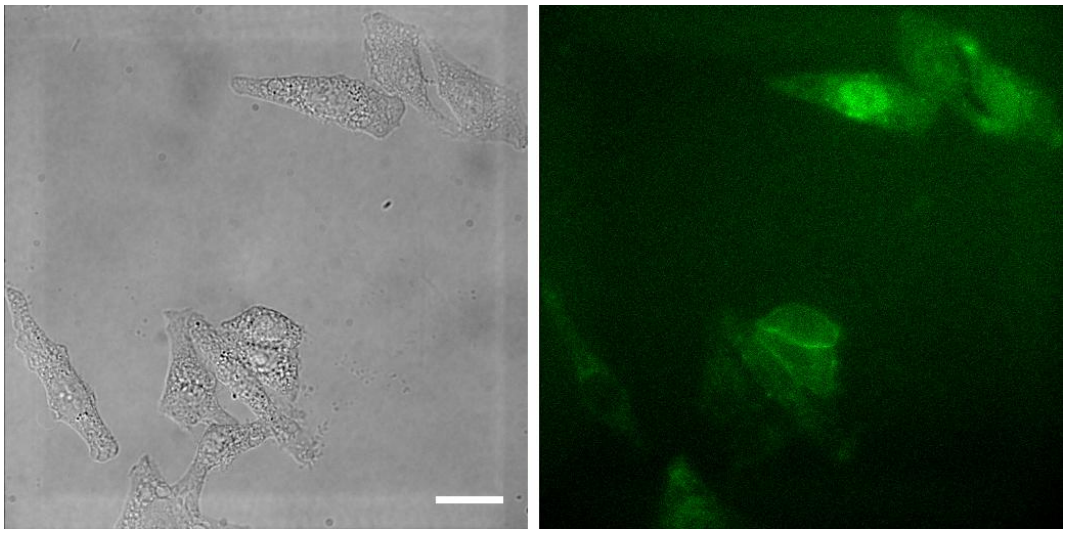

Figure 2.22 HeLa cells fixed by 4% PFA and labeled with CTB-FITC. HeLa cells were cultured in a confocal dish overnight at 37 ℃ in a 5% CO_2 incubator, and then washed with PBS twice. A fixative solution was added (4% PFA in PBS) and treated for 10 min at 4 ℃. Cells were washed with PBS twice and the images were taken by DIC. Scale bar = 25 μm.

CTB labeling under these conditions gave a range of staining for cells, with many very bright cells, and many dim cells. Higher concentrations of CTB and longer labeling times (5 μg CTB, 10 min at room temperature) gave only

slight improvements (**Figure 2.23**). We chose to use these conditions for fixed cells, and proceeded to identify a label for other biomolecules that could be expected to co-localize with integrins.

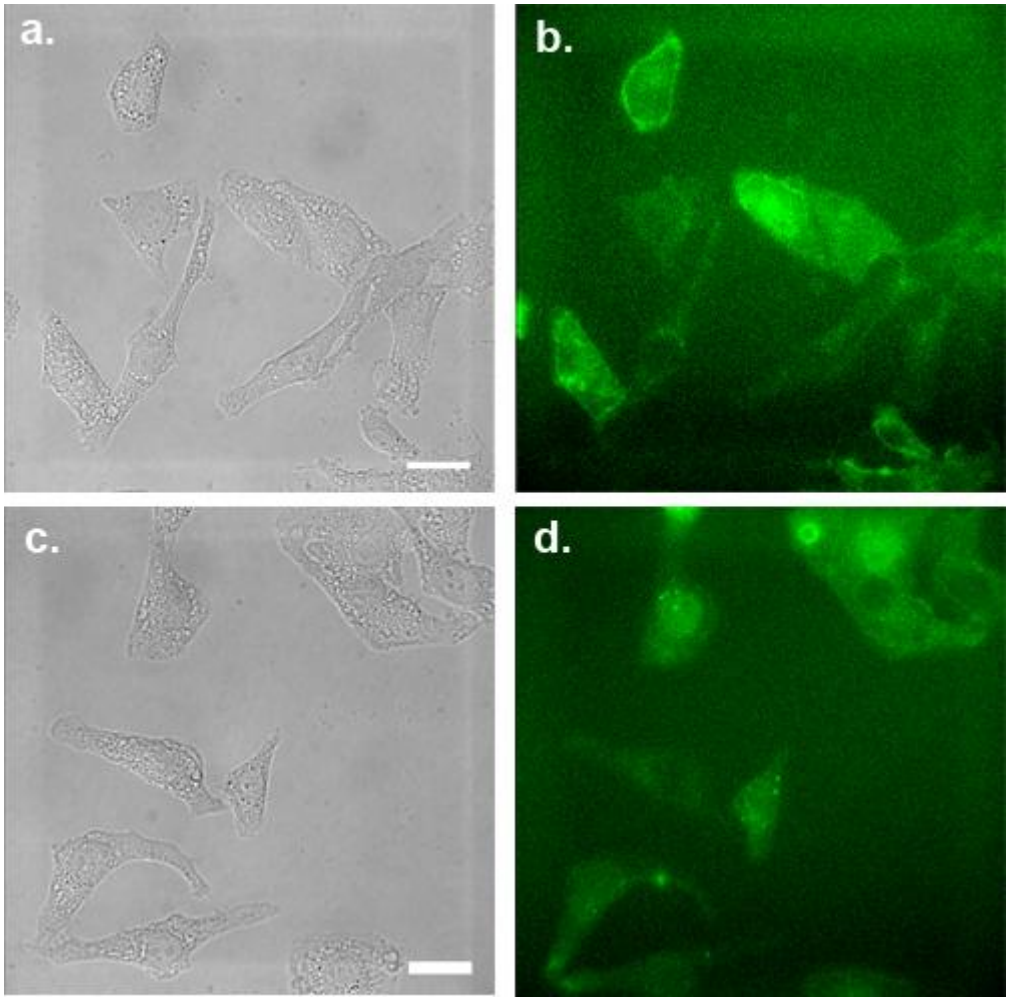

Figure 2.23 HeLa cells fixed by PFA and labeled with CTB-FITC. HeLa cells were cultured in a confocal dish overnight at 37 ℃ with 5% CO_2. Cells were washed with PBS twice. Cells were then treated with a fixative (4% PFA in PBS, 10 min at 4 ℃). Cells were washed with PBS twice CTB-FITC was added at either (**a & b**) 2 μg or (**c & d**) 5 μg for 10 min. Cells were washed again with PBS. Images were taken by DIC (left)

and TIRF (right) with a 488 nm laser. Scale bar = 25 μm.

Clones of HeLa transfected with a GFP-NEU3 fusion protein were provided by L.C. Morales and S. Sipione from the University of Alberta. The two clones employed here differed in expression levels of the GFP-NEU3 fusion protein. The first, GFP-NEU3/A10 (N-terminal), has lower expression of the GFP fusion as compared to the NEU3-GFP/C2 clone (C-terminal). Examination of these cells using fluorescence microscopy found GFP labeling of the cells at the membrane, as well as some intracellular staining. The A10 clone appeared to have more membrane localization than the C2 clone (**Figure 2.24**). Both cell lines show large changes in morphology from the standard kite-like morphology of HeLa cells. Instead, both cell lines are rounded, which may indicate changes to the cytoskeleton or adhesion receptors in these cells. We chose to use A10 cells as a model of NEU3-overexpressing cells.

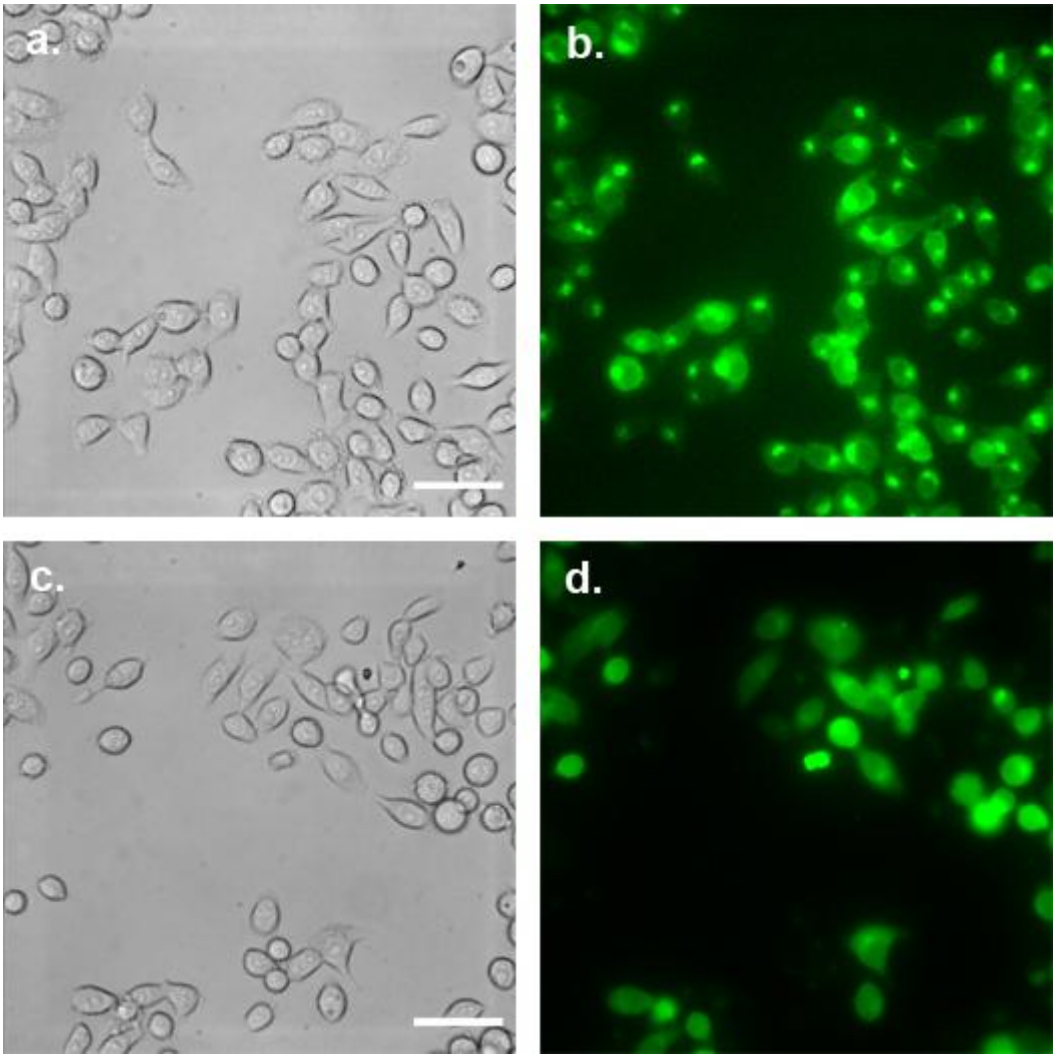

Figure 2.24 Fluorescence imaging of GFP-NEU3 expressing cells. GFP-NEU3 expressing HeLa cells, clones A10 (**a & b**) and C2 (**c & d**), were cultured in a confocal dish overnight at 37 ℃ in 5% CO_2, and then washed with PBS twice. The images were taken by epifluorescence microscopy. Scale bar = 100 μm.

To examine co-localization of integrins with gangliosides, we obtained two color images of HeLa cells stained with antibody for the α5 integrin, and with CTB-FITC. Fields were imaged by DIC, FITC (CTB-FITC), and TIRF (Cy5-anti-α5), and the channels were overlayed (**Figure 2.25**).

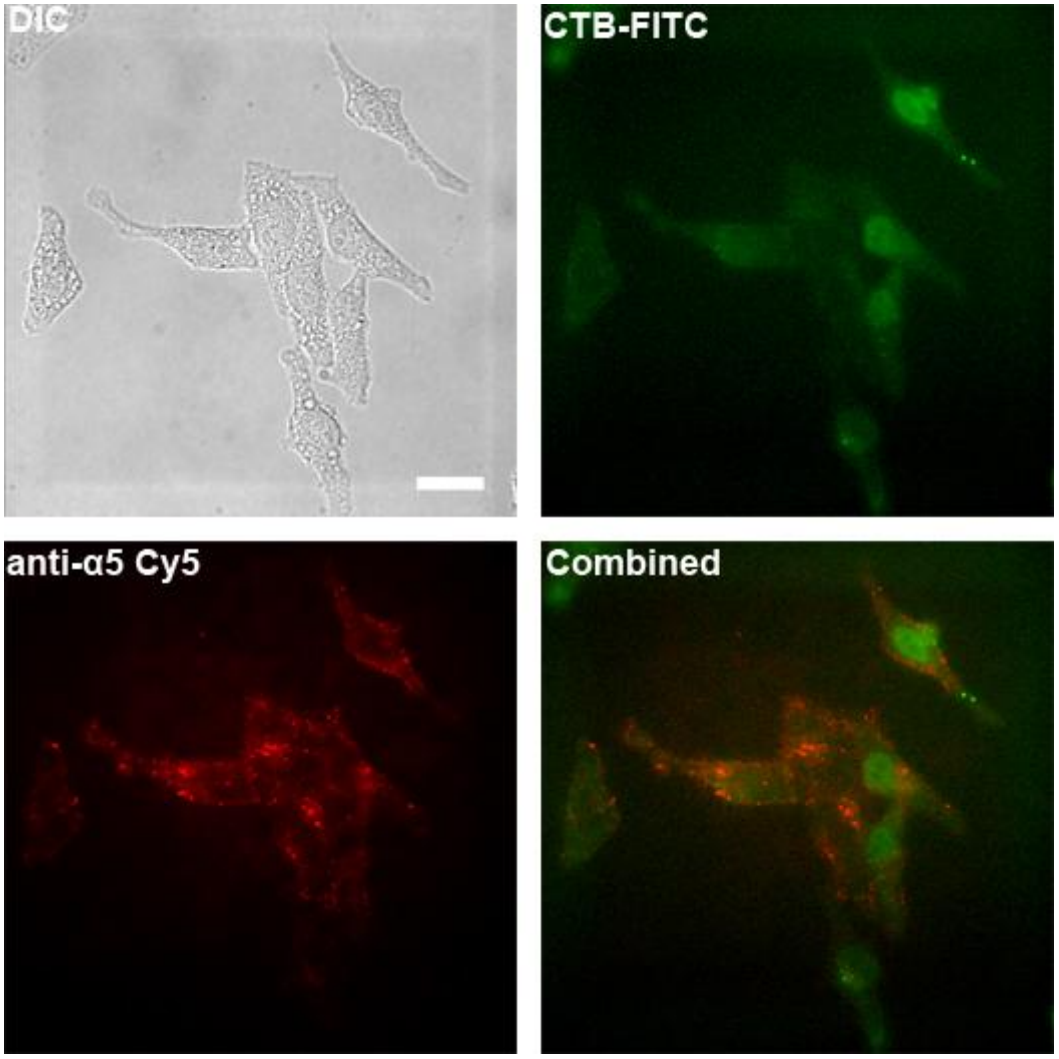

Figure 2.25 Labeling of fixed HeLa cells with CTB-FITC and Cy5-anti-α5. HeLa cells were cultured in a confocal dish overnight at 37 ℃ in 5% CO_2, and then washed with PBS twice. A fixative solution was added to cells (4% PFA in PBS) for 10 min at 4 ℃, followed by washing with PBS twice. CTB-FITC and Cy5-anti-α5 antibody were added for 10 min. Cells were then washed with PBS again. Images were acquired by TIRF. Scale bar = 25 μm.

The combined images indicated only minor or partial co-localization of the

integrin with CTB (**Figure 2.25**). The CTB-FITC images showed significant nuclear staining, similar to **Figures 2.20** and **2.21**.

We used three-color imaging in A10 cells to identify changes in localization to integrin, ganglioside, and NEU3 staining. A10 cells are difficult to work with, due to reduced spreading and attachment to surfaces, as mentioned above. We switched the CTB stain to a TRITC conjugate to avoid overlap with the GFP-NEU3 signal. We noted that the GFP signal was reduced in fixed cells, which may be a result of the PFA treatment (*55*). Overlayed images of A10 cells (**Figure 2.26**) showed significant nuclear staining by CTB. The α5 integrin maintained a similar staining pattern as in the wild-type HeLa cells. However, we did note that some regions showed co-localization of NEU3 and integrin staining.

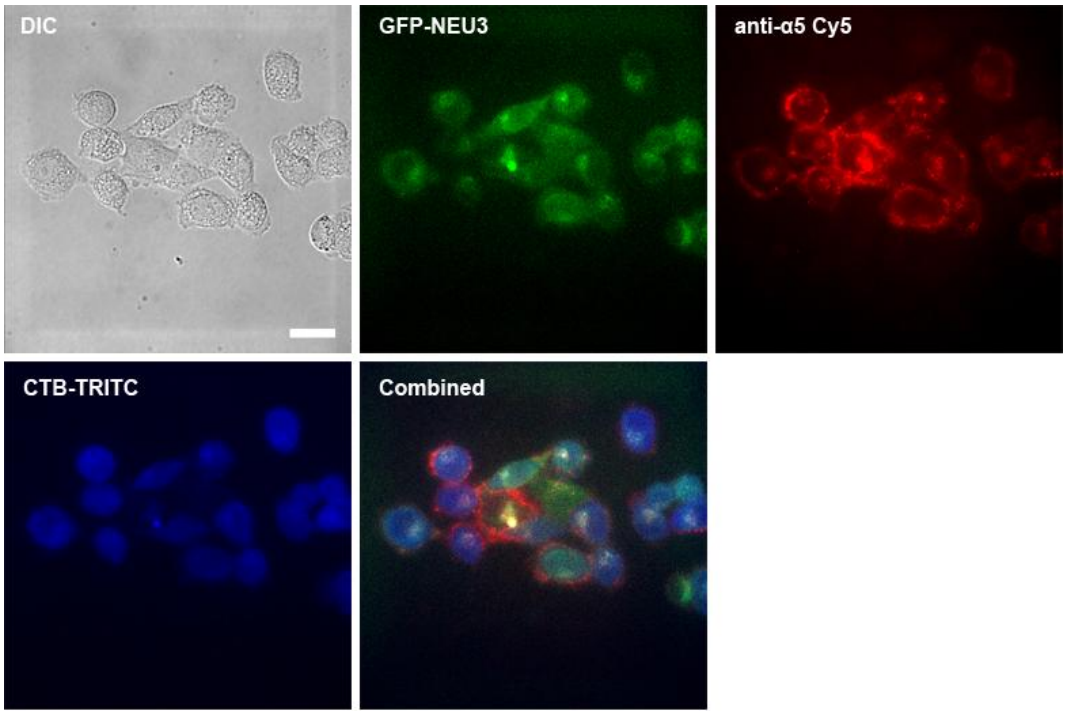

Figure 2.26 Fixed A10 cells labeled with CTB-TRITC and anti-α5 antibody. A10 cells were cultured in a confocal dish overnight at 37 ℃ in 5% CO_2, and then washed with PBS once. A solution of fixative (4% PFA in PBS) was added for 10 min at 4 ℃, followed by washing with PBS. CTB-TRITC and Cy5-anti-α5 were added for 10 min. Cells were washed again with PBS. Scale bar = 25 μm.

We next tried multi-color imaging in live cells. The protocol was similar to the one above; however, we skipped the fixative step and cells were stained at 20 ℃. These changes provided improved membrane staining and reduced intracellular staining with CTB (**Figure 2.27**). Then we applied the same protocol to live A10 cells with CTB-TRITC and Cy5-anti-α5 antibody (**Figure 2.28**). Again, live staining gave improved membrane staining for CTB. In A10 cells, we observed a dramatic change in localization for all three stains. The α5 integrin

formed large clusters on cells, and these regions also show co-localization of CTB and NEU3.

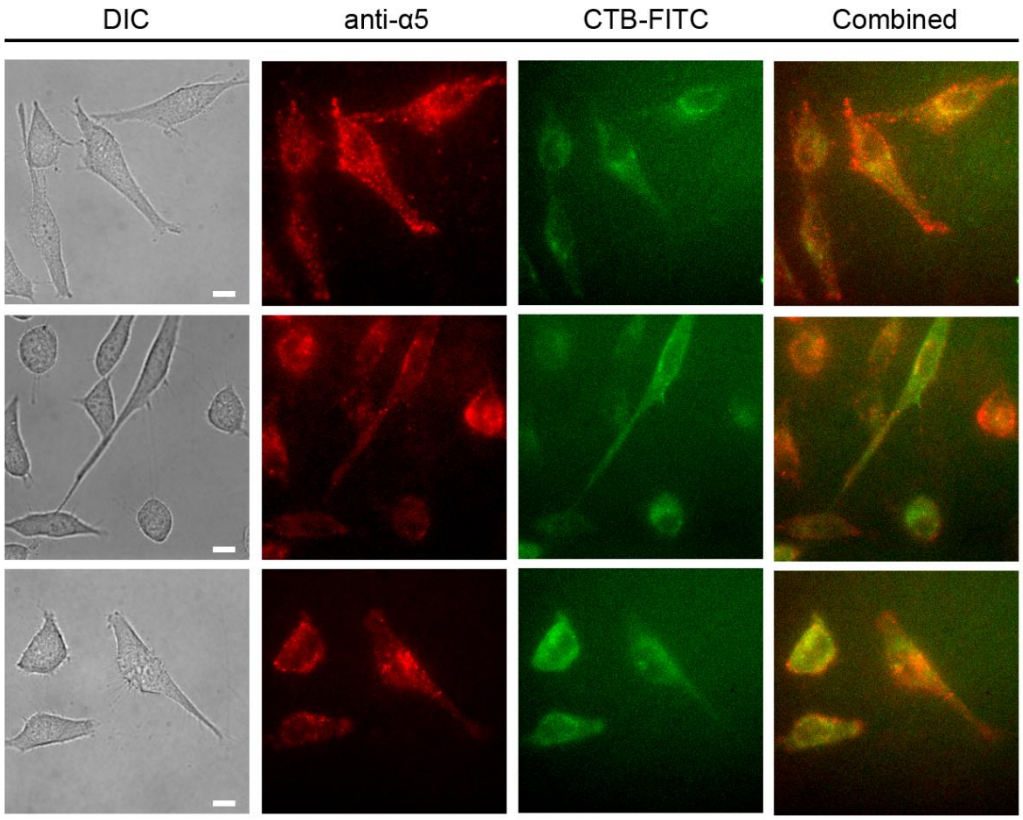

Figure 2.27 HeLa cells labeled with CTB-FITC and Cy5-anti-α5 antibody. HeLa cells were cultured in a confocal dish overnight at 37 ℃ in 5% CO_2, and then washed with PBS twice. CTB-FITC and Cy5-anti-α5 antibody were added for 10 min. Cells were then washed with PBS once. Fluorescence images were obtained by TIRF using either a 488 nm laser. Scale bar = 10 μm.

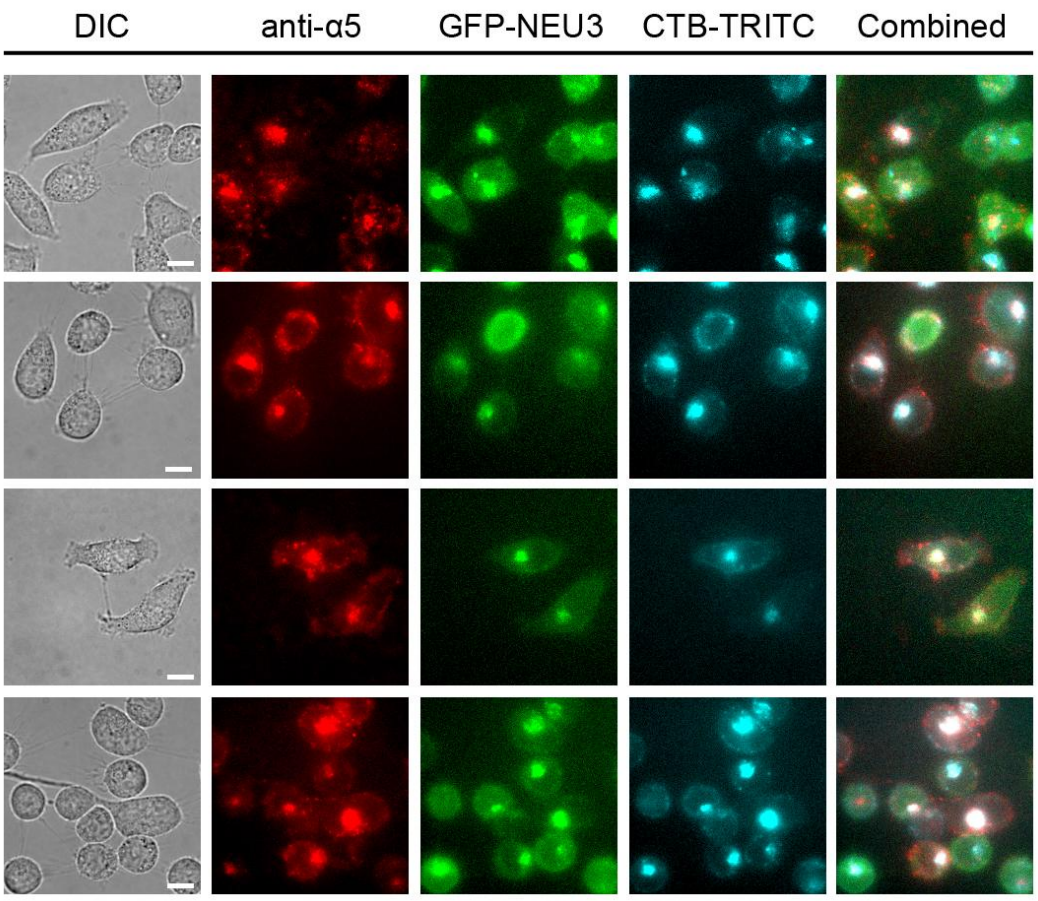

Figure 2.28 A10 cells labeled with CTB-TRITC and Cy5-anti-α5 antibody. HeLa cells were cultured in a confocal dish overnight at 37 ℃ in 5% CO_2, and then washed with PBS twice. CTB-TRITC and Cy5-anti-α5 antibody were added for 10 min. Cells were then washed with PBS once. Fluorescence images were obtained by TIRF using 488nm for GFP and 543 nm lasers for TRITC channel. Scale bar = 10 μm.

These multi-color experiments suggested that gangliosides, such as GM1, are colocalized with the α5 integrin in cells which overexpress NEU3. These clusters also contain the NEU3 enzyme, which may suggest that activation of NEU3, which we have shown can generate GM1 as a product, induces reorganization of adhesion receptors.

2.4.2 Lateral mobility of the α5 integrin

Adhesion receptors often exploit anchoring to the cytoskeleton as a mechanism to enhance or suppress attachment (*56*). As a result, experiments which provide information about the status of cytoskeletal attachment can give insight into the mechanism of adhesion. Our group has used measurement of receptor lateral mobility as a probe of adhesion receptor mechanisms (*57, 58*). Recently, we have started to employ single-molecule experiments as a way to rapidly determine the diffusion of multiple receptors in the membrane. Observation of individual receptors using total internal reflection fluorescence (TIRF) microscopy allows for detection of receptors in a restricted region close to the glass surface (*59*). Performing receptor tracking experiments in this mode, referred to as single dye tracking (SDT), allows us to obtain receptor trajectories for hundreds of samples in a single experiment. When interpreting trajectory data, we analyze individual trajectories using mean square displacement (MSD) to determine individual diffusion coefficients (*60, 61*). The range of diffusion coefficients observed for biomolecules on the cell surface is typically between 1 x 10^{-11} and 1 x 10^{-8} cm^2sec^{-1} (0.001 – 0.1 μm^2sec^{-1}). Lipids typically diffuse at rates close to the top of this range, while transmembrane proteins associated with the cytoskeleton will diffuse at rates closer to the bottom. Changes to the average

diffusion coefficient, or even changes to certain subpopulations, can be used to infer changes in cytoskeletal or inter-molecular contacts within the membrane.

Recent studies have shown that the β1 integrin may be regulated by clustering of GM1, resulting in down-regulation of adhesion to fibronectin via α5β1 and α4β1 integrins in T-cells.(*62*)

Our immunofluorescence studies had suggested that integrin mobility was significantly altered by the enzyme activity of NEU3. Additionally, these results may suggest that ganglioside products of NEU3, such as GM1, may alter the localization of integrins. We set out to study the lateral mobility of the α5β1 integrin under conditions that could lend support to a model of integrin regulation. We tested three key conditions including treatment of cells with DANA, GM1 and NEU3, to study the reorganization of integrin α5. HeLa cells were stained with Cy5-anti-α5 antibody, and cells were imaged by TIRF over 10 seconds to observe the movement of receptors. These experiments rely on sparse staining of integrin receptors and the signal-to-noise ratio provided by TIRF to allow observation of individual receptors. Data for each condition was obtained from 10 videos collected over two experiments. Data were analyzed according to a standard MSD analysis (*60*). Raw trajectories are individually converted to an MSD curve, which is then fit to determine the diffusion coefficient and type of diffusion using

$$< MSD >= 4Dt \quad (1)$$

, or in the case of anomalous diffusion

$$< MSD >= 4Dt^{\propto} \quad (2)$$

Fitting to eq. 1, lateral mobility is represented as diffusion (D) over a short period of time (400 ms), referred to as $D_{micro.}$ Diffusion over a longer period (3 s) was defined as D_{Macro}, using eq. 2. The degree of anomalous diffusion from D_{Macro} fits was measured by α. An α value close to 1 indicates Brownian diffusion, while numbers closer to zero indicate confined diffusion. Large α values indicate flow or directed diffusion.

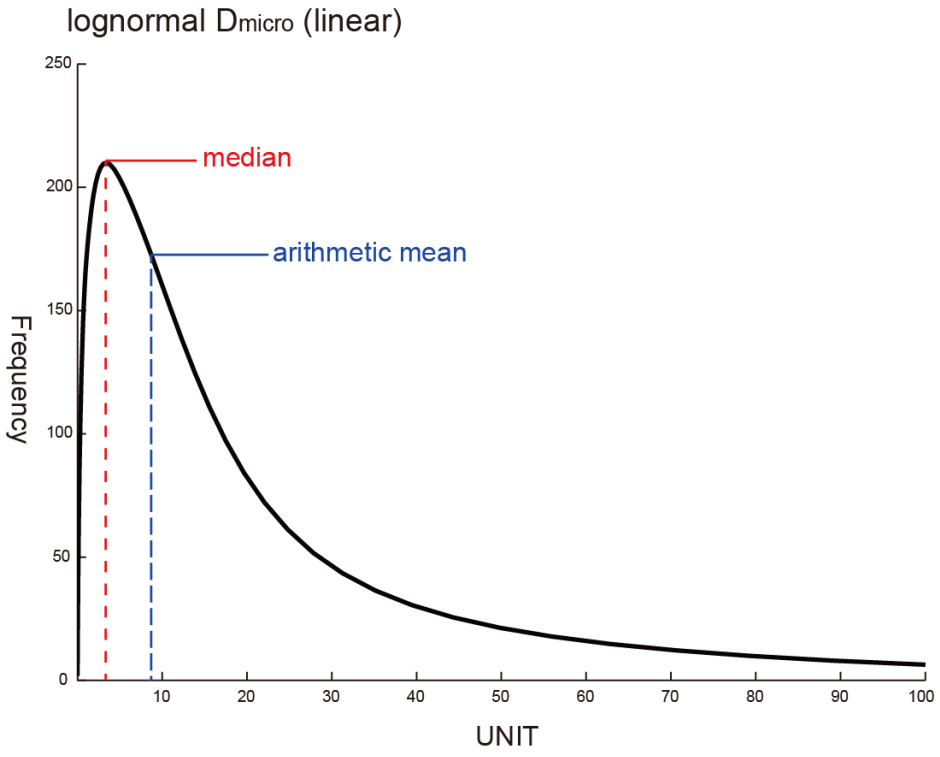
lognormal Dmicro (linear)
median
arithmetic mean
Frequency
UNIT
250
200
150
100
50
0
10
20
30
40
50
60
70
80
90
100

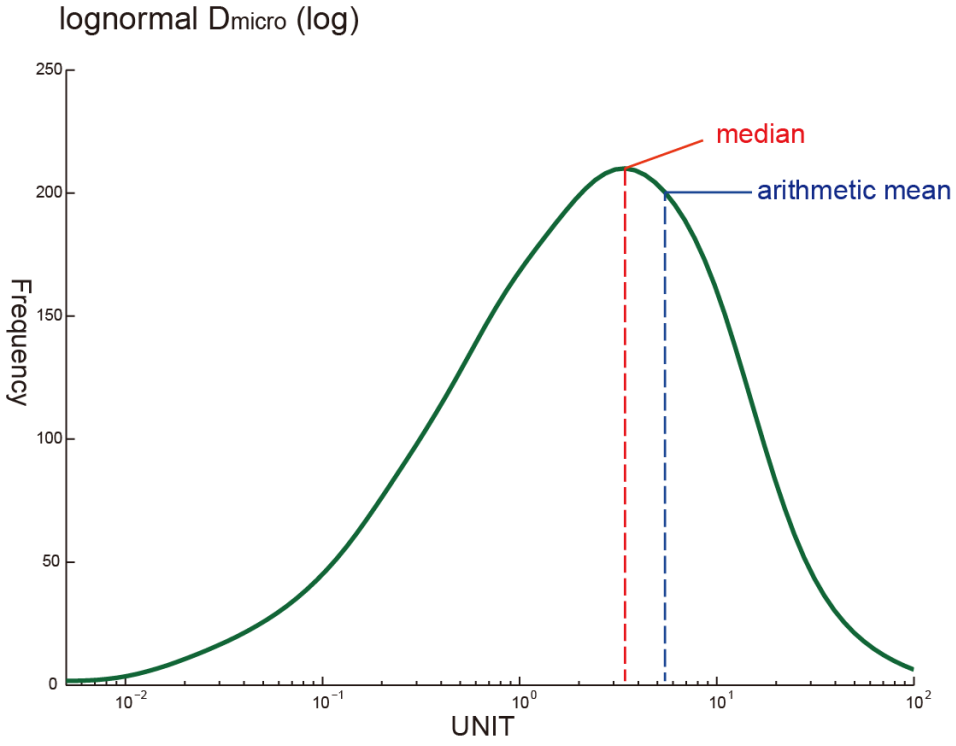
lognormal Dmicro (log)
median
arithmetic mean
Frequency
UNIT
250
200
150
100
50
0
10^-2
10^-1
10^0
10^1
10^2

Figure 2.29 Control condition D_{micro} values plotted in linear and log scales. Data were analyzed by MATlab R2012a using a custom script dezscribed in (*63*) to obtain diffusion coefficients. The data are plotted in both linear (top) and log (bottom) scales. These data appear to follow a lognormal distribution. Note that the arithmetic mean of a lognormal distribution is typically larger than the median of the distribution. In our analysis, we attempted to identify the median of lognormal distributions of diffusion coefficients.

The single dye tracking data obtained for either D_{micro} or D_{Macro} was fit to a lognormal distribution. The arithmetic means were calculated (**Table 2.5)** for both analyses. For fitting purposes, the data were transformed to logscale or fit to a lognormal distribution. Note that in this case, the arithmetic mean will not be coincident with the median of the curve(**Figure 2.29**).

Conditions	Trajectories	D_{micro}* (x10^{-10})	D_{Macro}* (x10^{-10})	Alpha
Control	1027	5.2 ±0.3	9.1 ±0.4	0.20 ±0.01
DANA	1249	5.6 ±0.3	9.3 ±0.5	0.23 ±0.01
GM1	1586	5.1 ±0.3	8.9 ±0.4	0.22 ±0.01
NEU3	2493	5.1 ±0.2	8.5 ±0.3***	0.18 ±0.01

Table 2.5 SDT data from α5β1 on HeLa cells. HeLa cells were cultured in a confocal dish overnight at 37 ℃ in 5% CO_2, and then washed twice with PBS. Cells were treated with the indicated condition for 3 hours. Cy5-Anti-α5 antibody was added and labeled for 10 min. Cells were then washed with PBS. Videos were taken by TRIF with 60x objective and 1.5 x magnifications. Data was analyzed using Matlab (*64*).

*Units were cm^2 sec^{-1}. *** $p<0.001$, compared to control.

The tracking data showed that integrin α5β1 diffusion had minor decreases after treatment with NEU3 and GM1 (**Table 2.5**). These results are consistent with our microscopy studies if the clustering of the integrin occurs through increased cytoskeletal attachment. Based on our in vitro studies of NEU3, treatment of cells with exogenous NEU3 would be expected to increase the concentration of GM1 and LacCer glycolipids. Although we observe only a small change in the lateral mobility (D_{micro}), there is a drop in this parameter for both GM1 (10 ng mL^{-1}) and NEU3 treatment.

In D_{Macro}, a significant decrease was only observed after the exogenous NEU3 treatment (**Table 2.5**) as compared with control.

In previous studies, our group has used a sub-population analysis of lateral mobility data. In T cells, we applied conformational-specific antibodies inhibitors to bind the LFA-1 receptor with PMA treatment and characterized LFA-1 diffusion profiles. The results were consistent with both inside-out and outside-in signal (*63*). In previous work, our group measured CD45 mobility by single-particle tracking, and the results provided more evidence that cytoskeletal interactions can dynamically regulate CD45 activity (*57*).

To confirm the presence of multiple populations, we performed an Akaike

Information Criterion (AIC) test (*65*). These tests indicated that D_{Macro} data sets were composed of at least two populations. Analysis of D_{micro} data sets suggested that there may be as many as three groups present. We performed fitting of the data using one and two populations.

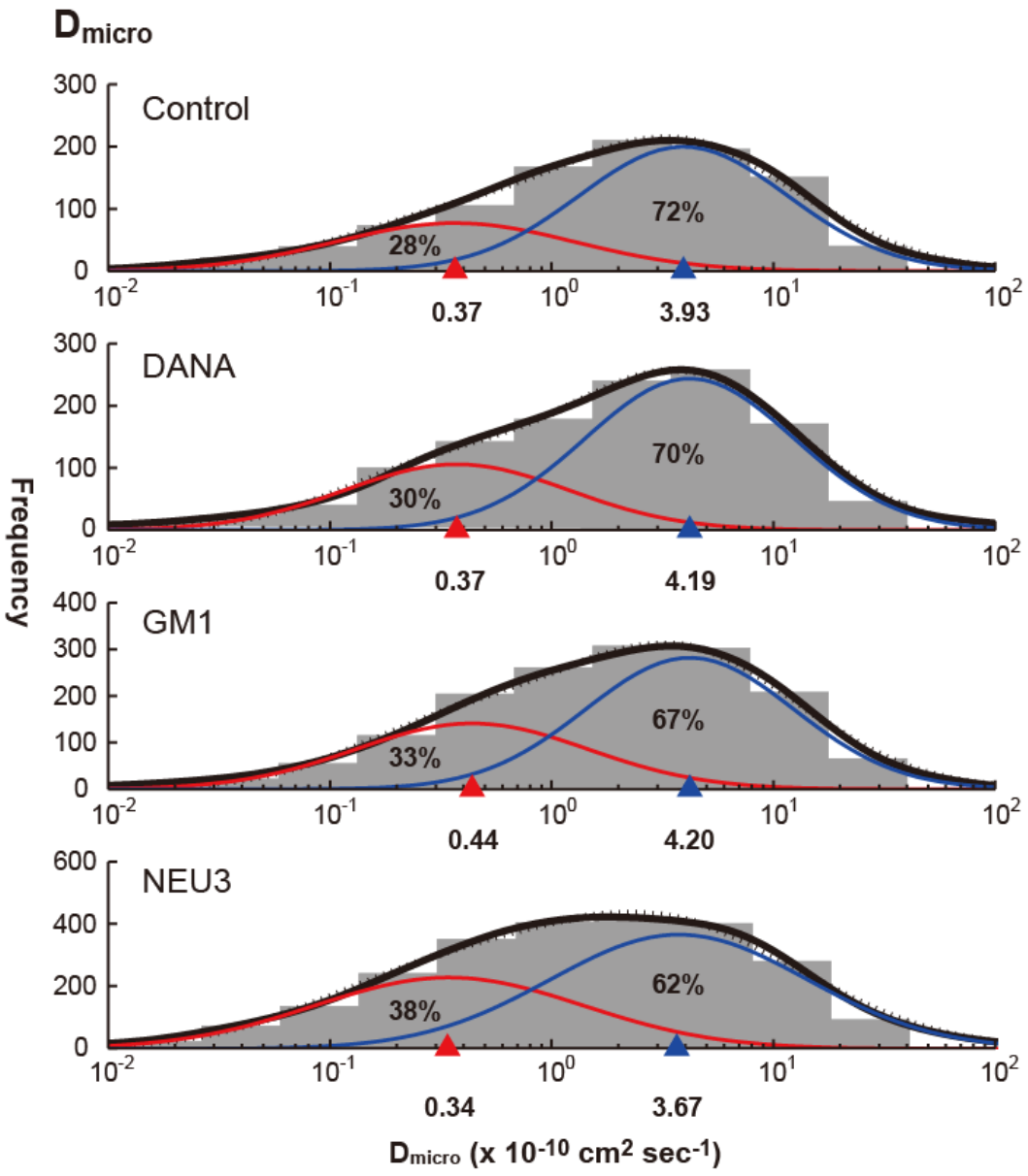

Figure 2.30 D_{micro} analysis of SDT data for α5β1 integrin on HeLa. Data were analyzed by MATlab R2012a using a custom script described in (*63*). In each condition, the red line indicates the fit of the slow-diffusing population and the blue line indicates a fit of the fast-diffusing population. The dashed line shows the sum of the two sub-population fits, and a solid black line indicates the raw population distribution based on a log-normal distribution. A triangle on the axis indicates the fit center.

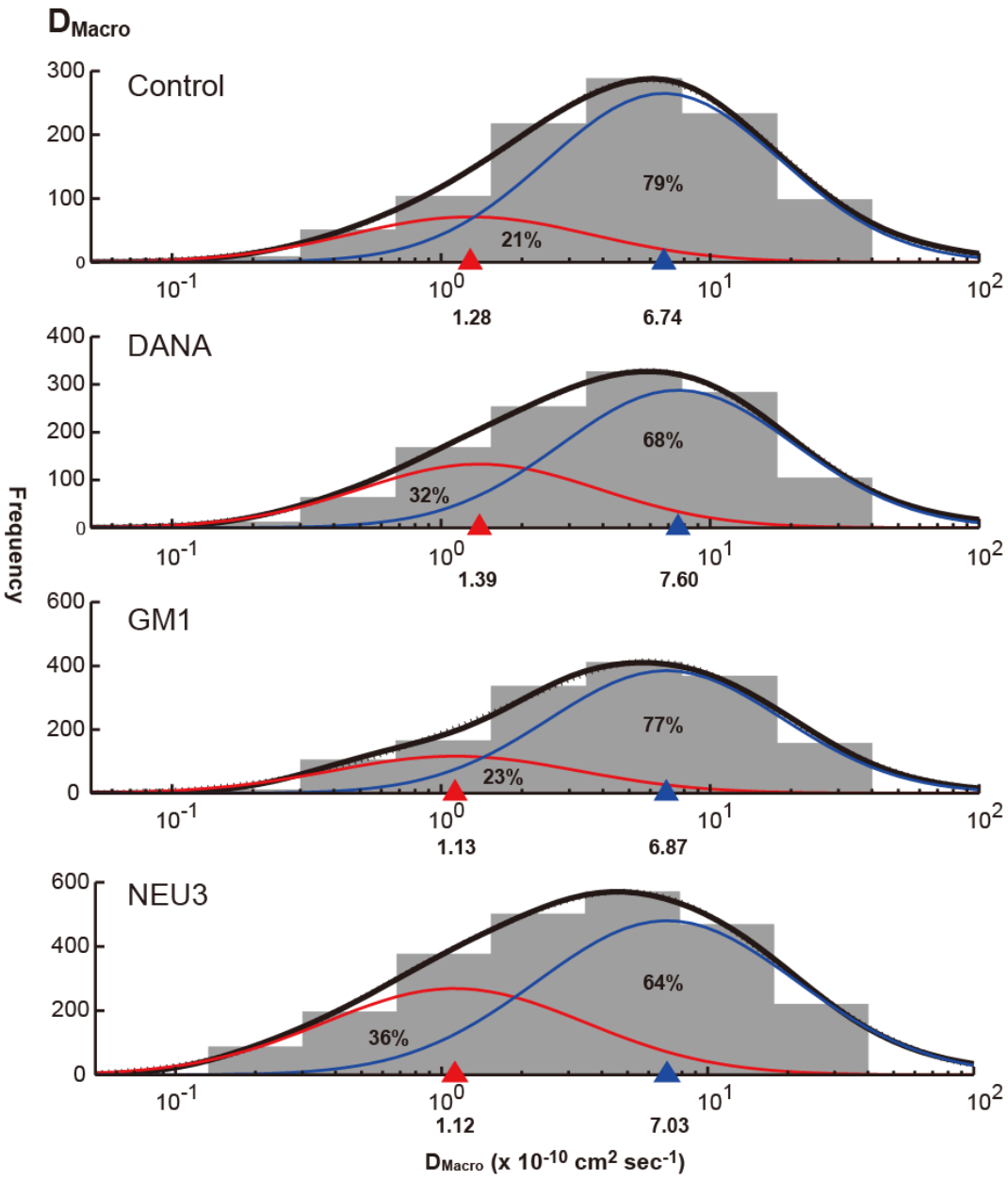

Figure 2.31 D_{Macro} analysis of SDT data for α5β1 integrin on HeLa. Data were analyzed by MATlab R2012a using a custom script described in (*63*). In each condition, the red line indicates the fit of the slow-diffusing population and the blue line indicates a fit of the fast-diffusing population. The dashed line shows the sum of the two sub-population fits, and a solid black line indicates the raw population distribution

based on a log-normal distribution. A triangle on the axis indicates the fit center.

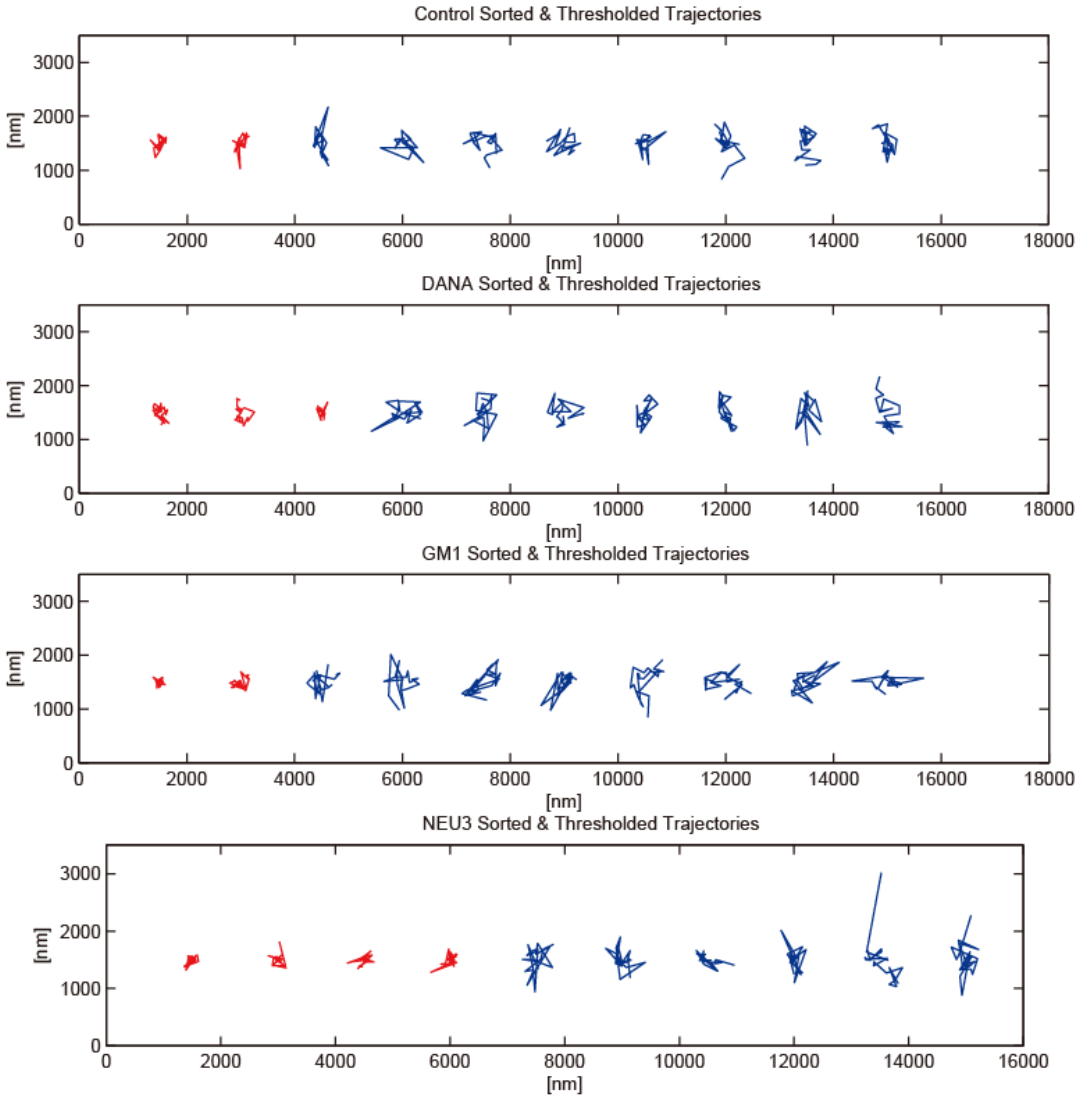

Figure 2.32 Sample trajectories from α5β1 integrin tracking on HeLa. Data were analyzed by MATlab R2012a. In each condition, the red trajectories are representative of the slow-diffusing population, and the blue trajectories are representative of the fast-diffusing population.

Subpopulation analysis of the D_{micro} results found a minor slow-diffusing

population (~0.4 x 10^{-10} cm^2 sec^{-1}) and a major fast diffusing population (~4.1 x 10^{-10} cm^2 sec^{-1}) (**Figure 2.30**). The D_{micro} data set did not show major changes in these populations; however, minor decreases in the slow population occur in NEU3 and GM1 conditions. We conclude that there was no major changes in D_{micro} diffusion profiles were observed.

The D_{Macro} analysis of SDT data from the α5β1 integrin showed similar trends as compared to the D_{micro} analysis (**Figure 2.31**). Again, we were able to fit the data to two populations including a slow-diffusing (~1.2 x 10^{-10} cm^2 sec^{-1}) and fast-diffusing (~7 x 10^{-10} cm^2 sec^{-1}) population. Treatment of cells with NEU3 shows an increase in the slow-diffusing population (from 23 to 36%). Treatment with GM1 shows a subtle increase in the slow-diffusing population (from 21 to 23%).

Analysis of D_{micro} and D_{Macro} data with a single log-normal distribution gave reasonable fits of the data (**Figure 2.33, 2.34**). The fit values are summarized in **Table 2.6**. Fitting of the D_{micro} data set to a single population found similar results to analysis using the arithmetic mean (**Table 2.6**). Treatment of cells with DANA resulted in an increase in D_{micro}, while treatment with GM1 and NEU3 both resulted in a decrease. The D_{Macro} single-population fits found the same trend; however, treatment with DANA appeared to cause a small decrease from control.

Conditions	D_{micro} (x 10^{-10} cm^2 sec^{-1})		
	D_{slow}	D_{fast}	Arithmetic Mean
Control	0.37 ±0.18	3.93 ±0.11	5.25 ±0.28
DANA	0.37 ±0.14	4.19 ±0.09	5.61 ±0.33
GM1	0.44 ±0.12	4.20 ±0.09	5.09 ±0.25
NEU3	0.34 ±0.13	3.67 ±0.10	5.11 ±0.23

Conditions	D_{Macro} (x 10^{-10} cm^2 sec^{-1})		
	D_{slow}	D_{fast}	Arithmetic Mean
Control	1.28 ±0.15	6.74 ±0.08	9.07 ±0.43
DANA	1.39 ±0.11	7.06 ±0.07	9.28 ±0.46
GM1	1.13 ±0.12	6.87 ±0.06	8.93 ±0.44
NEU3	1.12 ±0.08	7.03 ±0.06	8.52 ±0.30

Table 2.6 The logarithmic means for D_{micro} and D_{Macro} of α5 integrin diffusion on HeLa. Data was summarized from population diffusion figures. Error was determined as the standard error of the mean according to (*63*).

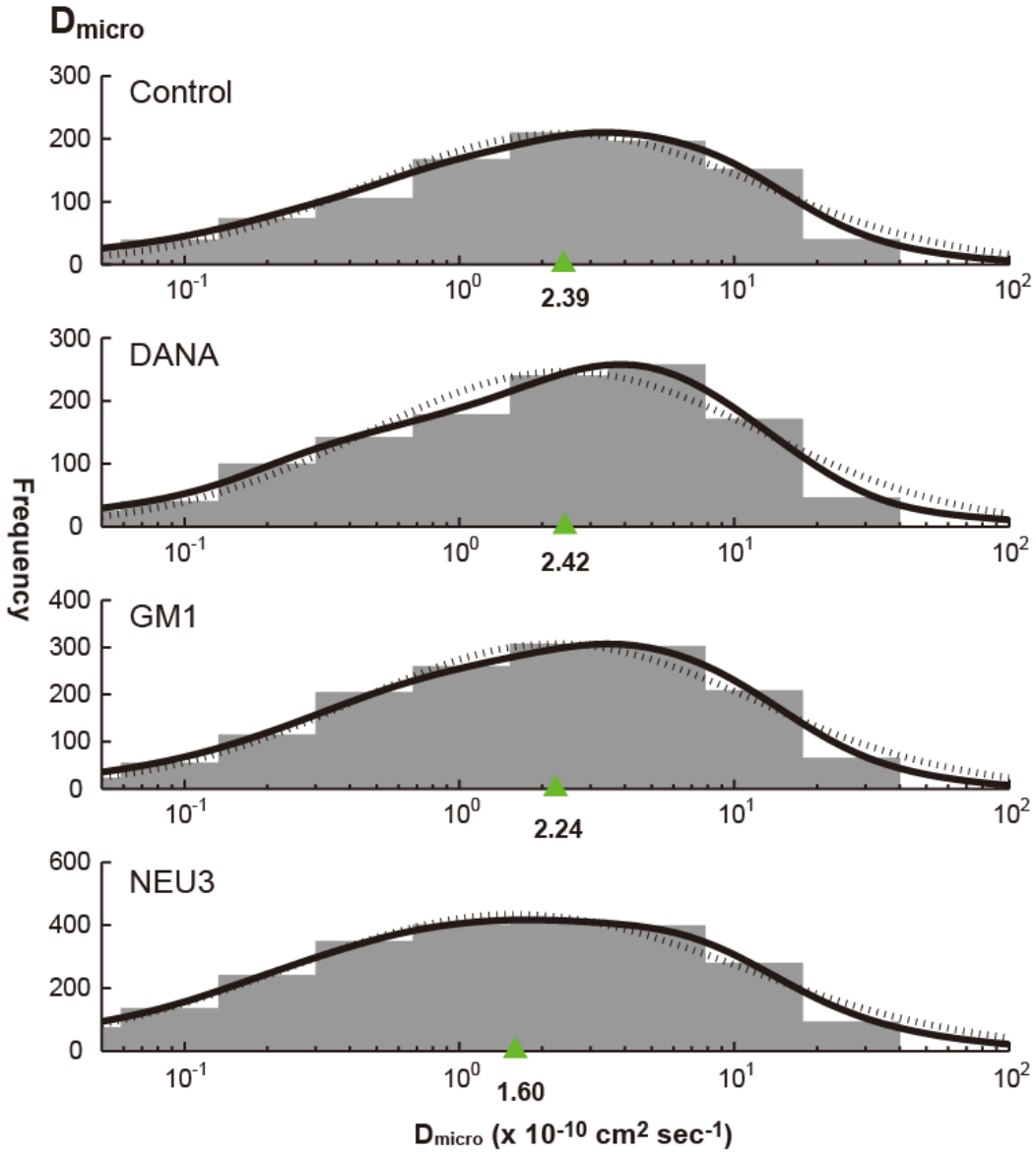

Figure 2.33 D_{micro} of the α5 integrin fit to a single population. Data were analyzed with custom scripts written in MATlab R2012a described in (*63*). In each condition, the solid line indicates the population density based on a log-normal distribution. The dashed line shows the curve-fit. The triangle marker on the axis indicates the fit center of the curve.

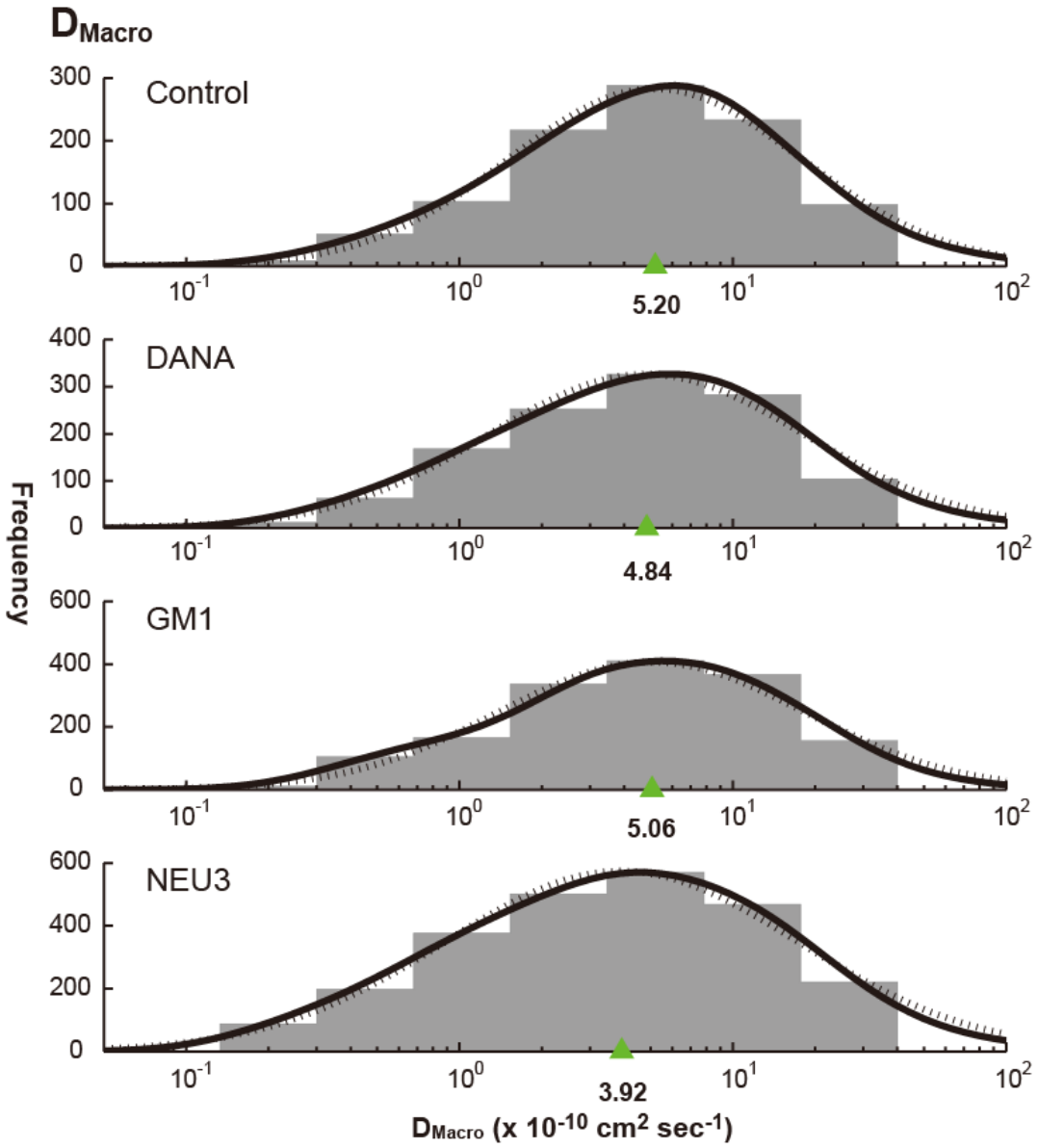

Figure 2.34 D_{Macro} of the α5 integrin fit to a single population. Data were analyzed with custom scripts written in MATlab R2012a described in (*63*). In each condition, the solid line indicates the population density based on a log-normal distribution. The dashed line shows the curve-fit. The triangle marker on the axis indicates the fit center of the curve.

Conditions	D_{micro} (x 10^{-10} cm^2 sec^{-1})		D_{Macro} (x 10^{-10} cm^2 sec^{-1})	
	D	Arithmetic Mean	D	Arithmetic Mean
Control	2.39 ±0.22	5.25 ±0.28	5.20 ±0.09	9.07 ±0.43
DANA	2.42 ±0.21	5.61 ±0.33	4.84 ±0.10	9.28 ±0.46
GM1	2.24 ±0.19	5.09 ±0.25	5.06 ±0.08	8.93 ±0.44
NEU3	1.60 ±0.28	5.11 ±0.23	3.92 ±0.10	8.52 ±0.30

Table 2.7 The logarithmic means for D_{micro} and D_{Macro} of α5 integrin diffusion on HeLa (one peak). Data was summarized from population diffusion figures. Error was determined as the standard error of the mean according to (*63*).

2.5 Conclusions and discussions

In this chapter, we described the use of cell migration assays, in vitro substrate assays, immuno-fluorescence, and single-molecule biophysics which provide crucial new insights into the regulation of integrin diffusion. We identified evidence that native human neuraminidase activity contributes to the regulation of integrin adhesion in an epithelial cell line (HeLa). In vitro substrate studies found that the human NEU3 and NEU4 isoenzymes converted complex

gangliosides, such as GT1b, to GM1. Both enzymes have α2,3- and α2,8-sialidase activity, and could therefore contribute to altering the composition of glycolipids found in the plasma membrane. Cell migration studies clearly demonstrate that neuraminidase enzymes known to modify glycolipid composition result in increased rates of cell migration. Importantly, the general sialidase inhibitor, DANA, significantly reduces cell migration – supporting a role for native sialidase activity in integrin regulation. Immunofluorescence studies indicate that the α5β1 integrin is generally found in microclusters which are well distributed at the cell surface, and does not co-localize with CTB-binding gangliosides. However, cells which overexpress NEU3 show the formation of large clusters of α5β1 integrin, which contain CTB-binding gangliosides and NEU3. Finally, lateral mobility studies of the α5β1 integrin demonstrate that treatment with NEU3 and GM1 resulted in reduced mobility of the integrin, supporting a role for cytoskeletal immobilization of the receptor to form clusters.

Human NEU3 and NEU4 target α2,3- and α2,8-linkages of sialic acid. Using HPTLC, we tested the sialidase activity of recombinant NEU3 and NEU4. These studies found that gangliosides including GT1b, GD1a, GD1b, and GM3 are substrates for both enzymes. GM1 was not a good substrate for either enzyme. Studies of glycolipids extracted from cells treated with recombinant enzymes were inconclusive. Only small changes in glycolipid composition were observed

by TLC. Based on our in vitro findings, we concluded that the low abundance of complex gangliosides limits our ability to observe the activity of NEU3 and NEU4 on extracted lipids. However, our in vitro results support the conclusion that the enzymes are capable of modifying membrane substrates.

Ganglioside composition affects integrin-mediated cell migration.

Using a cell migration assay, we probed the role of exogenously added neuraminidase enzymes, inhibitors, and glycolipids on integrin-mediated adhesion in HeLa cells. We found that NEU3 was able to increase cell migration rates, while inactive mutants of NEU3 (Y370F) had no effect. Other neuraminidase enzymes, such as NEU4 and *pf*NEU (at high concentration) gave the same effect. Treatment of cells with a general sialidase inhibitor, DANA, resulted in dramatic decreases in rates of cell migration. Additionally, treatment of cells with complex gangliosides, including GM1, resulted in decreased cell migration. On the other hand, treatment of cells with LacCer resulted in increased migration.

In our studies of A549 cells, we found that pfNEU and NEU4 had similar results. However, treatment of this cell line with NEU3 resulted in a decrease in cell migration rates. Although further work is required, we propose that these results are evidences that these two cell lines have different mechanisms regulate integrin-mediated adhesion. One possibility is that the target of NEU3 hydrolysis plays a negative regulatory role in these cells. We note that NEU4 is known to

modify both glycolipids and glycoproteins (*66*), while NEU3 only targets glycolipids. This finding could support the hypothesis that the two enzymes have different substrates.

Integrin α5, NEU3 and GM1 are co-localized on cell membrane.

In co-localization studies we found that the α5β1 integrin was not co-localized with CTB-binding gangliosides on wild-type cells. However, cells which overexpressed NEU3 demonstrated large reorganization of the integrin and CTB-binding gangliosides into a large cluster. These results lend support to the potential interaction of NEU3 with gangliosides that could help to induce integrin-clusters by altering ganglioside composition and membrane organization. These studies are ongoing and future work with alternative conditions may lead further support to these observations.

The lateral mobility of the α5β1 integrin is altered by gangliosides.

Using SDT, we obtained measurements of the lateral mobility of the α5β1 receptor. We found that integrin mobility was reduced in cells treated with conditions that result in receptor clusters, such as NEU3 and GM1. In contrast, treatment of cells with a sialidase inhibitor resulted in increased mobility. We concluded that these results were consistent with a model of diffusion which invokes cytoskeletal contact due to increased GM1 or LacCer content in the membrane.

In order to summarize our results, a model is provided below to integrate our observations from different assays (**Figure 2.32**). The integrin α5β1 may interact with GM3, and GM3 will inactivate α5β1 when it is bound.

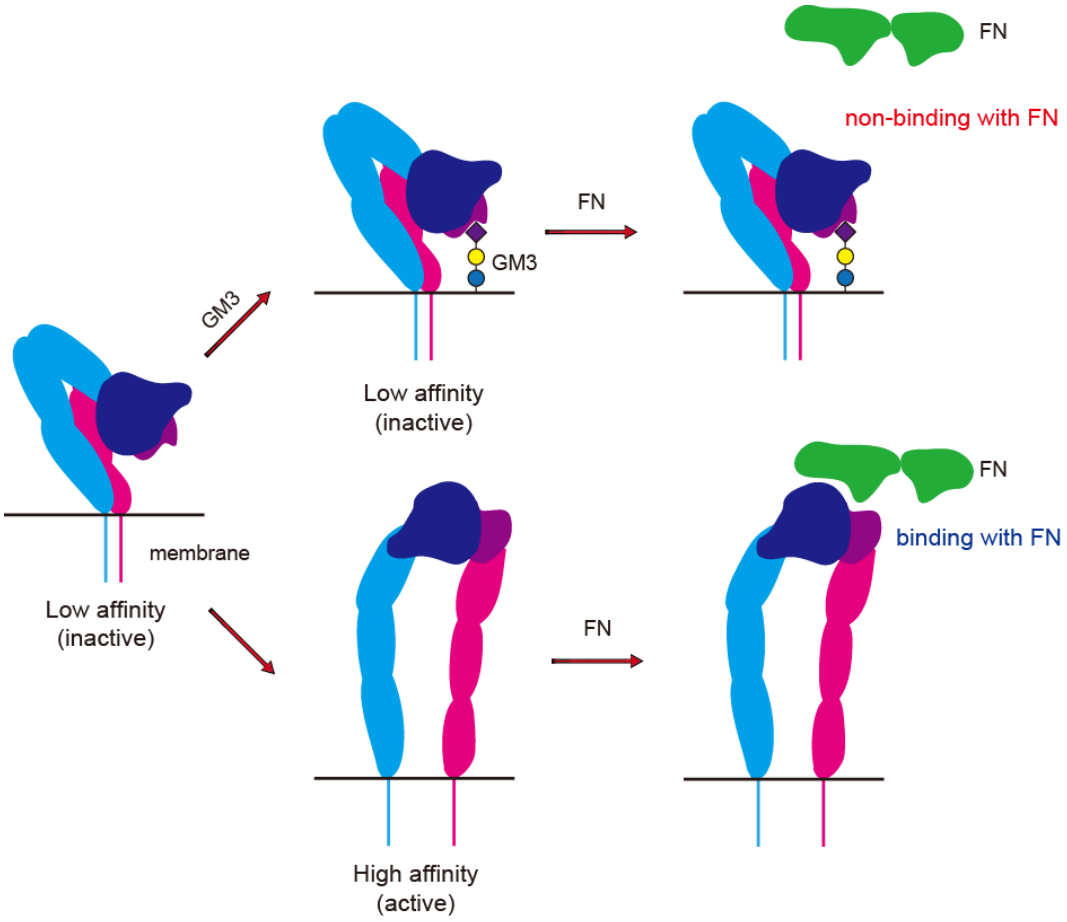

Figure 2.32 GM3-α5β1 integrin binding model. GM3 can bind with the low affinity state of α5β1 integrin and stabilize it, leading to the inhibition of binding between α5β1 integrin and fibronectin. Absence of GM3 will leading to α5β1 integrin changes to high affinity conformation and bind with fibronectin.

2.6 Materials and Methods

2.6.1 Reagents

Purified gangliosides LacCer, GM1 and GM3 were purchased from Avanti Polar lipids, Inc. (USA). GD1a, GD1b and GT1b were obtained from Santa Cruz Biotechnology (USA). Cy5-NHS ester was obtained from GE Healthcare (USA).

Human anti-CD49e (clone SAM-1) antibody was purchased from Santa Cruz Biotechnology (USA). A fluorescent conjugate of anti-CD49e was generated by reaction with the Cy5-NHS ester, and purified by gel filtration chromatography. FITC-labeled Cholera Toxin B was obtained from Sigma Aldrich (Milwaukee, WI, USA), and TRITC-labeled Cholera Toxin B subunit (CTB) from *Vibrio cholera* was obtained from List Biological Laboratories, Inc. (USA). Thymoquinone was obtained from Sigma Aldrich. Toxicity assays were performed using CellTilter 96 AQueous Non-Radioactive Cell Proliferation Assay (Promega, USA).

2.6.2 Cell lines

The HeLa cell line used was a generous gift of Dr. R.E. Campbell (University of Alberta). The A549 cell line was obtained from ATCC (Manassus, VA, USA).

Transfected cells were provided by C. Morales and Dr. S. Sipione (University of Alberta). Transfected cells express an N-terminal GRP-NEU3

fusion protein. Two clones were used in our experiments with vary only in their level of GRP expression (GFP-NEU3/A10 and NEU3-GFP/C2).

All cells were cultured in DMEM (Gibco, Invitrogen, USA) containing 10% Fetal Bovine Serum (Hyclone, Thermo, USA) and Penicillin/Streptomycin (Gibco, Invitrogen, USA). Transfected A10 and C2 cells were cultured in the same media supplemented with 800μg/mL G418.

2.6.3 Cell migration assays and data analysis.

Plates (12-well) were pre-treated with 10 μg/mL of fibronectin (FN) for 2 hours at 37 ℃ or 4 ℃ overnight, and then blocked with 0.2 mg/mL of BSA in PBS buffer for 1 hour at 37 ℃. Cells were counted and seeded into wells (HeLa, 4 x 10^5 cells/mL; A549, 5 x 10^5 cells/mL, 1 mL for each well) with fresh medium (1 mL). Plates were incubated overnight at 37 ℃ in a humidified incubator with 5% CO_2. The cell monolayer was carefully scratched with a gel-loading pipette tip (200 mL). Images of the wound were collected once every hour over 3 hours (6 images of each well), and each condition was run in four separate wells. Images were analyzed by NIS-Elements v3.5 and fit using linear regression according to $y = ax + b$, where a is the rate of migration, and b is the width of the wound at t = 0.

2.6.4 Cell toxicity.

Toxicity of conditions to cells were tested using an MTS assay followed

by the technical instruction from MTS assay kit company (Promega). A 96-well plate was loaded with 5 x 10^3 cells/well, and buffer containing the appropriate condition to be tested. Cells were incubated for 48 hours and then 20 μL of the MTS solution was added to each well and incubated for another 2 hours. The absorbance in each well was measured using a plate reader at 490 nm.

2.6.5 Lipid extraction and thin layer chromatography.

Cells were treated for 3 hours in a 12-well plate using the indicated conditions following the migration assay protocol. At the end of the incubation, cells were harvested with a cell scraper. Cells were suspended in PBS and washed 2 times, followed by extraction with a $CHCl_3$/MeOH (1:1) solution for 1 hour. After centrifuge and remove cell particle, dry the solution by N_2 and then dissolve the solid by $CHCl_3$/MeOH (1:1). The glycolipid solution was analyzed by HPTLC with AcOH/*n*-BuOH/0.5% aqueous $CaCl_2$ (1:2:1) as eluent. Lipids were then stained by an oricinol-H_2SO_4-EtOH solution and heated for 30 min at 100 ℃.

2.6.6 HPTLC analysis of Glycolipid substrates.

Gangliosides GM1, GM3, GD1a, GD1b and GT1b were dissolved in sodium bicarbonate buffer (200 μL, pH 4.7, 0.25 mg/mL final concentration). The indicated neuraminidase enzyme was then added to the solution (0.1 mg/mL final concentration) and incubated at 37 ℃ for 1 hour. The mixture was extracted with $CHCl_3$/MeOH (1:1, 200 μL), which was dried under a stream of N_2. The resulting

residue was desalted using a C_{18} column, and analyzed by HPTLC with AcOH/*n*-BuOH/0.5% aqueous $CaCl_2$ (1:2:1) as eluent for GM1 and GM3, and with $CHCl_3$/MeOH/0.25 aqueous KCl (60:40:8) as eluent for GD1a, GD1b and GT1b. Lipids were stained with an oricinol-H_2SO_4-EtOH solution and heated for 30 min at 100 ℃, and analyzed by densitometry using ImageJ (*67*).

2.6.7 Immunofluorescence imaging

Cells were cultured in a confocal dish overnight at 37 ℃ in a humidified incubator with 5% CO_2. Cells were washed with PBS before labeling. HeLa cells were labeled with Cy5-anti-CD49e (50 ng) and FITC-CTB (5 μg) for 10 min, and then washed again with PBS. A10 cells were labeled with Cy5-anti-CD49e (50 ng) and TRITC-CTB (5 μg) for 10min, and then washed with PBS. Live cells were imaged with a combination of epifluorescence and total-internal reflection fluorescence (TIRF) microscopy on a Nikon ECLIPSE *Ti* microscope system. Images were processed with NIS-Elements v3.5 (Nikon, USA). GFP, TRITC and FITC-conjugates of CTB were imaged by epifluorescence, Cy5-conjugates were imaged by TIRF.

2.6.8 Single-Dye Tracking

HeLa cells were cultured in a confocal dish overnight at 37 ℃ in a humidified incubator with 5% CO_2. Cells were washed with PBS twice, followed by addition of Cy5-anti-CD49e (50 ng) for 10 min at room temperature. Cells

were washed twice with PBS to remove excess antibody. Video images of labeled cells were taken in TIRF with a 60x objective (NA = 1.4) and 1.5x amplification on a Nikon ECLIPSE *Ti* microscope system. Data were processed using and NIS-Elements v3.5 (Nikon, USA). Single-dye trajectories were analyzed using U-Track (*64*), and the resulting data was processed using a custom software package developed in MATlab (Mathworks, Framingham MA, USA).

2.7 References

1. Berrier, A. L., and Yamada, K. M. (2007) Cell-matrix adhesion, *Journal of cellular physiology 213*, 565-573.
2. Morgan, M. R., Humphries, M. J., and Bass, M. D. (2007) Synergistic control of cell adhesion by integrins and syndecans, *Nature reviews. Molecular cell biology 8*, 957-969.
3. Ginsberg, M. H., Partridge, A., and Shattil, S. J. (2005) Integrin regulation, *Current opinion in cell biology 17*, 509-516.
4. Lahlou, H., and Muller, W. J. (2011) beta1-integrins signaling and mammary tumor progression in transgenic mouse models: implications for human breast cancer, *Breast cancer research : BCR 13*, 229.
5. Brownlie, R. J., and Zamoyska, R. (2013) T cell receptor signalling networks: branched, diversified and bounded, *Nature reviews. Immunology 13*, 257-269.
6. Paller, A. S., Arnsmeier, S. L., Chen, J. D., and Woodley, D. T. (1995) Ganglioside GT1b inhibits keratinocyte adhesion and migration on a fibronectin matrix, *J Invest Dermatol 105*, 237-242.
7. Wang, X. Q., Sun, P., and Paller, A. S. (2002) Ganglioside modulation regulates epithelial cell adhesion and spreading via ganglioside-specific

effects on signaling, *The Journal of biological chemistry 277*, 40410-40419.

8. Wang, X., Sun, P., Al-Qamari, A., Tai, T., Kawashima, I., and Paller, A. S. (2001) Carbohydrate-carbohydrate binding of ganglioside to integrin alpha(5) modulates alpha(5)beta(1) function, *The Journal of biological chemistry 276*, 8436-8444.

9. Wang, X. Q., Sun, P., and Paller, A. S. (2003) Ganglioside GM3 inhibits matrix metalloproteinase-9 activation and disrupts its association with integrin, *The Journal of biological chemistry 278*, 25591-25599.

10. Li, Y., and Chen, X. (2012) Sialic acid metabolism and sialyltransferases: natural functions and applications, *Applied microbiology and biotechnology 94*, 887-905.

11. Wandall, H. H., Rumjantseva, V., Sorensen, A. L., Patel-Hett, S., Josefsson, E. C., Bennett, E. P., Italiano, J. E., Jr., Clausen, H., Hartwig, J. H., and Hoffmeister, K. M. (2012) The origin and function of platelet glycosyltransferases, *Blood 120*, 626-635.

12. Crespo, P. M., Demichelis, V. T., and Daniotti, J. L. (2010) Neobiosynthesis of glycosphingolipids by plasma membrane-associated glycosyltransferases, *The Journal of biological chemistry 285*, 29179-29190.

13. Schwartz-Albiez, R., Merling, A., Martin, S., Haas, R., and Gross, H. J. (2004) Cell surface sialylation and ecto-sialyltransferase activity of human CD34 progenitors from peripheral blood and bone marrow, *Glycoconj J 21*, 451-459.

14. Vilcaes, A. A., Demichelis, V. T., and Daniotti, J. L. (2011) Trans-activity of plasma membrane-associated ganglioside sialyltransferase in mammalian cells, *The Journal of biological chemistry 286*, 31437-31446.

15. Miyagi, T., Wada, T., Yamaguchi, K., and Hata, K. (2004) Sialidase and malignancy: a minireview, *Glycoconj J 20*, 189-198.

16. Monti, E., Bonten, E., D'Azzo, A., Bresciani, R., Venerando, B., Borsani, G., Schauer, R., and Tettamanti, G. (2010) Sialidases in vertebrates: a family of enzymes tailored for several cell functions, *Advances in carbohydrate chemistry and biochemistry 64*, 403-479.

17. Miyagi, T., Wada, T., and Yamaguchi, K. (2008) Roles of plasma membrane-associated sialidase NEU3 in human cancers, *Biochimica et biophysica acta 1780*, 532-537.

18. Monti, E., Bassi, M. T., Papini, N., Riboni, M., Manzoni, M., Venerando, B., Croci, G., Preti, A., Ballabio, A., Tettamanti, G., and Borsani, G. (2000) Identification and expression of NEU3, a novel human sialidase associated to the plasma membrane, *The Biochemical journal 349*, 343-351.

19. Yamaguchi, K., Hata, K., Koseki, K., Shiozaki, K., Akita, H., Wada, T., Moriya, S., and Miyagi, T. (2005) Evidence for mitochondrial localization of a novel human sialidase (NEU4), *The Biochemical journal 390*, 85-93.

20. Sandbhor, M. S., Soya, N., Albohy, A., Zheng, R. B., Cartmell, J., Bundle, D. R., Klassen, J. S., and Cairo, C. W. (2011) Substrate recognition of the membrane-associated sialidase NEU3 requires a hydrophobic aglycone, *Biochemistry 50*, 6753-6762.

21. Zou, Y., Albohy, A., Sandbhor, M., and Cairo, C. W. (2010) Inhibition of human neuraminidase 3 (NEU3) by C9-triazole derivatives of 2,3-didehydro-N-acetyl-neuraminic acid, *Bioorganic & medicinal chemistry letters 20*, 7529-7533.

22. Zhang, Y., Albohy, A., Zou, Y., Smutova, V., Pshezhetsky, A. V., and Cairo, C. W. (2013) Identification of Selective Inhibitors for Human Neuraminidase Isoenzymes Using C4,C7-Modified 2-Deoxy-2,3-didehydro-N-acetylneuraminic Acid (DANA) Analogues, *Journal of medicinal chemistry 56*, 2948-2958.

23. Magesh, S., Moriya, S., Suzuki, T., Miyagi, T., Ishida, H., and Kiso, M. (2008) Design, synthesis, and biological evaluation of human sialidase inhibitors. Part 1: selective inhibitors of lysosomal sialidase (NEU1), *Bioorganic & medicinal chemistry letters 18*, 532-537.

24. Albohy, A., Zhang, Y., Smutova, V., Pshezhetsky, A. V., and Cairo, C. W. (2013) Identification of Selective Nanomolar Inhibitors of the Human Neuraminidase, NEU4, *ACS Medicinal Chemistry Letters*.

25. Decaestecker, C., Debeir, O., Van Ham, P., and Kiss, R. (2007) Can anti-migratory drugs be screened in vitro? A review of 2D and 3D assays for the quantitative analysis of cell migration, *Medicinal research reviews 27*, 149-176.

26. Liang, C. C., Park, A. Y., and Guan, J. L. (2007) In vitro scratch assay: a convenient and inexpensive method for analysis of cell migration in vitro, *Nature protocols 2*, 329-333.

27. Stephens, D. J., and Allan, V. J. (2003) Light microscopy techniques for live cell imaging, *Science 300*, 82-86.

28. Denk, W., Strickler, J. H., and Webb, W. W. (1990) Two-photon laser scanning fluorescence microscopy, *Science 248*, 73-76.

29. Muthing, J. (1996) High-resolution thin-layer chromatography of gangliosides, *J. Chromatogr. A 720*, 3-25.

30. Ando, S., Chang, N. C., and Yu, R. K. (1978) High-performance thin-layer chromatography and densitometric determination of brain ganglioside compositions of several species, *Analytical biochemistry 89*, 437-450.

31. Schneider, C. A., Rasband, W. S., and Eliceiri, K. W. (2012) NIH Image to

ImageJ: 25 years of image analysis, *Nat. Methods 9*, 671-675.

32. Vuori, K., and Ruoslahti, E. (1993) Activation of protein kinase C precedes alpha 5 beta 1 integrin-mediated cell spreading on fibronectin, *J. Biol. Chem. 268*, 21459-21462.

33. Zhang, Y., Albohy, A., Smutova, V., Pshezhetsky, A., and Cairo, C. W. (2013) Identification of selective inhibitors of human sialidase isoenzymes using *C*4, *C*7-modified 2-deoxy-2,3-didehydro-*N*-acetylneuraminic acid (DANA) analogs, *J. Med. Chem. 56*, 2948-2958.

34. Finlay, T. M., Jayanth, P., Amith, S. R., Gilmour, A., Guzzo, C., Gee, K., Beyaert, R., and Szewczuk, M. R. (2010) Thymoquinone from nutraceutical black cumin oil activates Neu4 sialidase in live macrophage, dendritic, and normal and type I sialidosis human fibroblast cells via GPCR Galphai proteins and matrix metalloproteinase-9, *Glycoconjugate J. 27*, 329-348.

35. Takahashi, K., Mitoma, J., Hosono, M., Shiozaki, K., Sato, C., Yamaguchi, K., Kitajima, K., Higashi, H., Nitta, K., Shima, H., and Miyagi, T. (2012) Sialidase NEU4 Hydrolyzes Polysialic Acids of Neural Cell Adhesion Molecules and Negatively Regulates Neurite Formation by Hippocampal Neurons, *J. Biol. Chem. 287*, 14816-14826.

36. Seyrantepe, V., Landry, K., Trudel, S., Hassan, J. A., Morales, C. R., and

Pshezhetsky, A. V. (2004) Neu4, a novel human lysosomal lumen sialidase, confers normal phenotype to sialidosis and galactosialidosis cells, *J. Biol. Chem. 279*, 37021-37029.

37. Azuma, Y., Sato, H., Higai, K., and Matsumoto, K. (2007) Enhanced expression of membrane-associated sialidase Neu3 decreases GD3 and increases GM3 on the surface of Jurkat cells during etoposide-induced apoptosis, *Biological & pharmaceutical bulletin 30*, 1680-1684.

38. Miyagi, T., Wada, T., Iwamatsu, A., Hata, K., Yoshikawa, Y., Tokuyama, S., and Sawada, M. (1999) Molecular cloning and characterization of a plasma membrane-associated sialidase specific for gangliosides, *The Journal of biological chemistry 274*, 5004-5011.

39. Tringali, C., Papini, N., Fusi, P., Croci, G., Borsani, G., Preti, A., Tortora, P., Tettamanti, G., Venerando, B., and Monti, E. (2004) Properties of recombinant human cytosolic sialidase HsNEU2. The enzyme hydrolyzes monomerically dispersed GM1 ganglioside molecules, *The Journal of biological chemistry 279*, 3169-3179.

40. Albohy, A., Mohan, S., Zheng, R. B., Pinto, B. M., and Cairo, C. W. (2011) Inhibitor selectivity of a new class of oseltamivir analogs against viral neuraminidase over human neuraminidase enzymes, *Bioorganic & medicinal chemistry 19*, 2817-2822.

41. Albohy, A., Li, M. D., Zheng, R. B., Zou, C., and Cairo, C. W. (2010) Insight into substrate recognition and catalysis by the human neuraminidase 3 (NEU3) through molecular modeling and site-directed mutagenesis, *Glycobiology 20*, 1127-1138.

42. Perillo, M. A., Yu, R. K., and Maggio, B. (1994) Modulation of the activity of Clostridium perfringens neuraminidase by the molecular organization of gangliosides in monolayers, *Biochimica et biophysica acta 1193*, 155-164.

43. Kramer, N., Walzl, A., Unger, C., Rosner, M., Krupitza, G., Hengstschlager, M., and Dolznig, H. (2013) In vitro cell migration and invasion assays, *Mutation research 752*, 10-24.

44. Singh, P., Carraher, C., and Schwarzbauer, J. E. (2010) Assembly of fibronectin extracellular matrix, *Annual review of cell and developmental biology 26*, 397-419.

45. Shoji, K., Ohashi, K., Sampei, K., Oikawa, M., and Mizuno, K. (2012) Cytochalasin D acts as an inhibitor of the actin-cofilin interaction, *Biochemical and biophysical research communications 424*, 52-57.

46. Finlay, T. M., Jayanth, P., Amith, S. R., Gilmour, A., Guzzo, C., Gee, K., Beyaert, R., and Szewczuk, M. R. (2010) Thymoquinone from nutraceutical black cumin oil activates Neu4 sialidase in live macrophage, dendritic, and normal and type I sialidosis human fibroblast cells via GPCR

Galphai proteins and matrix metalloproteinase-9, *Glycoconj J 27*, 329-348.

47. Tsakiridis, T., Tong, P., Matthews, B., Tsiani, E., Bilan, P. J., Klip, A., and Downey, G. P. (1999) Role of the actin cytoskeleton in insulin action, *Microscopy research and technique 47*, 79-92.

48. Keenan, T. W., Schmid, E., Franke, W. W., and Wiegandt, H. (1975) Exogenous glycosphingolipids suppress growth rate of transformed and untransformed 3T3 mouse cells, *Experimental cell research 92*, 259-270.

49. Cory, A. H., Owen, T. C., Barltrop, J. A., and Cory, J. G. (1991) Use of an aqueous soluble tetrazolium/formazan assay for cell growth assays in culture, *Cancer communications 3*, 207-212.

50. Gopalakrishna, P., Rangaraj, N., and Pande, G. (2004) Cholesterol alters the interaction of glycosphingolipid GM3 with alpha 5 beta 1 integrin and increases integrin-mediated cell adhesion to fibronectin, *Experimental cell research 300*, 43-53.

51. Zhang, Y., Lu, H., Dazin, P., and Kapila, Y. (2004) Functional differences between integrin alpha4 and integrins alpha5/alphav in modulating the motility of human oral squamous carcinoma cells in response to the V region and heparin-binding domain of fibronectin, *Experimental cell research 295*, 48-58.

52. Massin, F., Rubinstein, E., Faure, G. C., Martinet, Y., Boucheix, C., and

Bene, M. C. (2004) Tetraspan and beta-1 integrins expression pattern of the epithelial lung adenocarcinoma cell line A549 and its sensitivity to divalent cations, *Cytometry. Part B, Clinical cytometry 60*, 31-36.

53. Sanchez, J., and Holmgren, J. (2011) Cholera toxin - a foe & a friend, *The Indian journal of medical research 133*, 153-163.

54. Zeller, R. (2001) Fixation, embedding, and sectioning of tissues, embryos, and single cells, *Current protocols in pharmacology / editorial board, S.J. Enna Appendix 3*, 3D.

55. Brock, R., Hamelers, I. H., and Jovin, T. M. (1999) Comparison of fixation protocols for adherent cultured cells applied to a GFP fusion protein of the epidermal growth factor receptor, *Cytometry 35*, 353-362.

56. Cairo, C. W., and Golan, D. E. (2008) T cell adhesion mechanisms revealed by receptor lateral mobility, *Biopolymers 89*, 409-419.

57. Cairo, C. W., Das, R., Albohy, A., Baca, Q. J., Pradhan, D., Morrow, J. S., Coombs, D., and Golan, D. E. (2010) Dynamic regulation of CD45 lateral mobility by the spectrin-ankyrin cytoskeleton of T cells, *The Journal of biological chemistry 285*, 11392-11401.

58. Rajani, V., Carrero, G., Golan, D. E., de Vries, G., and Cairo, C. W. (2011) Analysis of molecular diffusion by first-passage time variance identifies the size of confinement zones, *Biophysical journal 100*, 1463-1472.

59. Dixit, R., and Ross, J. L. (2010) Studying plus-end tracking at single molecule resolution using TIRF microscopy, *Methods in cell biology 95*, 543-554.

60. Saxton, M. J., and Jacobson, K. (1997) Single-particle tracking: applications to membrane dynamics, *Annual review of biophysics and biomolecular structure 26*, 373-399.

61. Saxton, M. J. (2008) Single-particle tracking: connecting the dots, *Nature methods 5*, 671-672.

62. Mitchell, J. S., Brown, W. S., Woodside, D. G., Vanderslice, P., and McIntyre, B. W. (2009) Clustering T-cell GM1 lipid rafts increases cellular resistance to shear on fibronectin through changes in integrin affinity and cytoskeletal dynamics, *Immunology and cell biology 87*, 324-336.

63. Cairo, C. W., Mirchev, R., and Golan, D. E. (2006) Cytoskeletal regulation couples LFA-1 conformational changes to receptor lateral mobility and clustering, *Immunity 25*, 297-308.

64. Jaqaman, K., Loerke, D., Mettlen, M., Kuwata, H., Grinstein, S., Schmid, S. L., and Danuser, G. (2008) Robust single-particle tracking in live-cell time-lapse sequences, *Nature methods 5*, 695-702.

65. Vrieze, S. I. (2012) Model selection and psychological theory: a discussion of the differences between the Akaike information criterion (AIC) and the

Bayesian information criterion (BIC), *Psychological methods 17*, 228-243.

66. Seyrantepe, V., Landry, K., Trudel, S., Hassan, J. A., Morales, C. R., and Pshezhetsky, A. V. (2004) Neu4, a novel human lysosomal lumen sialidase, confers normal phenotype to sialidosis and galactosialidosis cells, *The Journal of biological chemistry 279*, 37021-37029.

67. Tangyuenyongwatana, P., Keeratinijakal, V., and Gritsanapani, W. (2012) Thin-layer chromatography-densitometry analysis of dimethoxyphenylbutadiene content in Zingiber cassumunar rhizomes, *Journal of AOAC International 95*, 1614-1617.

Chapter 3: Conclusions and future directions

3.1 Conclusions

In this project we used several methods to explore the role of human neuraminidase enzymes in the regulation of β1-integrin–fibronectin adhesion in human epithelial cells (HeLa and A549 cell lines). In our migration studies, we identified several conditions that implicate glycolipids in integrin-mediated adhesion. For example, NEU3 treatment of HeLa cells resulted in a significant increase in cell migration. We had originally hypothesized that NEU3 could regulate integrins through changes in glycolipid composition, and experiments in which specific glycolipids were exogenously added to the cells confirmed that these compounds could indeed modulate adhesion. Our results are consistent with GM3 as a key negative regulator of β1-integrins, along with NEU3 or NEU4 acting as a positive regulator by depleting GM3 levels in the membrane. Importantly, our results do not preclude the possibility that other glycolipids may play important roles in this system. In fact, it may be that other complex or low-abundance gangliosides may be playing important roles which remain undetected.

Our results support the possibility that the human NEU enzymes may play different roles in different cell types. For example, our data indicate that addition of NEU3 to cells can increase cell migration in one cell type (HeLa), while it is

inhibitory in another (A549). Critically, our results with the non-specific NEU inhibitor, DANA, clearly demonstrate that the family of human NEU enzymes plays an important role in integrin adhesion. DANA was able to inhibit β1-integrin cell migration in both cell types studied, supporting a role for native sialidases in integrin regulation.

This finding appears to extend to glycolipids as well, where GM3 is inhibitory in one cell line (HeLa), it is pro-adhesive in another (A549). Our studies reveal a surprising complexity of activity for glycolipid structures. We found that LacCer was pro-adhesive in both cell lines tested, while complex gangliosides (GM1, GD1a, GD1b, and GT1b) were all inhibitory to different degrees (**Figure 2.14**).

Analysis of NEU3 and NEU4 substrate specificity *in vitro* revealed that both enzymes have α2,3 and α2,8-sialidase activities. Additionally, we analyzed changes in cellular gangliosides of cells treated under conditions which altered cell migration. These experiments did not reveal large changes, though this may be a limitation of the technique (TLC), and therefore we were not able to draw any firm conclusions about these changes. Our *in vitro* experiments did confirm that GM3 is a good substrate for all the enzymes tested (NEU3, NEU4 and pfNEU); however, GM1 was not a substrate for any of these enzymes.

We used immunofluorescence to visualize the subcellular localization of

β1 integrins on epithelial cells (HeLa). We observed that the integrin is generally distributed in microclusters on the cell body, and that NEU-treated cells form larger integrin clusters. In wild-type cells, the integrin was not co-localized with cholera toxin-binding gangliosides, such as GM1. Cells which overexpress NEU3 showed large changes in morphology. Additionally, these cells formed large integrin clusters which contained gangliosides and the NEU3 enzyme. These results suggested that the integrin, gangliosides, and NEU3 can be co-localized.

Finally, we examined the diffusion of β1 integrins on HeLa using single dye tracking (SDT) experiments. Measurements of receptor diffusion can provide evidence of cytoskeletal involvement. In our case, we observed that integrin diffusion was decreased by NEU-treatment, consistent that the formation of clusters on the NEU3-overexpressing cells is a result of active cytoskeletal association.

3.2 Future Directions

Our result supported a role for regulation of cellular adhesion by the human neuraminidase enzyme isoenzymes, NEU3 and NEU4. The most likely mechanism for regulation is through modification of the ganglioside content of the plasma membrane. Although our results are consistent with a central role for GM3 or LacCer, it is possible that other gangliosides or other hNEU isoenzymes

are involved in this process. An unanswered question that will require future work is the observation that NEU4 has different effects on cell migration as compared with NEU3 in two cell types. Hence, further experiments will need to be designed which can provide evidence for the specific targets of each enzyme to resolve these questions. Some possible strategies for future experiments are described below.

3.2.1 Cell migration test with different ECMs.

We used fibronectin as the ECM substrate for our cell migration assays because it is the main ligand for α4β1 and α5β1. In control experiments, treatment of FN with hNEU had no effect on the rates of migration (**Figure 2.15**). However, it may be possible that other ECM substrates are affected by hNEU treatment. Potential substrates would include collagen or laminin. Recent studies have found that β4 integrins are involved in the growth of prostate cancer cells. The β4 integrin is the laminin receptor (*1*). The role of NEU3 in laminin-mediated adhesion has been studied and it suggested that NEU3 can activate ERK and FAK phosphorylation (*2, 3*). However, the role of hNEU which modify glycoproteins could be relevant in this system.

3.2.2 Cell invasion tests with NEU3 and NEU4.

In this project, we employed a two-dimensional cell migration assay. However, this assay may not accurately report on interactions that occur in

three-dimensional cell culture. Many methods are available to mimic tumor formation and metastasis *in vitro*, such including invasion assays (*4*). These assays are better mimics of the tissue environment as compared to the two-dimensional scratch assay. Invasion assays may use a Boyden chamber, also known as a transwell invasion assay. This chamber can be applied in both invasion and migration assays, and the only difference is whether the filter is pre-coated with ECM. In an invasion assay, the porous filter needs to be treated with ECM followed by seeding of cells (*5, 6*). Future studies should examine conditions such as NEU3, NEU4, and DANA treatment of epithelial or cancer cells. This assay configuration could also test the role of specific gangliosides. These results could support the conclusions drawn from the two-dimensional assays, or could indicate if these findings are an artifact of the assay configuration.

3.2.3 Identification of the NEU4 substrate.

The hNEU isoenzymes appear to have different effects depending on cell type. Our results in A549 cells suggest that NEU4 protein is a positive regulator of adhesion. However, NEU3 only showed a positive effect on adhesion in HeLa cells. This may be a result of different substrates in each cell line. For example, it is possible that NEU4 targets a glycoprotein substrate found on both cells (*7*), while NEU3 could target a glycolipid only present in one cell line. Alternatively, the same substrate may play a different role in each cell. To resolve these

questions, further work will be required to identify the primary targets of each enzyme in specific cell types.

3.2.4 Single dye tracking with more gangliosides and with A549 cell

We measured the lateral mobility of the α5β1 integrin on cells, and changes to receptor mobility upon treatment known to alter cell migration. For these experiments, we used single dye tracking, and we proposed a hypothetical model to explain our results (**Sec 2.6**). However, additional work will be required to verify this model. In dye tracking studies, we tested NEU3, GM1 and DANA treatment. Additional tests of GM3 and NEU4 conditions would help to support a role for GM2. It may also be worth acquiring higher speed trajectories to provide improved resolution in these experiments, which may help to distinguish the very small changes observed in **Figure 2.28** and **Figure 2.29**. Additional studies with other cell lines, including A549, could provide insight as to whether the effects observed are specific to the HeLa cell line.

3.2.5 Ganglioside-α5β1 integrin model

In our model, GM3 inhibits FN-integrin interactions by stabilizing an inactive conformation of the integrin α5β1 receptor (**Figure 3.1**).

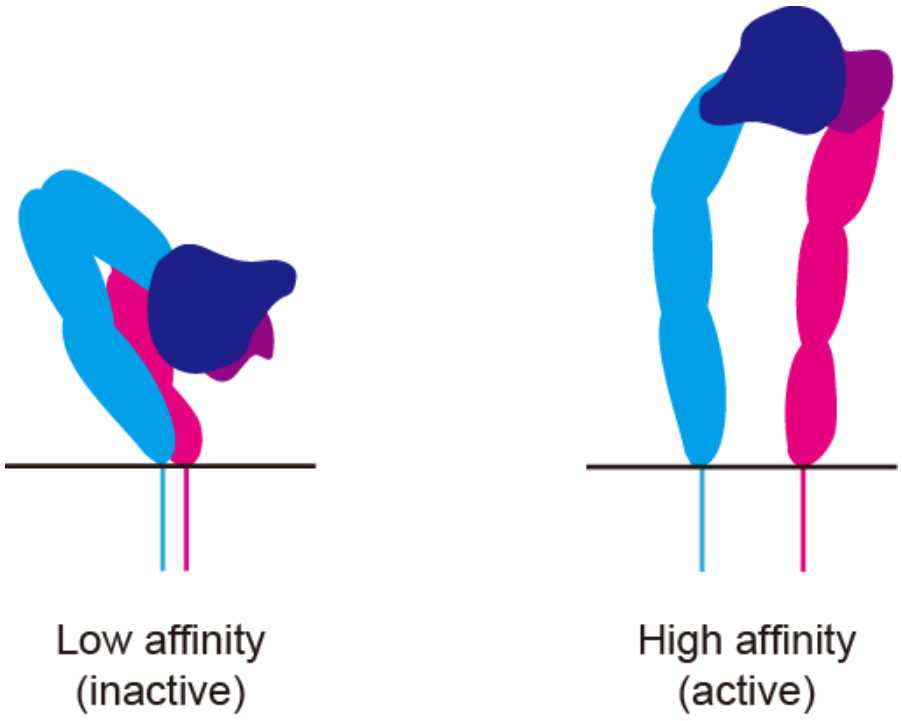

Figure 3.1 Two conformational states of the integrin heterodimer. On the cell membrane, most integrins may be maintained in a low affinity (inactive) folded conformation, which can't bind easily with the ECM. After activation (either outside-in or inside-out) , integrins may undergo a conformational change to a high affinity (active) state. This conformation is results in improved binding to ECM (*8*).

However, the action of NEU3 alters the structure of GM3 to LacCer. With increased levels of LacCer present, FN-integrin adhesion is increased. Our model would predict that the absence of GM3 could allow for more of the high-affinity conformation of the integrin to be generated. We propose that a molecular interpretation of this model could be based on direct ganglioside-integrin binding interactions. It is possible that the α5β1 integrin contains a lectin domain which

binds to GM3, or another ganglioside substrate of NEU3. If the binding of the ganglioside target to the lectin domain (*9, 10*) prevents a conformational change required for integrin-FN interactions it would fit with our observations. This model would also suggest that competitive inhibition of the GM3-integrin interaction would be anti-adhesive, consistent with our observations in **Figure 2.13**. Exogenous addition of GM3 would also be expected to be inhibitory, as was observed in HeLa cells (**Figure 2.14**).

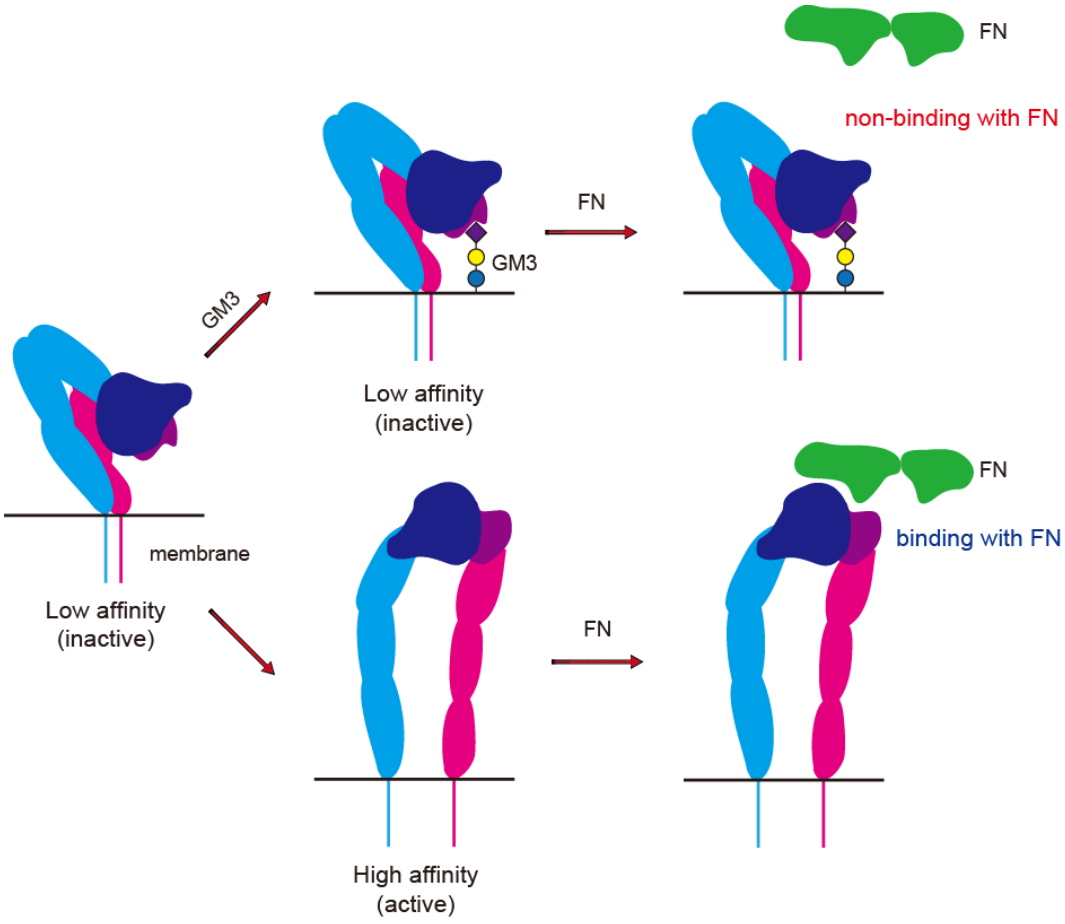

Figure 3.2 Proposed GM3-α5β1 integrin model. We hypothesize that GM3 can bind to the low affinity state

of the α5β1 integrin, stabilizing this conformation and inhibiting binding to its ECM target, fibronectin. In the absence of GM3, α5β1 integrins are more able to change conformation to a high affinity state, and bind to fibronectin.

In order to test this model, it would be ideal to verify the direct binding of GM3 to the integrin. Direct binding experiments could be conducted using a variety of methods. Surface Plasmon resonance (SPR) is a common technique used to test the binding affinity interaction between biomolecules (*11*, *12*). In this method, the sensor surface can display a binding epitope, and a target protein in solution is measured for binding. Difficulties with this experiment will include access to large amounts of the integrin. If SPR evidence of GM3-integrin binding were observed, it would be worthwhile to express specific domains of the integrin and test each for binding to identify the protein-ganglioside binding site.

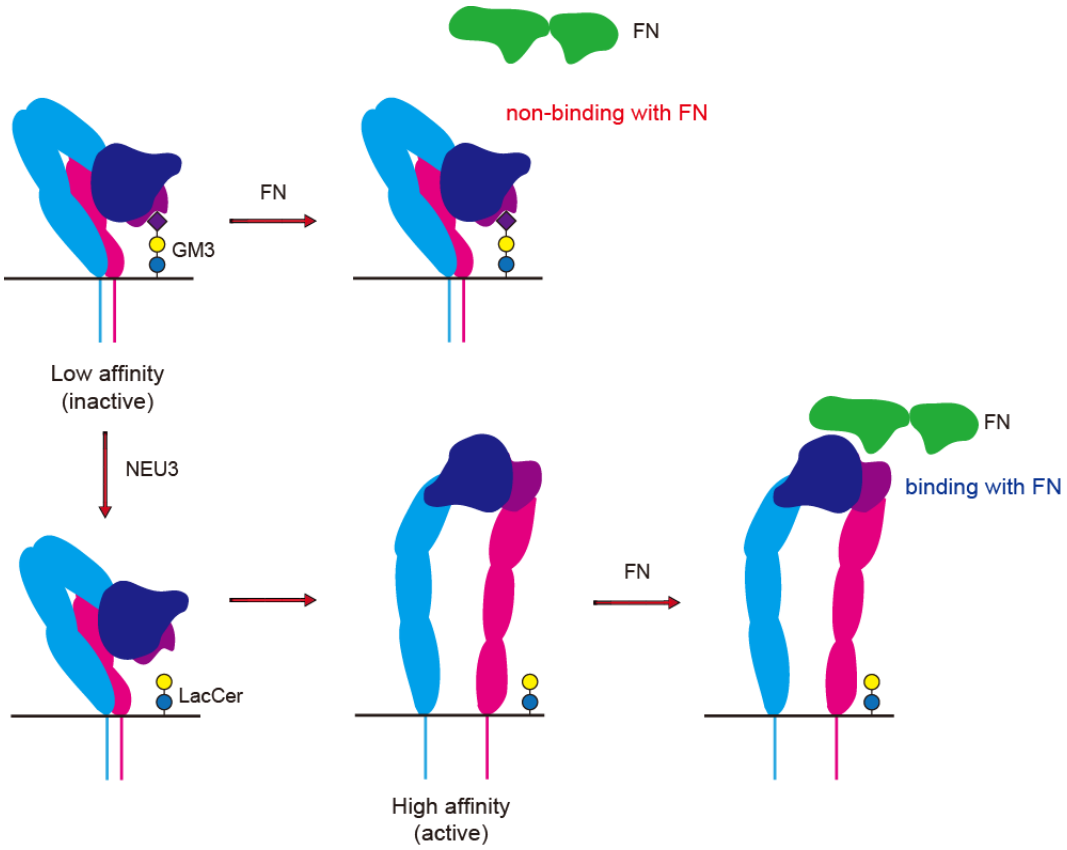

Figure 3.3 Proposed GM3-α5β1 integrin interactions in the presence of NEU3. In our model, NEU3 cleaves sialic acid from GM3, generating LacCer. LacCer has reduced affinity for the α5β1 integrin lectin domain, leading to a free integrin. The α5β1 integrin may then change to high affinity status and then bind with fibronectin.

This experiment could also be used to detect binding of the integrin to FN. For example, integrin co-incubated with GM3 would be expected to have reduced FN binding from our model (**Figure 3.3**).

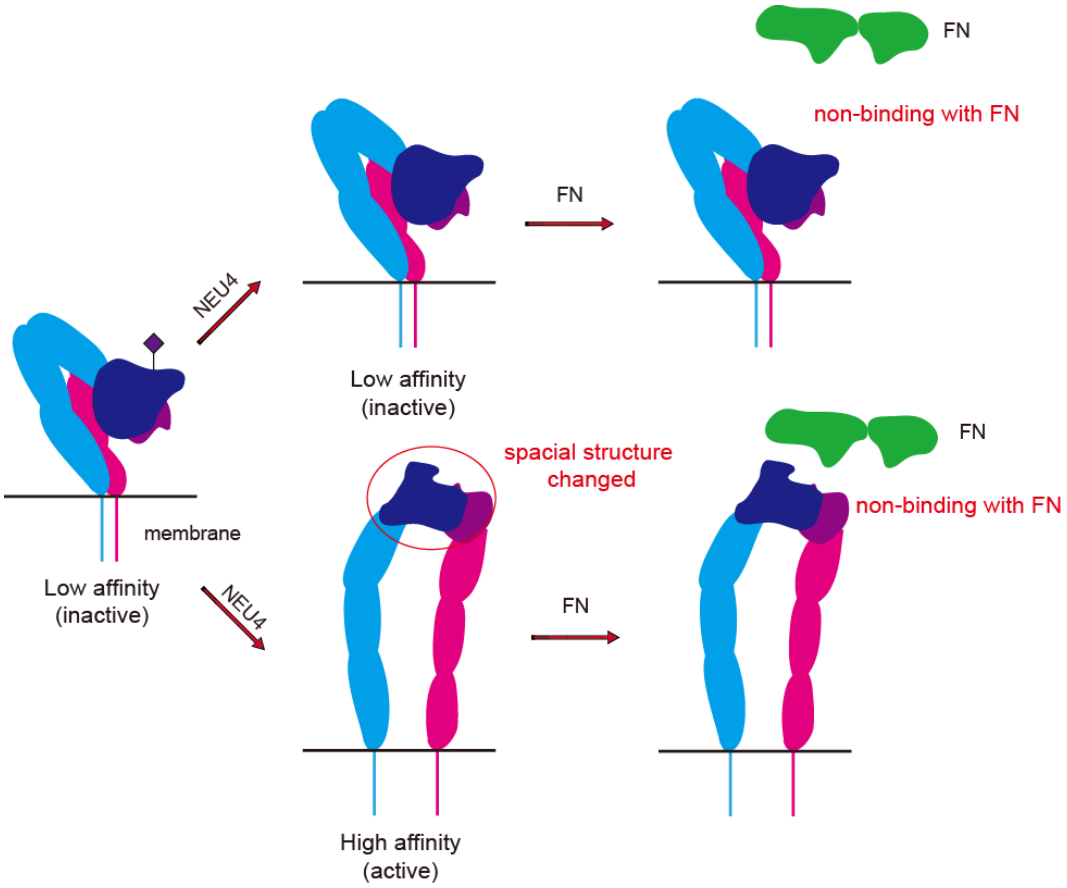

Figure 3.4 Proposed model for α5β1 integrin modulation by NEU4.

Establishment of an SPR, or other binding assay, could also test the effect of enzymes like NEU4 on the α5β1 integrin-FN interaction. Other gangliosides, including GM1, GD1a, GD1b and GT1b, could also be tested for direct binding.

3.3 References

1. Yoshioka, T., Otero, J., Chen, Y., Kim, Y. M., Koutcher, J. A., Satagopan, J., Reuter, V., Carver, B., de Stanchina, E., Enomoto, K., Greenberg, N. M., Scardino, P. T., Scher, H. I., Sawyers, C. L., and Giancotti, F. G. (2013) beta4 Integrin signaling induces expansion of prostate tumor progenitors, *The Journal of clinical investigation*.
2. Kato, K., Shiga, K., Yamaguchi, K., Hata, K., Kobayashi, T., Miyazaki, K., Saijo, S., and Miyagi, T. (2006) Plasma-membrane-associated sialidase (NEU3) differentially regulates integrin-mediated cell proliferation through laminin- and fibronectin-derived signalling, *The Biochemical journal 394*, 647-656.
3. Tringali, C., Lupo, B., Silvestri, I., Papini, N., Anastasia, L., Tettamanti, G., and Venerando, B. (2012) The plasma membrane sialidase NEU3 regulates the malignancy of renal carcinoma cells by controlling beta1 integrin internalization and recycling, *The Journal of biological chemistry 287*, 42835-42845.
4. Kramer, N., Walzl, A., Unger, C., Rosner, M., Krupitza, G., Hengstschlager, M., and Dolznig, H. (2013) In vitro cell migration and invasion assays,

Mutation research 752, 10-24.

5. Albini, A., and Benelli, R. (2007) The chemoinvasion assay: a method to assess tumor and endothelial cell invasion and its modulation, *Nature protocols 2*, 504-511.
6. Marshall, J. (2011) Transwell((R)) invasion assays, *Methods in molecular biology 769*, 97-110.
7. Yamanami, H., Shiozaki, K., Wada, T., Yamaguchi, K., Uemura, T., Kakugawa, Y., Hujiya, T., and Miyagi, T. (2007) Down-regulation of sialidase NEU4 may contribute to invasive properties of human colon cancers, *Cancer science 98*, 299-307.
8. Arnaout, M. A., Goodman, S. L., and Xiong, J. P. (2007) Structure and mechanics of integrin-based cell adhesion, *Current opinion in cell biology 19*, 495-507.
9. Jakubowski, P., Calvete, J. J., Eble, J. A., Lazarovici, P., and Marcinkiewicz, C. (2013) Identification of inhibitors of alpha2beta1 integrin, members of C-lectin type proteins, in Echis sochureki venom, *Toxicology and applied pharmacology 269*, 34-42.
10. Xia, Y., Borland, G., Huang, J., Mizukami, I. F., Petty, H. R., Todd, R. F., 3rd, and Ross, G. D. (2002) Function of the lectin domain of Mac-1/complement receptor type 3 (CD11b/CD18) in regulating neutrophil

adhesion, *Journal of immunology 169*, 6417-6426.

11. Szunerits, S., Maalouli, N., Wijaya, E., Vilcot, J. P., and Boukherroub, R. (2013) Recent advances in the development of graphene-based surface plasmon resonance (SPR) interfaces, *Analytical and bioanalytical chemistry 405*, 1435-1443.

12. Guo, X. (2012) Surface plasmon resonance based biosensor technique: a review, *Journal of biophotonics 5*, 483-501.

Appendix

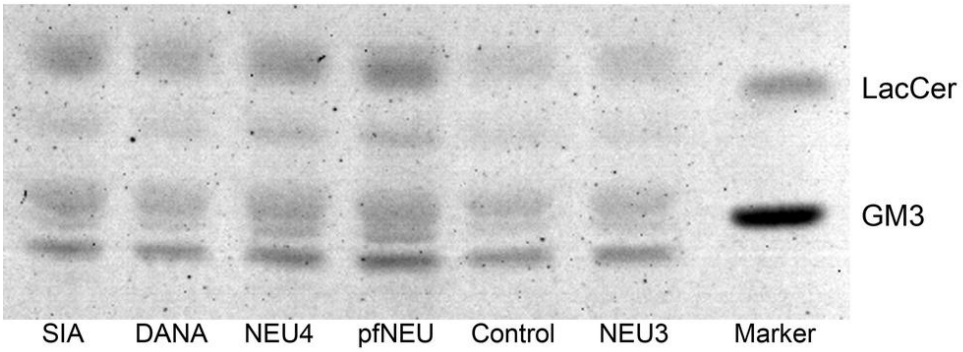

Figure A-01 A549 cell gangliosides extraction on TLC plate. HeLa cells were treated with same concentration of migration assay for 3 hours at 37℃, 5% CO_2, and then harvest by cell scraper. The suspension was washed with PBS twice and centrifuge to get the cell pellet. Gangliosides would be extracted by 1:1 methanol and chloroform for 30 min and then remove the precipitate by centrifuge. The solution was dried by N_2 and then dissolved again in small amount of 1:1 methanol and chloroform. The TLC plate was separated by 1:2:1 acidic acid, n-butanol and 0.5% $CaCl_2$ (aq) and then stained by oricinol sulfuric acid stain.

Analysis of GD1a, GD1b and GT1b by HPTLC required additional produced optimization. GT1b was treated with the same protocols as for GM1 and GM3, but staining did not show the bands for the substrates. Heating the plate for a longer time (about 1 hour) did not improve development (**Figure A-02**).

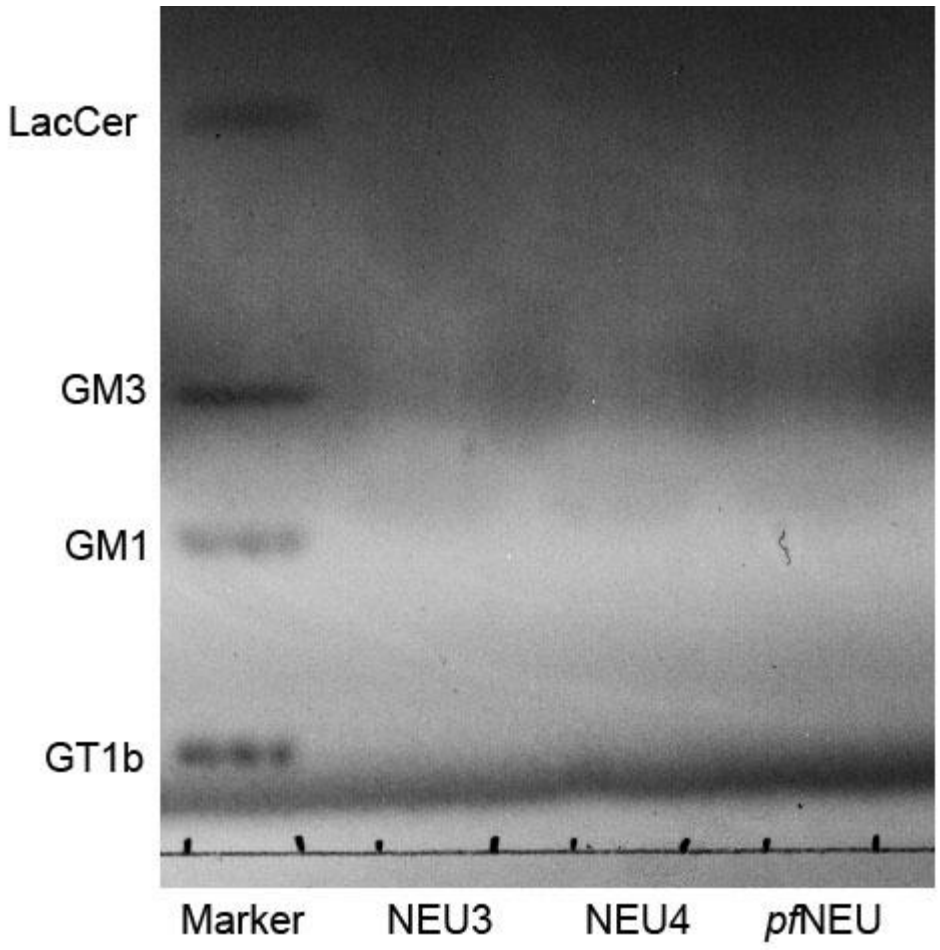

Figure A-02 TLC for GT1b (first run). GT1b treated with sialidases for 1 hour at 37℃ and then precipitated by 1:1 methanol and chloroform. Liquid was separated by centrifuge and removed aqueous layer. After drying the organic layer by N_2, solid was dissolved in 1:1 methanol and chloroform again and then run on TLC by 1:2:1 acetic acid/n-butanol/0.5% $CaCl_2$ (aq.). TLC was stained by orcinol sulfuric acid and heat for 1 hour at 80℃.

The TLC did not show lipids from extraction of the organic layer. Centrifuged to remove the precipitate was followed the drying the liquid mixture with N_2 and then dissolved in 1:1 methanol and chloroform again.

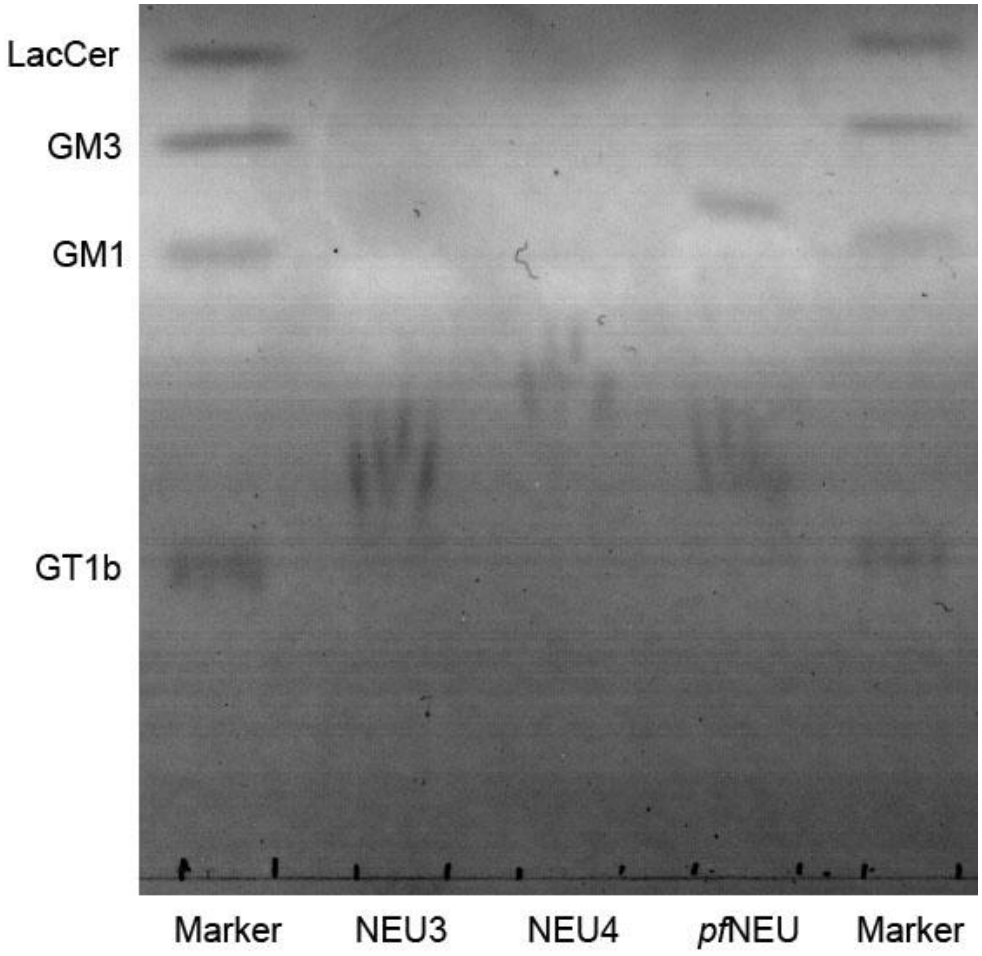

Figure A-03 TLC for GT1b (second run). GT1b treated with sialidases for 1 hour at 37℃ and then precipitated by 1:1 methanol and chloroform. Liquid was separated by centrifuge and removed proteins. After drying the liquid by N_2, solid was dissolved in 1:1 methanol and chloroform again and then run on TLC by 1:2:1 acetic acid/n-butanol/0.5% $CaCl_2$ (aq.). TLC was stained by orcinol sulfuric acid and heat for 1 hour at 80℃.

This TLC protocol was improved, but the bands were still not well

resolved (**Figure A-03**). We expected that the salt added in the buffer for the first reaction step could be the source of the problem. Desalting the sample with C18 tip after reaction was performed before. This improvement allowed us to analyzed ganglioside substrates after enzyme treatment.

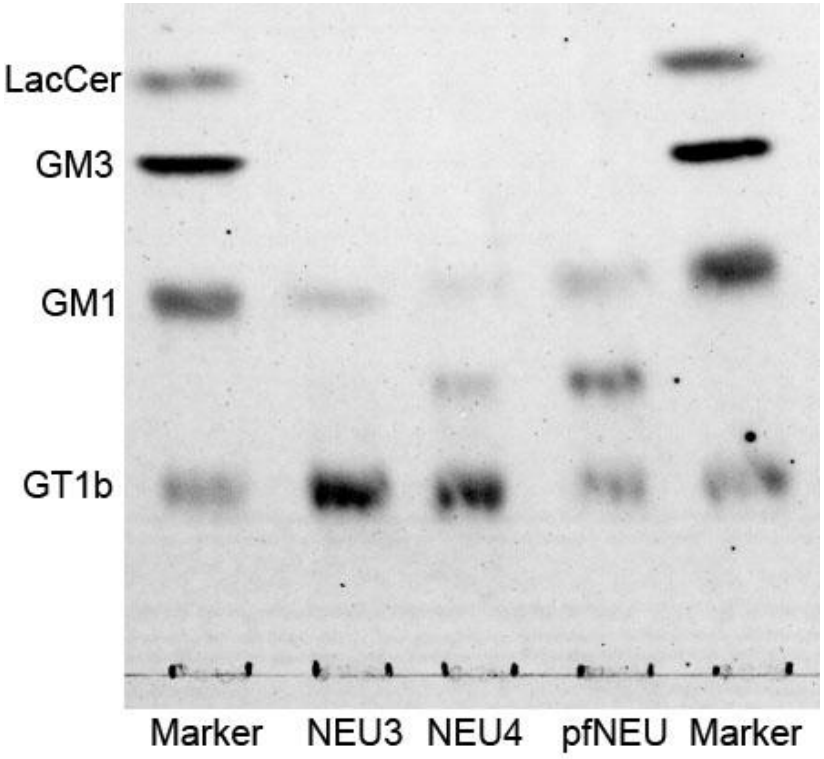

Figure A-04 TLC for GT1b (desalted and glycerol free). All sialidases changed buffer with 10k spin column to water in order to remove glycerol, and then GT1b treated with sialidases for 1 hour at 37℃. Protein was precipitated by 1:1 methanol and chloroform, and liquid was separated by centrifuge and removed proteins. After drying the liquid by N_2, solid was desalted by C18 tip and dried by N_2 again. Then the solid dissolved in 1:1 methanol and chloroform and then run on TLC by 1:2:1 acetic acid/n-butanol/0.5% $CaCl_2$ (aq.). TLC was stained by orcinol sulfuric acid and heat for 30 min at 80℃.

From our previous studies GM1 was not cleaved by sialidases to GA1. To confirm that our TLC was not affected by glycerol impurities from hNEU buffer, a 10K spin column was applied to change buffer to water. The glycerol is used to make neuraminidase more stable in solution, and it can still remain in the solid after several purify steps. This time we used glycerol-free sialidases in the reaction and then ran TLC. This protocol improved the resolution of the GM3 band (**Figure A-04**).

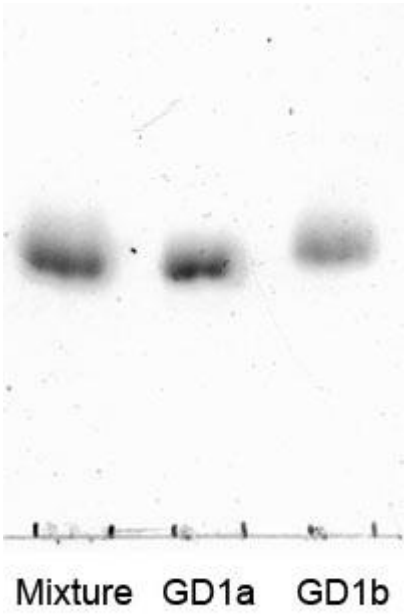

Figure A-05 Eluent testing for GD1a and GD1b (1:2:1). GD1a and GD1b were mixed with same amount and run TLC in 1:2:1 acetic acid, n-butanol and 0.5% $CaCl_2$ (aq). TLC was stained by orcinol sulfuric acid and heat for 30 min at 80 ℃.

The solvent system used to separate glycolipids can have strong effect on separation. Although we first used 1:2:1 acetic acid, n-butanol and 0.5% $CaCl_2$, other system have been used in the literature (**Figure A-05**). Separation of GD1a and GD1b has been required with 60:35:8 chloroform, methanol and 0.25% KCl (aq) and 60:40:7:3 chloroform, methanol, 0.25% KCl (aq) and ammonium hydroxide. Prepared these two eluent system, we found that ammonium hydroxide was not miscible and had two layers at first, which because miscible after standing for 2 hours. Results showed that both of them could resolve GD1a and GD1b in a mixture by TLC (**Figure A-06**).

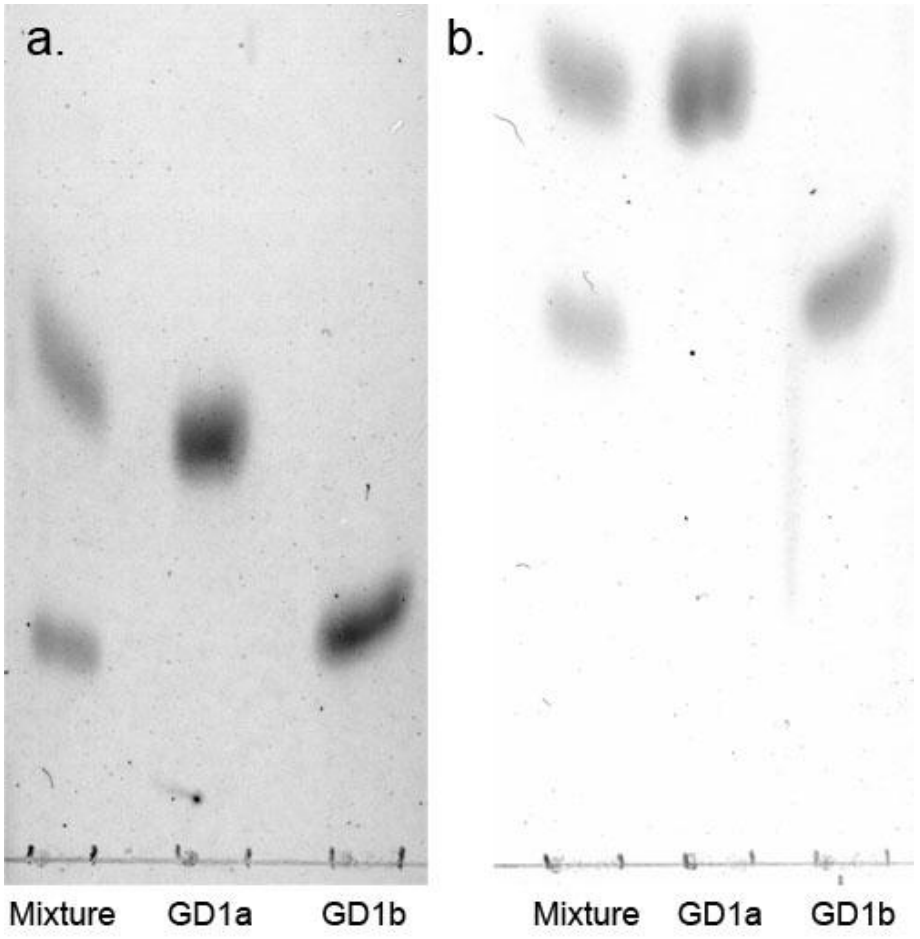

Figure A-06 Eluent testing for GD1a and GD1b. Gangliosides tested with a. 60:40:7:3 of chloroform, methanol, 0.25% KCl (aq) and ammonium hydroxide and b. 60:35:8 of chloroform, methanol and 0.25% KCl (aq). GD1a and GD1b were mixed with same amount and run TLC plates in two eluent, after that stained by orcinol sulfuric acid and heat for 30 min at 80 ℃.

Both of these eluent systems moved very fast on TLC plates. The system used in **a.** was better than **b.** for separation (**Figure A-06)**. In order to make a good band on TLC, we still made some change for the eluent, and we used

60:40:8 of chloroform, methanol and 0.25% KCl (aq), then a more clear result came out.

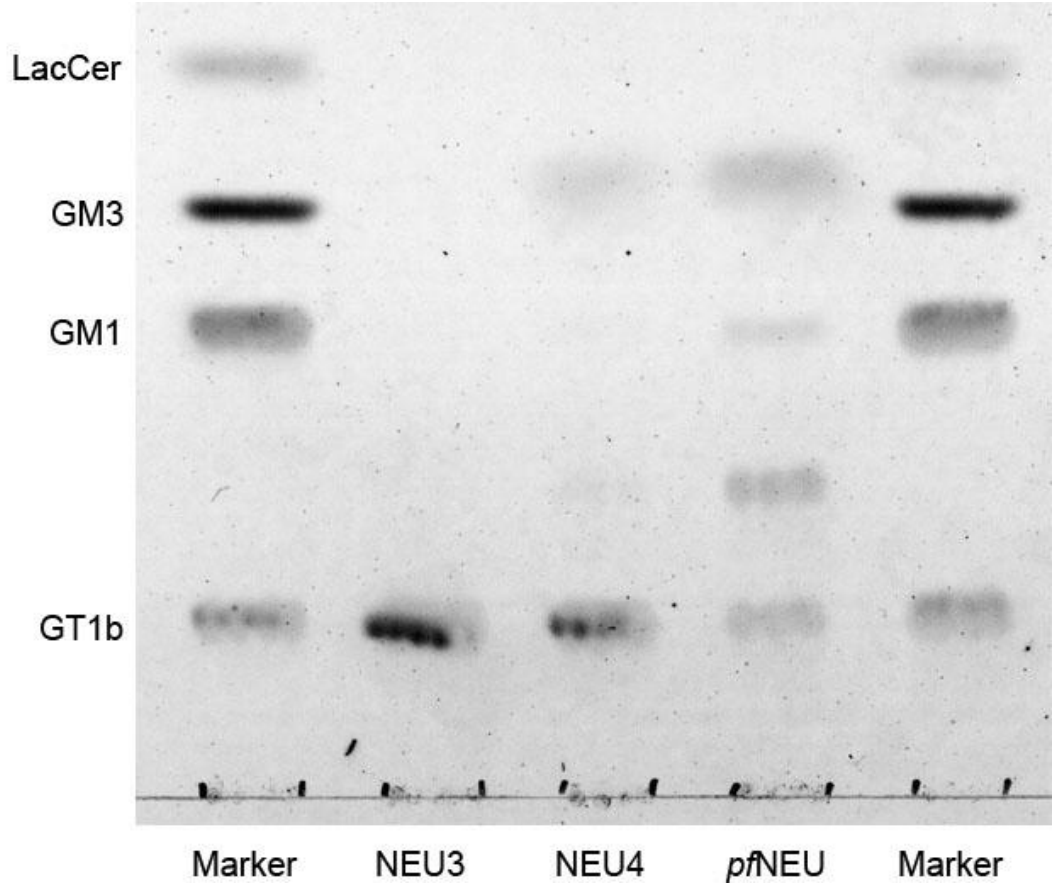

Figure A-07 TLC analysis of GT1b (desalted). GT1b was treated with sialidase for 1 hour at 37 ℃ and then precipitated by 1:1 methanol and chloroform. The sample was centrifuged and the aqueous layer was removed. After drying, the organic layer was dissolved in 1:1 methanol and chloroform again and then run on TLC by 1:2:1 acetic acid/n-butanol/0.5% $CaCl_2$ (aq.). The plate was stained by orcinol sulfuric acid and heated for 30 min at 80 ℃